

Electronic Thesis and Dissertation Repository

12-5-2023 11:30 AM

Hydrogen Bond Activation of Donor Acceptor Cyclopropanes

Matthew H.J. Pamerter, *The University of Western Ontario*

Supervisor: Michael A. Kerr, *The University of Western Ontario*

A thesis submitted in partial fulfillment of the requirements for the Master of Science degree in Chemistry

© Matthew H.J. Pamerter 2023

Follow this and additional works at: <https://ir.lib.uwo.ca/etd>

 Part of the [Organic Chemistry Commons](#)

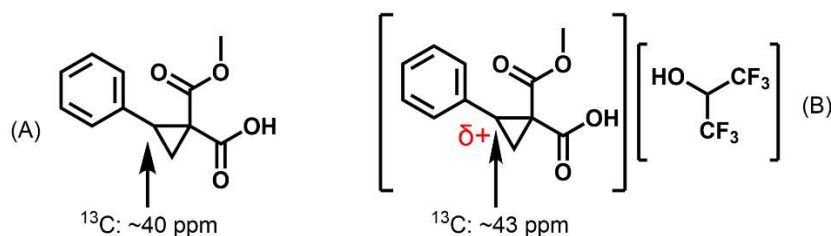
Recommended Citation

Pamerter, Matthew H.J., "Hydrogen Bond Activation of Donor Acceptor Cyclopropanes" (2023). *Electronic Thesis and Dissertation Repository*. 9892.
<https://ir.lib.uwo.ca/etd/9892>

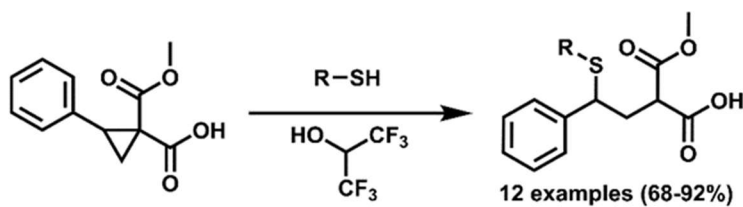
This Dissertation/Thesis is brought to you for free and open access by Scholarship@Western. It has been accepted for inclusion in Electronic Thesis and Dissertation Repository by an authorized administrator of Scholarship@Western. For more information, please contact wlsadmin@uwo.ca.

Abstract

Donor acceptor cyclopropanes (DACs) are versatile organic building blocks used in the synthesis of many pharmaceutically relevant heterocycles. The combination of a high ring strain cyclopropane core and vicinal donor and acceptor substituents cause DACs to behave like 1,3-zwitterions. Recently, DACs have been activated by a hydrogen bond donor solvent in place of a Lewis acid catalyst, allowing the elimination of heavy metals commonly used in these transformations. Hexafluoroisopropanol (HFIP) as a hydrogen bond donor cosolvent was found to cause a downfield shift of the DACs electrophilic carbon in the ^{13}C NMR spectrum. This indicates increased electrophilicity at this position (**Structure A vs B**). NMR spectroscopy titrations were used to study the host-guest interaction between DACs and HFIP. The data collected was compared to the effects of binding a Lewis acid catalyst such as scandium triflate ($\text{Sc}(\text{OTf})_3$). The HFIP conditions used previously by the Kerr group caused a further downfield shift than commonly used catalytic amounts of scandium triflate.



To further expand the application of the HFIP method, the ring-opening addition reaction of DACs with thiol nucleophiles is reported here. Yields were comparable or slightly improved when compared to similar transformations that used a metal-based catalyst. Electron donating and withdrawing properties of the thiol reagents had very strong effects on the results, resulting in two sets of conditions for this methodology.



Keywords: donor-acceptor cyclopropane, nucleophilic ring opening, NMR spectroscopy titration, hydrogen bond activation, thiol nucleophile.

Summary for Lay Audience

New species of plants and fungi are constantly being discovered, while the number is debated some sources estimate that up to 6 million species of fungi could be present on Earth. Natural products, which are molecules isolated from various plants and fungi are also constantly being discovered. Many of these compounds have potentially useful biological properties for which further study is desired. Synthetic organic chemists are tasked with the challenge of recreating these natural products for further testing, as well as making similar products that could end up being useful things like drugs. Building these molecules can be a long process with many steps, and synthetic chemists rely on previously tested reactions they can use as steps toward their product. Method-oriented synthesis is the discovery of these reactions that can be used as steps. This contributes to the base knowledge of the scientific community. This thesis will discuss the development and results of a reaction along with analytical experiments to support the findings. The goal of this work was to eliminate the need for a metal catalyst in a field of chemistry that commonly relies on one to push the reaction forward. These catalysts are usually based around a metal that is toxic and expensive and therefore removing it is beneficial. Accompanying the results of this reaction are analytical studies that show how this new method can be more effective than the older metal catalyst methods.

Acknowledgments

First off, I would like to thank Dr. Michael Kerr for his guidance and support throughout my years as a member of his research group. Having a supervisor who is so knowledgeable and encouraging made it easy to face and overcome any obstacles that came my way and I could not have asked for a better group to be part of for my research. I would like to thank my fellow group member Shane for being my mentor as I entered the group and completed my undergraduate research project. I would also like to thank the Kerr group, Alec, Maeve, and Tim for making the lab space as supportive and enjoyable as possible. I greatly look forward to continuing my studies with Dr. Kerr and his group. A huge thank you to Mat Willans in the NMR spectroscopy department for his assistance and additional training required for my research. I would like to thank Western University and the Chemistry Department for making this project possible.

Table of Contents

Abstract.....	ii
Summary for Lay Audience.....	iii
Acknowledgments.....	iv
Table of Contents.....	v
List of Tables.....	vii
List of Figures.....	viii
List of Appendices.....	ix
List of Schemes.....	xi
Abbreviations.....	xii
1. Introduction.....	1
1.1. Donor Acceptor Cyclopropanes.....	1
1.2. Reactions of Donor-Acceptor Cyclopropanes.....	3
1.3. Natural Product Targets of Donor-Acceptor Cyclopropanes.....	8
1.4. Donor-Acceptor Cyclopropane Activation by Hydrogen Bond Donor.....	12
1.5. NMR Spectroscopy Titration Studies.....	14
1.6. ¹³ C NMR Spectroscopy Studies of Donor-Acceptor Cyclopropanes.....	16
1.7. Purpose of Thesis.....	17
2. Results and Discussion.....	19
2.1. NMR Spectroscopy Titrations.....	19
2.1.1. Methodology of Titrations.....	19
2.1.2. Methodology of Fitting Titration Data.....	20
2.1.3. HFIP Titration of Hemimalonate and Diester DAC.....	26
2.1.4. Comparison with Metal Catalyst Titration.....	28

2.2.	Ring Opening Reactions with Thiol Nucleophiles.....	31
2.2.1.	Reaction Optimization	32
2.2.2.	Substrate Scope.....	35
3.	Conclusions and Future Directions.....	38
4.	Experimental.....	41
4.1.	NMR Titrations	41
4.1.1.	Sample Preparation: Job's Plot.....	41
4.1.2.	Sample Preparation: HFIP titrations	41
4.1.3.	Sample Preparation: Sc(OTf) ₃ titrations	42
4.2.	Synthesis of Cyclopropanes	42
4.3.	General Procedures for Ring Opening Additions	42
4.4.	Characterization of ring open adducts.....	43
5.	References.....	50
	Appendix.....	56
	Curriculum Vitae	72

List of Tables

Table 2.1: Optimization of ring opening conditions for thiophenol, temp at 60 °C (Inc. = incomplete, No rxn = no reaction).....	32
---	----

List of Figures

Figure 1.1: Cycloalkane ring strain energies	2
Figure 1.2: Cyclopropane ring strain	2
Figure 1.3: Diester and hemimalonate DAC structure.....	3
Figure 1.4: Slow exchange host-guest NMR spectra model.....	15
Figure 1.5: Fast exchange host-guest NMR spectra model	15
Figure 1.6: ^{13}C NMR study of DAC donor groups, modified from Waser ³³	17
Figure 2.1: DAC carbon centers labeled.....	19
Figure 2.2: Chemical shift of C2 in hemimalonate 2.1a at varying mol equivalents of HFIP	20
Figure 2.3: Jobs plot for hemimalonate 2.1a and HFIP	22
Figure 2.4: Stacked ^{13}C Spectra (2.4a) and initial fitting of expanded data set (2.4b)	24
Figure 2.5: Dimerization of hemimalonate 2.1a in 2:2 complex with HFIP	25
Figure 2.6: Hemimalonate 2.1a dilution experiment	26
Figure 2.7: Hemimalonate 2.1a and HFIP titration. Blue points represent experimental data, black line represents the calculated fit.....	27
Figure 2.8: Diester 2.1b and HFIP titration. Red points represent experimental data, black line represents the calculated fit	27
Figure 2.9: ^{13}C NMR titration of hemimalonate 2.1a with $\text{Sc}(\text{OTf})_3$. Blue represents Sc titration data, red shows HFIP titration data.....	29
Figure 2.10: ^{13}C NMR titration of diester 2.1b with $\text{Sc}(\text{OTf})_3$. Blue represents Sc titration data, red shows HFIP titration data	30
Figure 2.11: Thiol substrate scope	35
Figure 2.12: Pyridine thiol adduct ^1H spectra.....	36
Figure 2.13: DAC donor group substrate scope.....	37
Figure 3.1: Summary of NMR spectroscopy titration method	38

List of Appendices

Table A.1: HFIP titration of hemimalonate 200 mM	56
Table A.2: Jobs plot HFIP titration of hemimalonate, total concentration 1 M	57
Table A.3: HFIP titration of hemimalonate 5 mM	57
Table A.4: HFIP titration of diester 5 mM	58
Table A.5: HFIP and Sc(OTf) ₃ titration of hemimalonate 100 mM	59
Table A.6: HFIP and Sc(OTf) ₃ titration of diester 100 mM	59
Figure A.1: ¹ H NMR Spectra for 2.20a.....	60
Figure A.2: ¹³ C NMR Spectra for 2.20a.....	60
Figure A.3: ¹ H NMR Spectra for 2.20b	61
Figure A.4: ¹³ C NMR Spectra for 2.20b.....	61
Figure A.5: ¹ H NMR Spectra for 2.20c	62
Figure A.6: ¹³ C NMR Spectra for 2.20c.....	62
Figure A.7: ¹ H NMR Spectra for 2.20d	63
Figure A.8: ¹³ C NMR Spectra for 2.20d.....	63
Figure A.9: ¹ H NMR Spectra for 2.20e	64
Figure A.10: ¹³ C NMR Spectra for 2.20e.....	64
Figure A.11: ¹ H NMR Spectra for 2.20f	65
Figure A.12: ¹ H NMR Spectra for 2.20g	66
Figure A.13: ¹³ C NMR Spectra for 2.20g.....	66
Figure A.14: ¹ H NMR Spectra for 2.20h	67
Figure A.15: ¹³ C NMR Spectra for 2.20h.....	67
Figure A.16: ¹ H NMR Spectra for 2.20i	68
Figure A.17: ¹³ C NMR Spectra for 2.20i.....	68
Figure A.18: ¹ H NMR Spectra for 2.20j	69
Figure A.19: ¹³ C NMR Spectra for 2.20j.....	69
Figure A.20: ¹ H NMR Spectra for 2.20k	70
Figure A.21: ¹³ C NMR Spectra for 2.20k.....	70

Figure A.22: ^1H NMR Spectra for 2.201	71
Figure A.23: ^{13}C NMR Spectra for 2.201	71

List of Schemes

Scheme 1.1: DAC Structure and zwitterion intermediate.....	3
Scheme 1.2: Lewis acid coordination to diester DAC.....	4
Scheme 1.3: DAC nucleophilic ring opening	4
Scheme 1.4: Kerr group DAC ring opening with indole nucleophiles ⁸	5
Scheme 1.5: Diester DAC ring opening with thiols by Nolin	5
Scheme 1.6: DAC general annulation mechanism	6
Scheme 1.7a-h: Annulation reactions of DACs ¹¹⁻¹⁹	7
Scheme 1.8: Total synthesis of FR901483 pyrrolidine formation.....	9
Scheme 1.9: Total synthesis of (+)-phyllantidine tetrahydro-1,2-oxazine formation.....	9
Scheme 1.10: Total synthesis of (+)-nakadomarin A tetrahydro-1,2-oxazine formation..	10
Scheme 1.11: Total synthesis of (-)-allosecurinine pyrroloisoxazolidine formation.....	11
Scheme 1.12: Total synthesis of (+)-isatisine A tetrahydrofuran formation	11
Scheme 1.13: Conversion of diester DAC to hemimalonate	12
Scheme 1.14: Hemimalonate DAC ring opening with indoles by Kerr ²⁶	12
Scheme 1.15: Hypothesized hydrogen bonding between hemimalonate DAC carboxylic acid groups.....	13
Scheme 1.16: DAC ring opening activated by hydrogen bond donor solvent.....	13
Scheme 1.17: DAC ring opening using TfOH-HFIP hydrogen bond donor system	14
Scheme 1.18: Activation of DAC with a hydrogen bond donor.....	16
Scheme 1.19: Proposed reaction scheme for DAC ring-opening addition with thiols	18
Scheme 2.1: DAC ring opening with sulfoximines	29
Scheme 2.2: Proposed nucleophiles for hemimalonate DAC ring opening.....	31
Scheme 2.3: Optimized addition of dodecane thiol to DAC 2.6	32
Scheme 2.4: p-nitro thiophenol substrate with 2,6-lutidine additive	33
Scheme 2.5: p-methoxy thiophenol substrate with 2,6-lutidine additive.....	34
Scheme 2.6: Conditions "A" and "B" for ring-opening reactions.....	34
Scheme 3.1: Summary of DAC ring opening by thiol nucleophiles.....	40
Scheme 3.2: Initial work on dihydrothiophene synthesis by DAC annulation with thioamides.....	40

Abbreviations

- A – acceptor group
- Å – angstrom
- acac – acetylacetonate
- AcOH – acetic acid
- Ar – aryl
- atm – atmospheres
- B400 – Bruker 400 NMR spectrometer
- B600 – Bruker 600 NMR spectrometer
- Bn - benzyl
- CDCl₃ – deuterated chloroform
- CPME – cyclopentyl methyl ether
- D – donor group
- DAC – donor-acceptor cyclopropane
- DCE – dichloroethane
- DCM - dichloromethane
- E - electrophile
- esp – $\alpha,\alpha,\alpha',\alpha'$ -tetramethyl-1,3-benzenedipropionic acid
- Eq – equivalents
- f – mol fraction
- g – grams
- h – hours
- HFIP – hexafluoroisopropanol
- HIV – human immunodeficiency virus
- HSQC – heteronuclear single quantum coherence
- iPrOH - isopropanol
- K – association constant
- kbar – kilo bar

kJ – kilojoules
L.A – Lewis acid
M – molar
Me – methyl
MeOH – methanol
MHz – megahertz
mL – milliliters
mmol – millimoles
MS – molecular sieves
NMR – nuclear magnetic resonance
NTf – trifluoro methanesulfonamide
Nu – nucleophile
OTf – trifluoro methanesulfonate
PFAS – poly-fluoroalkyl substances
Ph – phenyl
PMB – para-methoxy benzyl
ppm – parts per million
rt – room temperature
TBAI – tetrabutylammonium iodide
TBDPS – tert-butyldiphenylsilyl
TfOH – trifluoromethanesulfonic acid
THF - tetrahydrofuran
TLC – thin layer chromatography
TMS – trimethylsilyl
tol – toluene
Ts – toluene sulfonyl
v – volume

1. Introduction

Synthetic organic chemists are tasked with the challenge of recreating many complex organic molecules found in nature. These molecules, which we know as natural products, can exhibit characteristics that make them useful in a variety of research fields. The study of natural products and their synthetic variations can lead to the discovery of things such as new pharmaceutical agents. Synthetic organic chemistry can be divided into two main areas of research. The first is target-oriented synthesis, which includes the design of pathways to synthesize these natural products and related synthetic compounds. The second is method development. In this area of research new methods are discovered and probed to test the scope and yield of transformations possible with the method. These tested reactions can then be applied to target-oriented synthesis pathways as one of the steps toward the desired end product. The work presented in this thesis falls in the method development research area. The reaction studied involves the ring opening of a class of molecules called donor-acceptor cyclopropanes. This type of reaction usually proceeds with a metal-based catalyst, which can be harmful and expensive. The introduction of the hydrogen bond donor solvent hexafluoroisopropanol (HFIP) allows for the elimination of these metal-based catalysts. While HFIP does have some negative impacts on health and the environment, the discovery of other hydrogen bond donor alternatives could lead to a greener route for these reactions. This introduction will begin with a look at a donor-acceptor cyclopropane structure and reactivity.

1.1. Donor Acceptor Cyclopropanes

Donor-acceptor cyclopropanes (DACs) have been of great interest over the last few decades in the field of organic chemistry due to their use as versatile synthetic building blocks. The reactivity of this class of molecules arises from its 3-membered carbocycle core, cyclopropane. Unlike the 109.5° angles preferred by sp^3 hybridized carbons, the cyclopropane ring with its 60° bond angles is under significantly higher ring strain.

Figure 1.1 shows the different ring strain energies resulting from carbocycle sizes up to 10 carbon atoms.¹

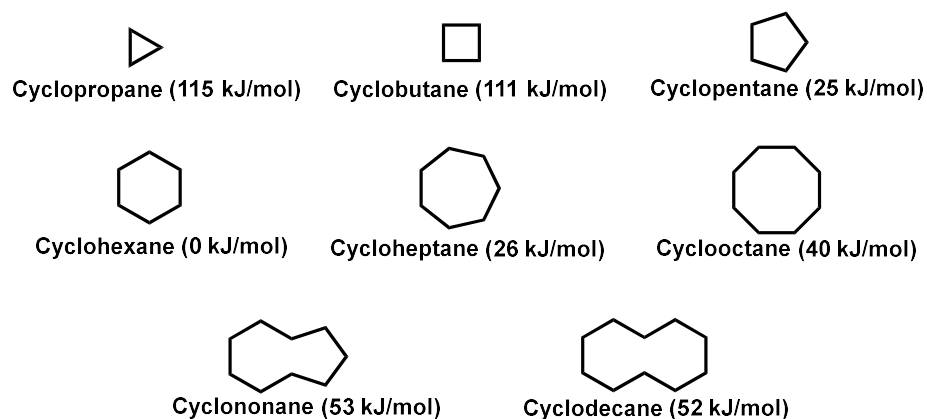


Figure 1.1: Cycloalkane ring strain energies

Cyclopropane, like cyclobutane, has a ring strain energy far from the other carbocycles. These two ring structures also have a $\Delta H_{\text{formation}}$ of +53 kJ/mol and +28.4 kJ/mol, respectively. The positive values generally indicate these compounds are unstable, unlike the other cyclic structures such as cyclohexane with a $\Delta H_{\text{formation}}$ of -156 kJ/mol.² This indicates these rings are unstable compared to the others. In the cyclopropane this instability is caused by the 60 ° bond angles preventing the sp^3 orbitals to improperly overlap, resulting in a “bent” carbon-carbon bond. Additionally, due to the cyclopropane's planar structure, it also exhibits steric strain from its substituents being locked in eclipsed formation (**Figure 1.2**).

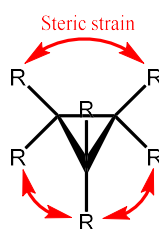
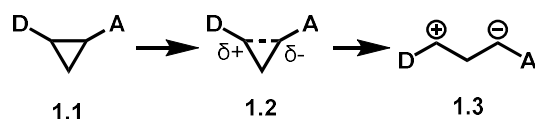


Figure 1.2: Cyclopropane ring strain

While this ring strain contributes to cyclopropane reactivity, it alone does not allow cyclopropanes to undergo the many possible transformations that DACs can. Through the introduction of vicinal electron donor and acceptor substituents, the bond between the two can be polarized making the DAC an ideal target for various reactions.



Scheme 1.1: DAC Structure and zwitterion intermediate

Scheme 1.1 illustrates this polarization. Structure **1.1** shows the DAC structure substituted with donor “D” and acceptor “A” groups. It should be noted that the donor group in these molecules is defined as a group that will stabilize the developing partial positive charge observed next to the donor group in **1.2**. In many cases, the donor group in these molecules is a phenyl group because of its ability to stabilize the positive charge by resonance through its ring. Generally, after the introduction of a catalyst, the DAC can be considered as the ring open zwitterion intermediate **1.3**, which now has a reactive electrophilic and nucleophilic site. These DACs can undergo a variety of reactions at both the electrophilic position (donor group carbon) and nucleophilic position (acceptor group carbon) giving possibilities to access many 1,3 functionalized, and annulation products.³ One of the most common DAC structures in this field of study and used by the Kerr group, is a DAC substituted with a phenyl group in the donor position and two methyl esters at the acceptor position. This DAC **1.5** will be referred to as the diester DAC as seen in **Figure 1.3**. Replacing one of the esters with a carboxylic acid group gives another structure used by the Kerr group in DAC chemistry, the hemimalonate DAC **1.6**.

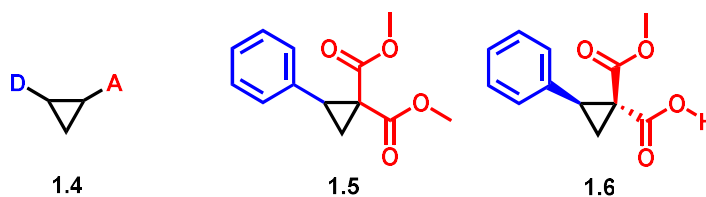
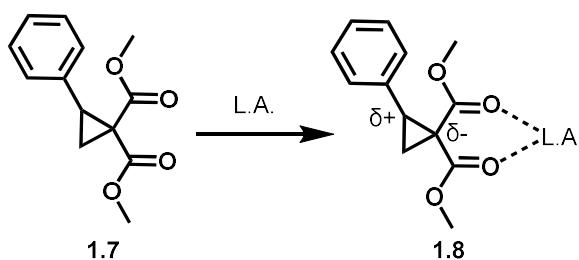


Figure 1.3: Diester and hemimalonate DAC structure

1.2. Reactions of Donor-Acceptor Cyclopropanes

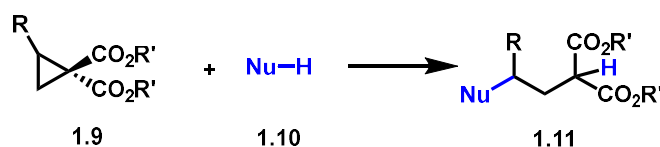
The reactive nature of DACs is a result of the high ring strain energy and the vicinal donor and acceptor groups. In most cases, these features alone are not enough and

DACs require further activation to undergo transformations. A Lewis acid catalyst is commonly used to drive these reactions. Lewis acid catalysts are a group of substances that readily accept an electron pair. These compounds can be boron-based, aluminum compounds, alkali/alkaline metal-based, and commonly seen in many current DAC reactions are lanthanide-based Lewis acid catalysts.^{4,5}



Scheme 1.2: Lewis acid coordination to diester DAC

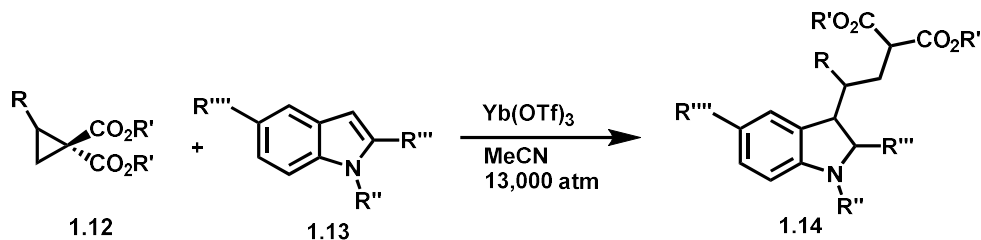
In DAC chemistry these catalysts function by binding to the acceptor group or groups of the molecule. In **Scheme 1.2** a Lewis acid (L.A.) coordinates to the acceptor groups of DAC **1.8** which pulls electron density away from the ring and towards the L.A. While the methyl esters function as the acceptor groups in the DAC they act as Lewis bases, or electron-pair donors, in the binding to a Lewis acid. This “activates” the DAC by polarizing the ring further, making it more susceptible to attack by a nucleophile. Through this activation many ring opening and annulation transformations are possible. In **Scheme 1.3** the general reaction for nucleophilic ring opening additions of DACs is shown.



Scheme 1.3: DAC nucleophilic ring opening

In ring-opening addition reactions of DACs, a nucleophile **1.10** will attack the electrophilic center adjacent to the donor group in DAC **1.9** driving the reaction towards the ring-open adduct **1.11**. Through this mechanism, a variety of functional groups may be installed such as indoles, amines, azides, nitriles, thiols, and carbon nucleophiles such as aryls groups.^{3,6,7} One example of this from the Kerr group employs

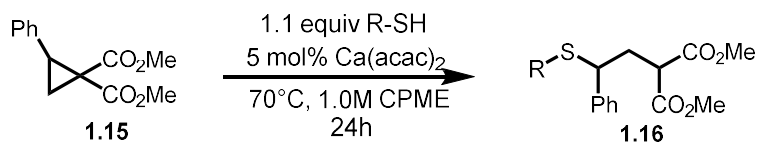
indoles as the nucleophile to ring open diester DACs as shown in **Scheme 1.4**.⁸ The Lewis acid catalyst ytterbium trifluoromethane sulfonate ($\text{Yb}(\text{OTf})_3$) is used to activate the DAC allowing a variety of substituted indoles to be inserted.



Scheme 1.4: Kerr group DAC ring opening with indole nucleophiles⁸

This is one of many ring-opening examples by the Kerr group and is an important starting point leading to the work discussed in this thesis. Indoles were later used as nucleophiles to ring open the hemimalonate DAC, the cyclopropane in this research studies. Later in this chapter, the progression from this ytterbium-catalyzed reaction to new methods with indole nucleophiles will be discussed.

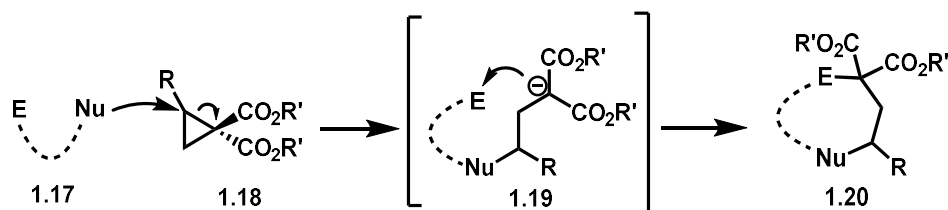
Directly relating to this thesis is the work done by Nolin, which demonstrates the use of thiol nucleophiles in the ring opening of diester DACs.⁹ The method developed utilized calcium acetylacetonate as the catalyst for this transformation in mild conditions (**Scheme 1.5**). Examples of 7 thiol reagents were reported with yields ranging from 75-94% for ring open adducts **1.16** and 8 examples of donor groups on the diester DAC ranging from 73-94%.



Scheme 1.5: Diester DAC ring opening with thiols by Nolin

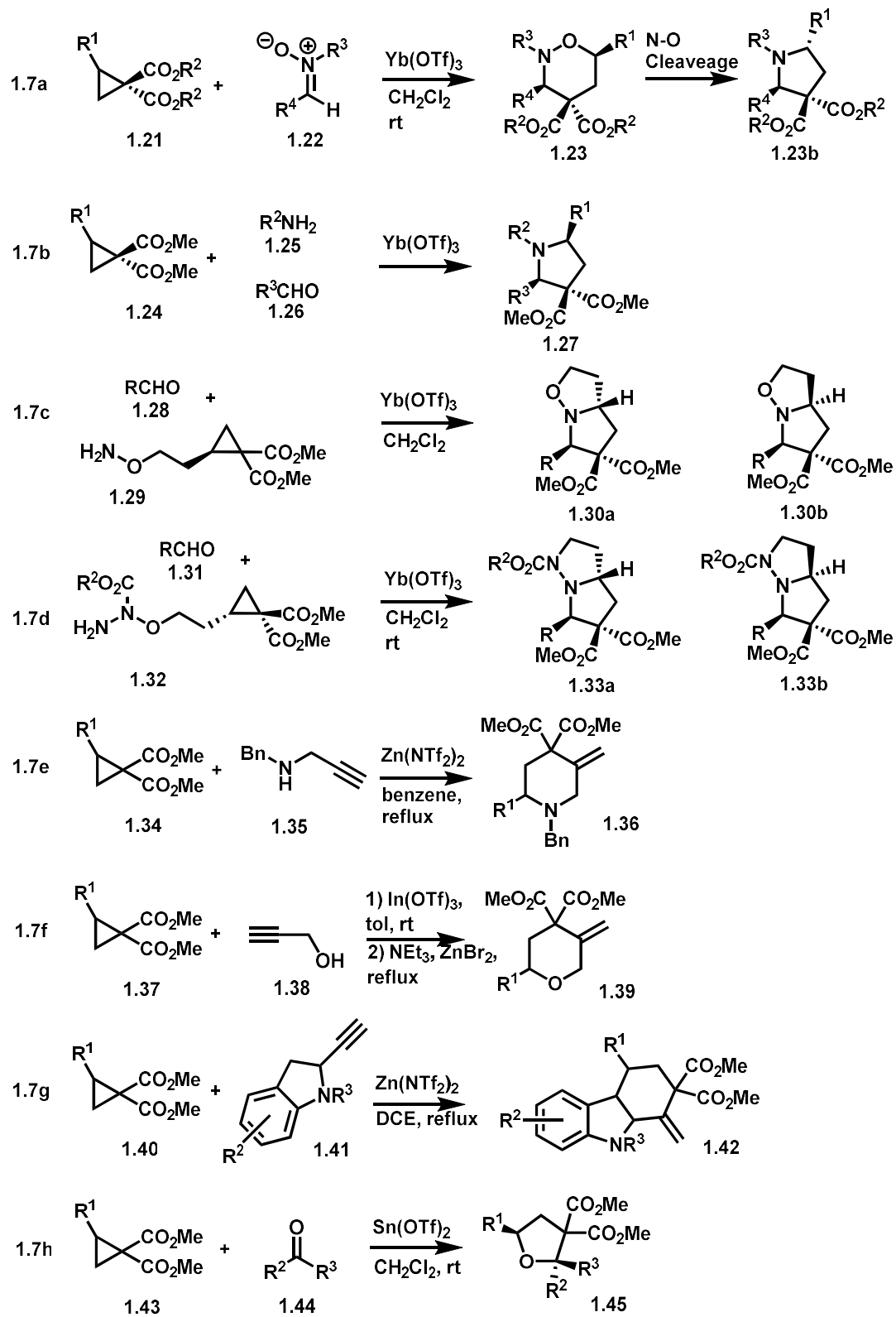
This reaction is a great comparison to the method developed in this thesis yielding similar adducts and using many of the same thiol nucleophiles. The results of Nolin's work act as an excellent comparison for the yield and scope results of this thesis. While the work in this thesis covers ring-opening reactions, DACs also undergo annulation

reactions. These reactions can occur when the substrate contains both an electrophilic and nucleophilic center. **Scheme 1.6** shows how the mechanism begins with a ring opening of the DAC **1.18** by the nucleophile **1.17**, this generates the ring open intermediate **1.19** with a negative charge. This new negative charge then attacks the electrophilic position that was part of substrate **1.17**, closing the ring and resulting in the new cyclic product **1.20**. In the cases where **1.17** contains a heteroatom (such as *N*, *O*, or *S*) then heterocycles will be synthesized.¹⁰



Scheme 1.6: DAC general annulation mechanism

Scheme 1.7 summarizes several possible transformations that can be accomplished through DAC annulation reactions. The Kerr group found that cyclopropane diesters **1.21** will react with nitrones **1.22** in a dipolar homo [3+2] cycloaddition to form tetrahydro-1,2-oxazines **1.23a** as shown in Scheme **1.7a**.¹¹ Nitron **1.22** may also be generated in situ by an aldehyde and hydroxylamine. These oxazine adducts may also undergo *N-O* cleavage to access pyrrolidines such as **1.23b**.¹² In scheme **1.7b**, cyclopropane diesters **1.24** react with imines that are generated in situ by amine **1.25** and aldehyde **1.26**.¹³ This reaction can access highly functionalized pyrrolidines **1.27**. Bicyclic heterocycle systems can also be built through intramolecular reactions such as schemes **1.7c** and **1.7d**. In scheme **1.7c** a cyclopropyl alkoxyamine **1.29** combined with aldehyde **1.28** gives an oxime ether that will in turn undergo an intramolecular annulation when treated with Lewis acid catalyst Yb(OTf)₃ to yield 2,5-trans-pyrroloisoxazolidines **1.30a**.¹⁴ It was found that if the order was reversed and the catalyst was added to alkoxyamine **1.29** followed by aldehyde **1.28** then the *cis* adduct **1.30b** will instead be synthesized. Similarly, the Kerr group also found that hydrazinoethyl cyclopropanes **1.32** would undergo intramolecular annulations in scheme **1.7d**.¹⁵

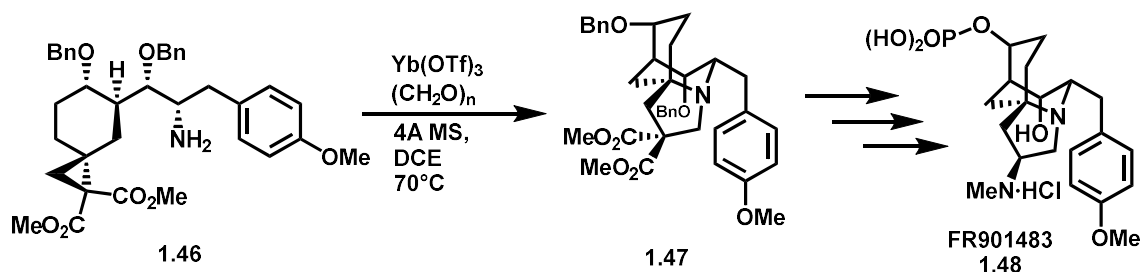
Scheme 1.7a-h: Annulation reactions of DACs¹¹⁻¹⁹

Cyclopropane **1.32** combined with aldehyde **1.31** and catalyst will yield bicyclo pyrazolidines **1.33a** and **1.33b**. Much like the work with oxime ethers, the trans **1.33a** and cis **1.33b** adducts can be accessed by adding the aldehyde before or after the catalyst, respectively. Schemes **1.7e** and **1.7f** show how cyclopropane diesters will react with propargyl amines **1.35** and propargyl alcohols **1.38** to yield piperidines **1.36** and tetrahydropyrans **1.39**, respectively.^{16,17} DAC chemistry with indoles has been demonstrated in the ring opening reaction section. **Scheme 1.7g** presents how cyclopropane diesters **1.40** will also undergo ring opening and subsequent conia-ene ring closure with 2-alkynyl indoles **1.41**.¹⁸ This approach allows DACs to be used as a building block for tetrahydro carbazoles **1.42**. Finally, in scheme **1.7h**, Johnson's work with aldehydes gives another example of oxygen heterocycles possibilities.¹⁹ Cyclopropane diesters **1.43** activated by Lewis acid catalyst will perform a cycloaddition reaction with aldehydes **1.44** to give substituted tetrahydrofurans (THF) **1.45**. These reactions demonstrate the wide range of transformations possible with DAC chemistry and provide an understanding of their importance in the development of total synthesis strategies.

1.3. Natural Product Targets of Donor-Acceptor Cyclopropanes

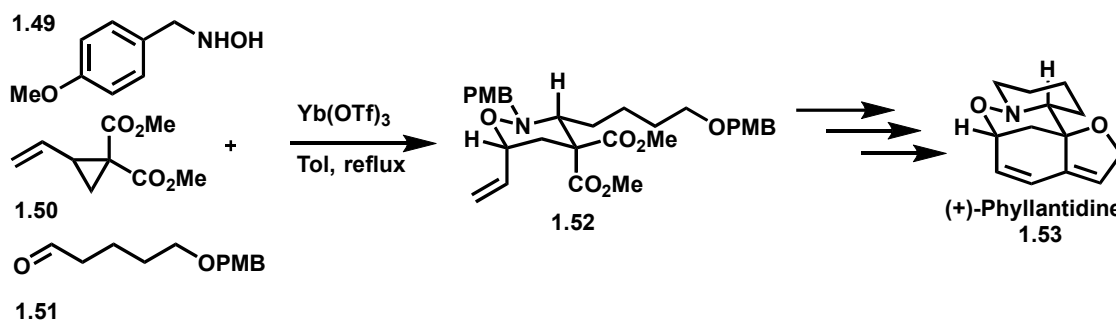
A large reason for the interest in DACs is their synthetic application to natural product targets. Many of these natural products and pharmaceutically relevant targets are based around heterocycles, approximately 80% of approved drugs contain one in them.²⁰ Additionally, 59% of drugs contain a heterocycle that includes nitrogen in it such as the commonly seen indole heterocycle.²⁰ DACs allow many opportunities for the addition or synthesis of various heterocycles. Annulation reactions of DACs are specifically useful in the synthesis of natural products, allowing for efficient construction of heterocycle cores. The Kerr group has taken advantage of DACs as synthetic building blocks in the pursuit of several natural product targets. The first of these natural products is FR901483 **1.48**, an immunosuppressive alkaloid with a complex tricyclic core making it an interesting target for synthetic chemists. The key step (**Scheme 1.8**) of the synthetic pathway relies on an intramolecular annulation forming the pyrrolidine

ring at the core FR901483.²¹ Cyclopropane **1.46** is added to paraformaldehyde and $\text{Yb}(\text{OTf})_3$, generating an imine in situ from the amine group on **1.46** that then undergoes an intramolecular annulation to form the pyrrolidine ring in **1.47**. With several more modifications, FR901483 **1.48** is synthesized in a total of 18 steps.



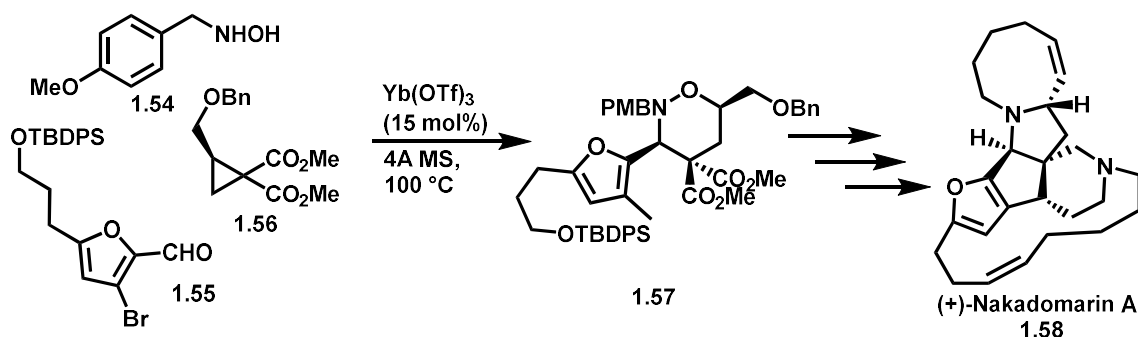
Scheme 1.8: Total synthesis of FR901483 pyrrolidine formation

The synthesis of (+)-phyllantidine **1.53** poses a great synthetic challenge due to the tetrahydro-1,2-oxazine structure at its core, a heterocycle that has few methods to directly synthesize.²² Kerr group took advantage of their work done with nitrones and DACs to prepare these structures and applied the reaction in the key step of synthesizing the core of this compound (Scheme 1.9). The synthesis begins with 3 components, hydroxylamine **1.49** and aldehyde **1.51** first form a nitron in situ which then undergoes an annulation reaction with vinyl diester cyclopropane **1.50**. Through this strategy, the tetrahydro-1,2-oxazine core **1.52** is built in one step from 3 similarly sized starting components. This led to the first synthesis of (+)-phyllantidine in 6 % yield over 12 steps.



Scheme 1.9: Total synthesis of (+)-phyllantidine tetrahydro-1,2-oxazine formation

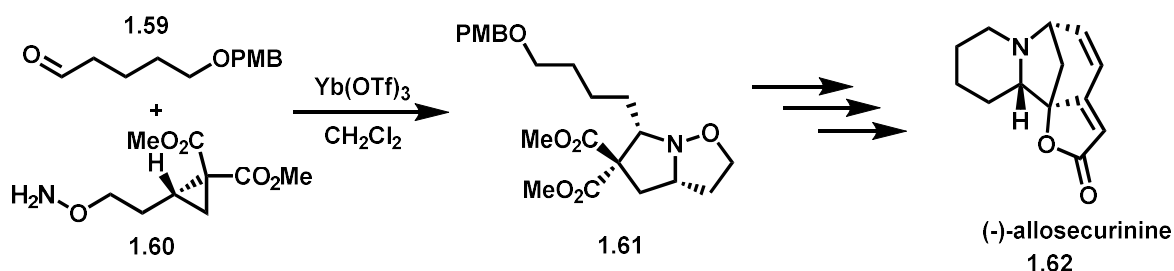
(+)-nakadomarin A **1.58** uses a similar strategy to that as seen in the (+)-phyllantidine synthesis. Initial study of this complex alkaloid showed the potential of bioactivity such as inhibiting a cyclin-dependent kinase associated with several types of cancer as well as antimicrobial activity.²³ Synthesizing this compound allows easier access to material for running further studies on the molecule's anticancer, antifungal, and antibacterial properties. The key step of this total synthesis shown in **Scheme 1.10** once again takes advantage of the nitron and DAC annulation method to construct its core. Hydroxylamine **1.54** and furyl aldehyde **1.55** form a nitron that then with the addition of cyclopropane **1.56** completes an annulation reaction giving tetrahydro-1,2-oxazine **1.57**. In this case, this heterocycle is not part of the natural product but instead used as a pathway by reductive *N-O* cleavage to the pyrrolidine ring present in (+)-nakadomarin A **1.58**. This strategy synthesizes **1.58** in a more direct pathway than previously reported syntheses accomplishing it in 22 steps.



Scheme 1.10: Total synthesis of (+)-nakadomarin A tetrahydro-1,2-oxazine formation

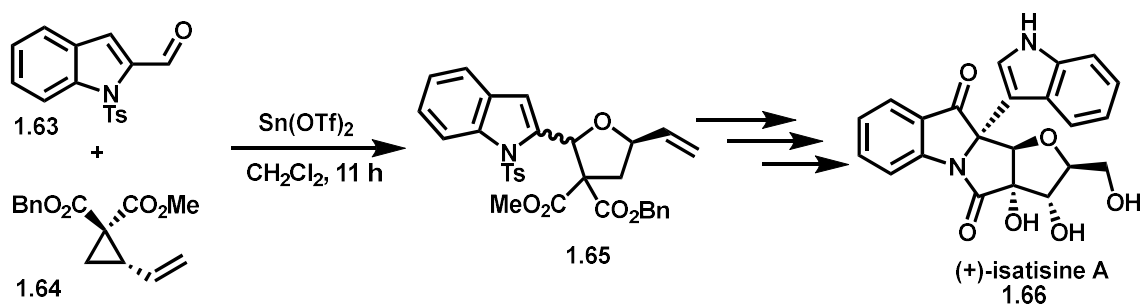
(-)-Allosecurinine **1.62** is an alkaloid from the family of securinega alkaloids, most of which share a unique azabicyclo [3.2.1] ring system at their core.²⁴ This structural feature along with the biological activity of the compounds in this family make for an excellent synthetic target. In **Scheme 1.11** the key step of the synthesis makes use of the work done by the Kerr group on intramolecular annulations with oxime ethers to selectively build cis and trans pyrrolidines. The synthesis begins with the addition of Yb(OTf)₃ to cyclopropane **1.60**, followed by aldehyde **1.59** to generate the oxime ether in situ for annulation. Aldehyde **1.59** is added following the catalyst to selectively

synthesize the cis isomer of pyrroloisoxazolidine **1.61**. This strategy resulted in the successful synthesis of (-)-allosecurinine in just 15 steps with an overall yield of 5%.



Scheme 1.11: Total synthesis of (-)-allosecurinine pyrroloisoxazolidine formation

The last of these total synthesis strategies shown is for (+)-isatisine A **1.66**, an alkaloid found in the Chinese shrub *Isatis indigotica*. The acetone derivative isolated after processing the shrub's leaves has shown anti-HIV-1 activity.²⁵ The biological activity of (+)-isatisine A itself however could not be determined with the limited amount of product produced through this route. Developing a synthetic pathway for this compound would give material to run further biological testing. The synthesis relies on the cycloaddition of an aldehyde to DAC to construct the tetrahydrofuran ring at the compound's core. **Scheme 1.12** illustrates the key reaction, where vinyl cyclopropane **1.64** activated by Sn(OTf)₂ is combined with indole-2-carboxaldehyde **1.63** performing a cycloaddition that results in the tetrasubstituted tetrahydrofuran **1.65**. This approach allowed for the synthesis of (+)-isatisine A in 14 steps with an overall yield of 6%.²⁵



Scheme 1.12: Total synthesis of (+)-isatisine A tetrahydrofuran formation

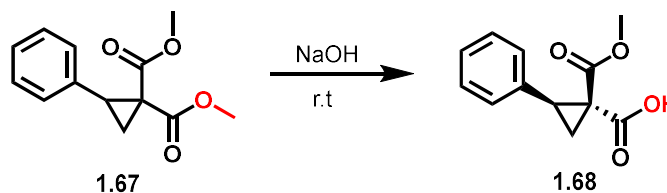
These natural product targets give examples of the practical applications of DAC chemistry and their importance as unique building blocks. In these reactions, the use of

many Lewis acid catalysts is observed. The next section will instead discuss an alternate method of DAC activation, and how the Kerr group is involved in this area.

1.4. Donor-Acceptor Cyclopropane Activation by Hydrogen Bond

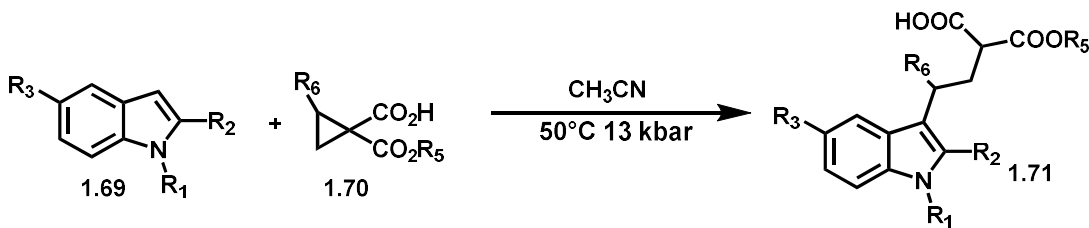
Donor

A more recent area of interest in the study of DAC methodology is the use of hydrogen bond donors in place of metal-based catalysts to activate the DAC in a similar way to Lewis acid catalysts. In recent work by the Kerr group, it was shown that the simple saponification of the diester DAC **1.67** could convert one of the esters to a carboxylic acid, this is referred to as the hemimalonate DAC **1.68**.²⁶



Scheme 1.13: Conversion of diester DAC to hemimalonate

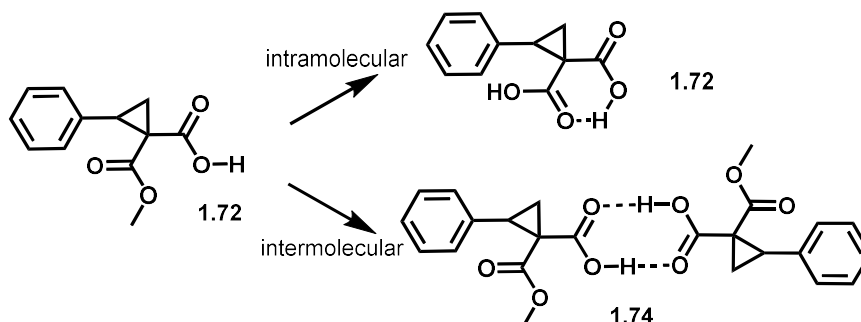
This discovery was of great interest as the hemimalonate DAC showed increased reactivity compared to the diester DAC. The Kerr group found in this work that the hemimalonate DAC **1.70** could undergo a ring-opening addition using indoles **1.69** as the nucleophile in the absence of a catalyst (**Scheme 1.14**).



Scheme 1.14: Hemimalonate DAC ring opening with indoles by Kerr²⁶

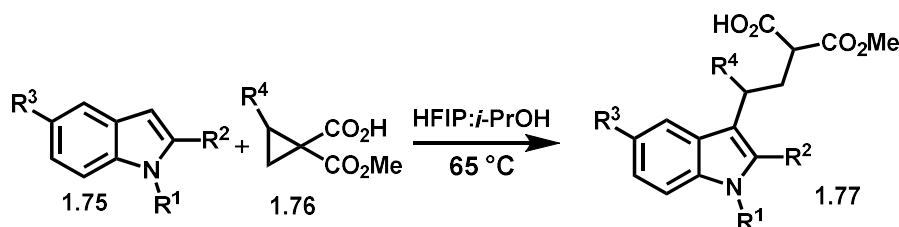
This hemimalonate DAC is hypothesized to undergo intra- and/or inter-molecular hydrogen bond activation through its acid group as shown in **Scheme 1.15**, causing

increased electrophilicity at the donor group carbon. This is supported by a downfield shift on that carbon of ~ 8 ppm from the diester observed in the ^{13}C NMR spectrum.



Scheme 1.15: Hypothesized hydrogen bonding between hemimalonate DAC carboxylic acid groups

Building off this, the Kerr group set out to further take advantage of this hydrogen bonding activation through the addition of an external hydrogen bond donor. While many possible compounds would fit this description, fluorinated alcohols proved to be extremely effective thanks to strong electron-withdrawing trifluoromethyl groups. Introducing 1,1,1,3,3,3-hexafluoroisopropanol (HFIP) as a cosolvent in **Scheme 1.16** allowed the hemimalonate DAC **1.76** to undergo ring opening reactions with indoles **1.75**.²⁷ Compared to the previous ring openings with indole nucleophiles, this reaction proceeded under more mild conditions.

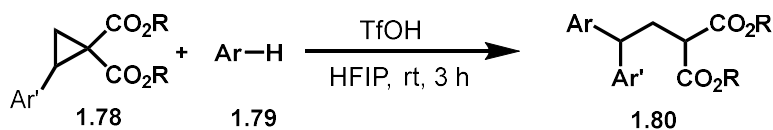


Scheme 1.16: DAC ring opening activated by hydrogen bond donor solvent

This method is exciting because besides having activation rely on the solvent instead of a metal catalyst it also can be done at atmospheric pressure and mild heating.

In similar work, Moran also introduced HFIP as a hydrogen bond donor alternate to metal catalysts, in this case along with a catalytic amount of trifluoromethanesulfonic

acid (TfOH). Here they were able to ring open diester DACs **1.78** with several aryl groups **1.79** and select other nucleophiles (**Scheme 1.17**).²⁸



Scheme 1.17: DAC ring opening using TfOH-HFIP hydrogen bond donor system

These select reactions are closely related to the work in this thesis as this research revolves around the study of the hemimalonate DAC and its reactivity through activation by HFIP as a hydrogen bond donor. Through the substitution of a hydrogen bond donor solvent for metal-based Lewis acid catalysts, harmful and expensive metal compounds can be avoided in these reactions. HFIP does belong to the family of polyfluoroalkyl substances (PFAS) which can have harmful effects on the environment due to their slow degradation.²⁹ HFIP specifically is not of current environmental concern due to the quantity it is produced in, but should still be collected with a rotary evaporator and chilled collection flask to avoid release into the environment. HFIP is known to cause skin and eye irritation but otherwise has low acute toxicity. In fact, Sevoflurane is an inhaled fluorinated anesthetic that metabolizes to HFIP in the body.³⁰ Majority of this HFIP then coordinates to glucuronic acid to be excreted in urine.

1.5. NMR Spectroscopy Titration Studies

In the first section of this thesis, the HFIP-DAC system was studied further through mechanistic experiments. The binding of the DAC to HFIP or Lewis acid is a host-guest system where the level of activation observed in the DAC is based on the strength of association and ratio of the host-to-guest molecule. NMR spectroscopy is one method that can be used to study host-guest interactions. This is done by gathering spectra of varying host-to-guest ratios and observing the change in chemical shift of the same target in a molecule³¹. A host-guest system can be seen as either a fast exchange or a slow exchange system. In a slow exchange system, the rate of association and dissociation is quite slow and therefore if we are to observe the complex with NMR spectroscopy separate peaks would be present for the free host and complexed host

molecules such as modeled in **Figure 1.4**. In fast exchange, the rate is very rapid, and therefore instead of observing separate peaks, a single peak with a weighted average shift of the free host and complexed host chemical shift is seen such as in **Figure 1.5**.³²

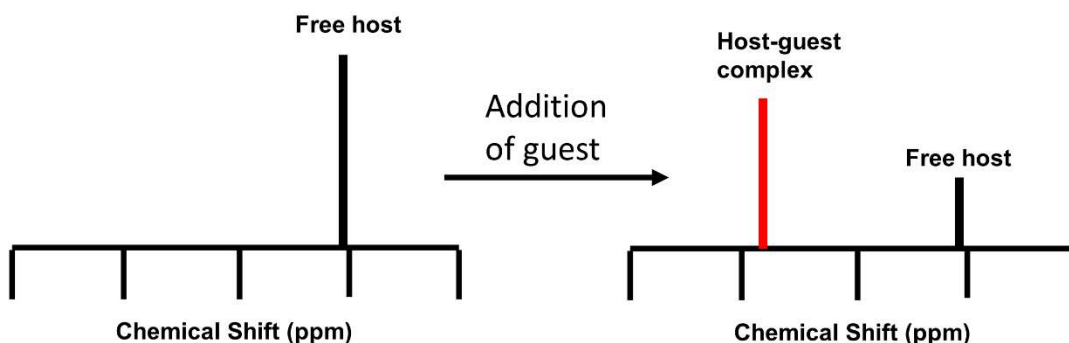


Figure 1.4: Slow exchange host-guest NMR spectra model

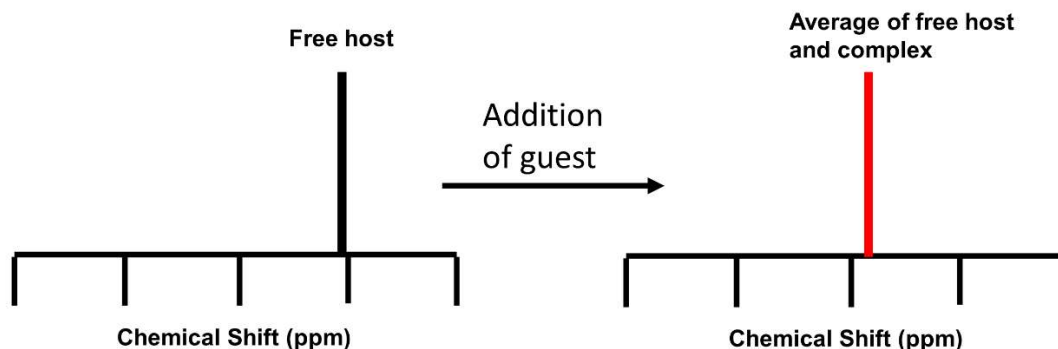


Figure 1.5: Fast exchange host-guest NMR spectra model

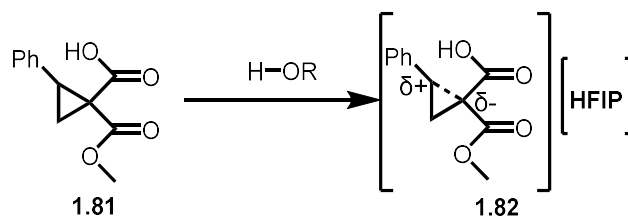
Since the interaction between host and guest in the case of DAC and HFIP is a hydrogen bond this is expected to be a fast exchange system. The resulting data from the titration experiment can be plotted as chemical shift vs. mol equivalents of guest molecule added. The resulting curve shows the average chemical shift of the target peak moving closer to the chemical shift for the molecule in a completely complexed form as the host becomes increasingly saturated with guest molecules. This curve can then be fit

to solve for the unknown association constant K and the chemical shift of the target peak in the host-guest complex δ_c .

1.6. ^{13}C NMR Spectroscopy Studies of Donor-Acceptor

Cyclopropanes

NMR spectroscopy titrations to study host-guest interactions are normally done using ^1H NMR spectra. The same theory also applies to ^{13}C spectra which was used in the work reported in this thesis. In this case, the electron density around carbon centers can be observed as binding between host and guest takes place. Through the introduction of the hydrogen bond donor, increased DAC reactivity is observed due to the formation of a hydrogen bond that pulls electrons away from the cyclopropane ring like in **1.82**. This weakens the bond between donor and acceptor groups as shown in **Scheme 1.18**.



Scheme 1.18: Activation of DAC with a hydrogen bond donor

The pull of electron density away from the ring causes the site of nucleophilic attack, donor group carbon, to be increasingly electrophilic as the molecule more closely resembles a 1,3 zwitterion. This change can be observed using NMR spectroscopy as a decreasing electron density around a nucleus will cause it to shift further downfield. Waser demonstrates this very well while studying a new donor group installed on a DAC.³³ The paper focuses on the introduction of a triazene donor group, shown on the far left of **Figure 1.6**, while also comparing other possible and past studied donor groups. The figure shows the chemical shift of the carbon with the R donor group (C^2), the carbon that is most electrophilic in the DAC, and the shift further downfield is related to its shift towards increased electrophilicity. This work used the carbon NMR spectroscopy data to show the increased electrophilicity of the C^2 position when

substituted with the triazene donor group. The same idea can be applied to adding a catalyst or a hydrogen bond donor to affect the electrophilic nature of the C² position.

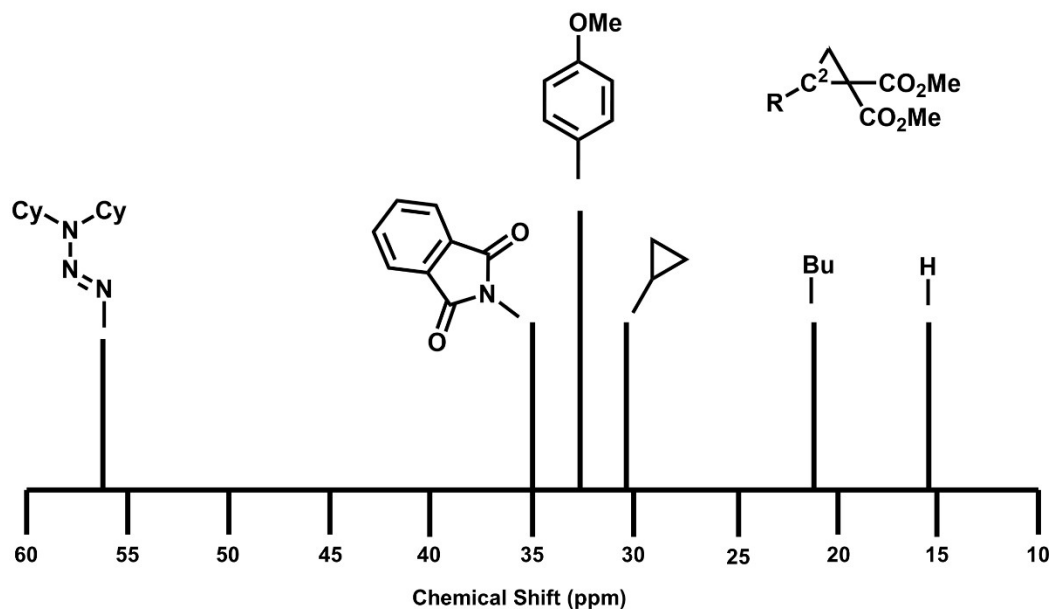
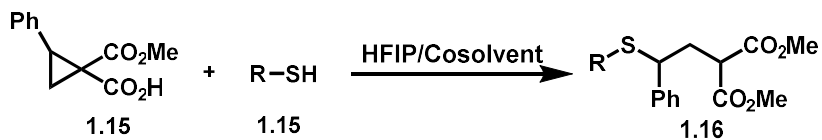


Figure 1.6: ¹³C NMR study of DAC donor groups, modified from Waser³³

1.7. Purpose of Thesis

The aim of the work reported in this thesis is broken into two main sections revolving around the hemimalonate DACs activation through HFIP as a hydrogen bond donor. First, ¹³C NMR spectroscopy was used to conduct titrations on the host-guest interaction between the DAC and HFIP. This provided data on the strength of binding between the two and allowed visualization of the electronic effects on the DAC from association. This data supports the previously found optimal ratio of HFIP to use in reactions based on the observed plateau in HFIP's effect on the DAC's chemical shift. A similar titration experiment was then conducted with a metal catalyst commonly used in the field of DAC chemistry. HFIP and catalyst titration results were then compared to determine if HFIP can match or surpass the ability of these catalysts to activate DACs. A benchmark of metal catalyst mol% was set based on similar methods in the field. The second section of this thesis probes the reactivity of the hemimalonate DAC to further expand the range of nucleophiles that can be used in ring-opening reactions.

Thiols were selected as the nucleophile of interest in this work and a reaction for their use as nucleophiles with the hemimalonate DAC was optimized (**Scheme 1.19**). A variety of thiols and substituted thiophenols were used to test the limits of the reaction. The yields were competitive with similar reactions found in the literature.⁹



Scheme 1.19: Proposed reaction scheme for DAC ring-opening addition with thiols

2. Results and Discussion

2.1. NMR Spectroscopy Titrations

NMR spectroscopy titrations allow us to observe the change in chemical shift values of compounds forming a complex together at varying concentrations and equivalent ratios. This method was used in the first section of work reported in this thesis to study the association between DACs and HFIP.

2.1.1. Methodology of Titrations

The first step in this method was to determine a target carbon site to track through the titration. DACs contain electrophilic and nucleophilic carbon positions thanks to their substituents that through catalyst activation have increasingly polarized character, therefore these two carbons ideally should show the largest change in chemical shift. The electrophilic carbon was selected as it is generally the primary reactive site in these molecules as well as it is a tertiary center in the studied DAC as opposed to the quaternary nucleophilic center which could be more difficult to observe in ^{13}C NMR. This carbon center **C2** is the same studied in work by Waser discussed previously (**Figure 1.6**) and indicated again in **Figure 2.1**.³³

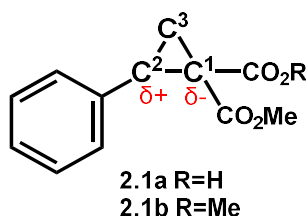


Figure 2.1: DAC carbon centers labeled

To determine the peak associated with this carbon an HSQC experiment was run with both pure DAC and a DAC/HFIP mixture of approximately 100 mol equivalents HFIP. The peak for **C2** was identified in the ^{13}C spectra at 39-44 ppm (parts per million) depending on the amount of HFIP added and DAC concentration. The **C2** peak had no other carbon peaks overlap in that region which made for simple identification. A proof-of-concept trial was done with the hemimalonate DAC and HFIP (mol

equivalents:0,1,2,3,5,10,20,50) and the stacked plot in **Figure 2.2** was generated. The downfield shift observed upon HFIP addition is indicative of increased electrophilic character.

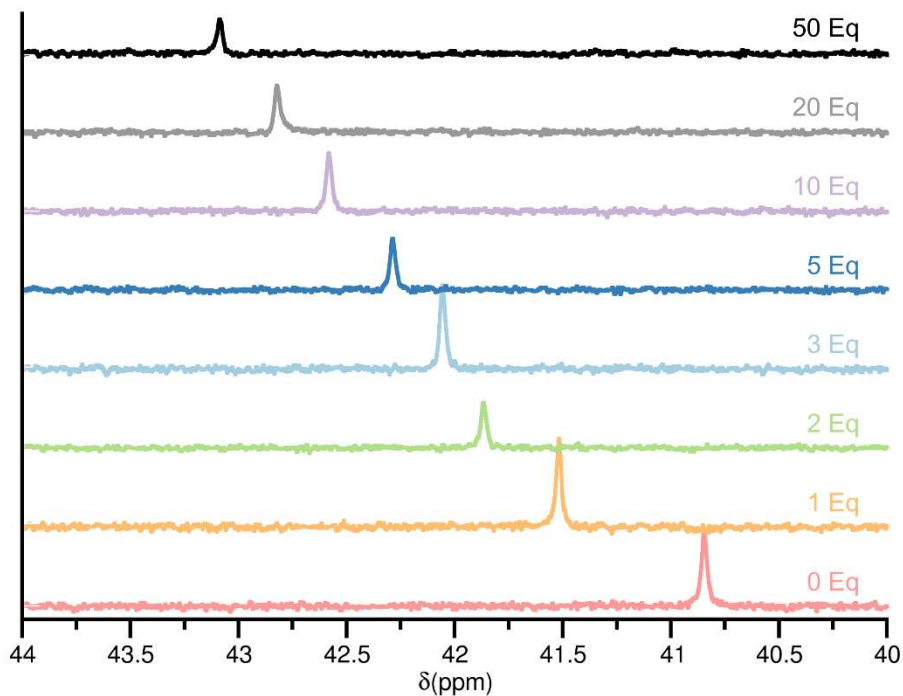


Figure 2.2: Chemical shift of C2 in hemimalonate 2.1a at varying mol equivalents of HFIP

2.1.2. Methodology of Fitting Titration Data

Following the results of the trial titration, the next step was to expand the data set to include more ratios of HFIP to DAC then plot and fit the data. Using that data an association constant between HFIP and the DAC can then be determined. First, the type of host-guest system must be determined. In the initial titration data, one C² peak is observed that gradually shifts with increasing amounts of HFIP added. As discussed previously this is indicative of a fast exchange system. This means the chemical shift of completely complexed DAC is unknown without saturating the system with an extreme ratio of HFIP, however, this too can be calculated by fitting the titration data. The stoichiometry of the association must also be determined to accurately fit the data and it was found that the simplest method to do this was to utilize a Jobs plot.³⁴ A Jobs plot is

an effective way to confirm a 1:1 stoichiometric ratio between the host and guest however it is not a dependable method to determine other host-to-guest ratios such as 2:1 systems. For the Jobs plot experiment, another ^{13}C NMR Spectroscopy titration was run but with the difference of keeping the combined concentration of host and guest the same and instead varying the ratios of both (0.1 mol fraction intervals from 0.1-1 DAC). After collecting the observed chemical shift for each mol fraction of host and guest, **Equation 1** was used to determine the concentration of host-guest complex at each data point³⁵. The $\delta_{H_m G_n}$ term representing the chemical shift of the host-guest complex must be estimated based on previous titration data since this value is unknown.

$$[H_m G_n] = \frac{\Delta\delta[H]_0}{\delta_{H_m G_n} - \delta_h} \quad \text{Eq. 1}$$

$[H_m G_n]$ = concentration of DAC (H) HFIP (G) complex of stoichiometric ratios 'm' and 'n'. $\Delta\delta$ = difference between observed chemical shift and chemical shift of free DAC. $[H]_0$ = initial concentration of free DAC. $\delta_{H_m G_n}$ = chemical shift of DAC when complexed to HFIP. δ_h = chemical shift of free DAC.

If the maximum concentration of complexed host-guest aligns with the point where there is an equal initial concentration of host and guest (mol fraction $f_h = 0.5$), then there is 1:1 stoichiometry for the complex. In this case for the DAC-HFIP association, this maximum at $f_h = 0.49$ is observed in **Figure 2.3** which indicates 1:1 stoichiometry.

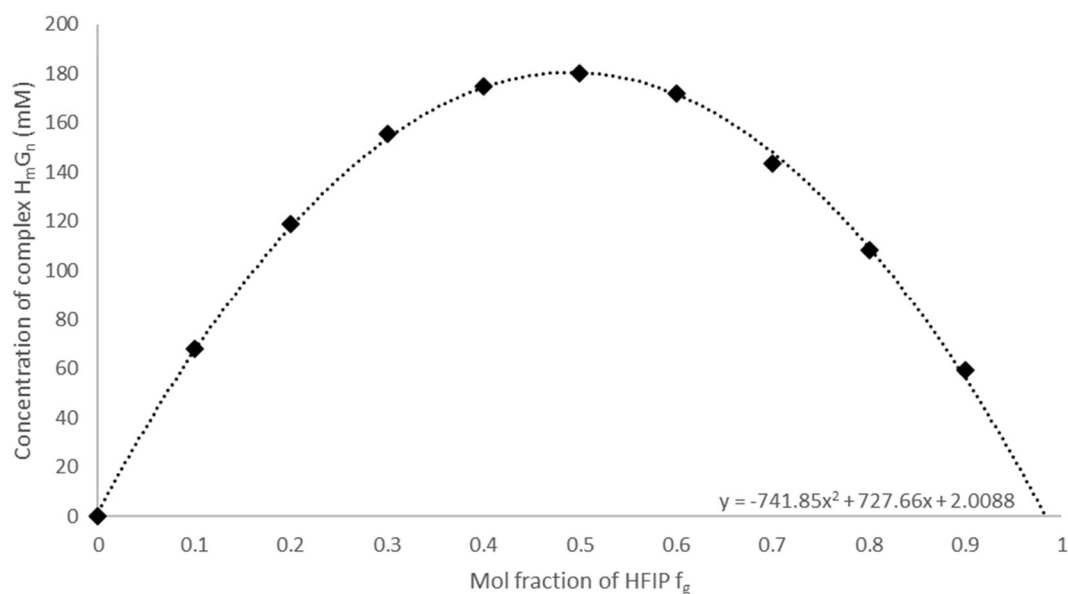


Figure 2.3: Jobs plot for hemimalonate 2.1a and HFIP

This means that the association constant will be determined by **Equation 2**, and from this, our fitting formula can be derived.

$$K = \frac{[H_1G_1]}{[H][G]} \quad \text{Eq. 2}$$

Equation 2 can be rewritten with **[H]** and **[G]** replaced by the difference from initial concentrations (**[H]₀** and **[G]₀**) and concentration of the complex (**[C]** replaces **[HG]**) giving **Equation 3**.

$$K = \frac{[C]}{([H]_0 - [C])([G]_0 - [C])} \quad \text{Eq. 3}$$

Substituting **[C]** for **n_c[H]₀**, where **n_c** is the mol fraction of complexed host, and introducing **R** as the mol ratio of guest to host (**[G]₀/[H]₀**) allows this equation to be rewritten as quadratic **Equation 4**.

$$K = \frac{n_c/[H]_0}{(1-n_c)(R-n_c)}$$

$$n_c^2 - \left(1 + R + \frac{1}{K[H]_0}\right)n_c + R = 0 \quad \text{Eq. 4}$$

Equation 5 is the root of this quadratic equation, defined in terms of **b** which is shown in **Equation 6**.

$$n_c = \frac{b - \sqrt{b^2 - 4R}}{2} \quad \text{Eq. 5}$$

$$b = 1 + R + \frac{1}{K[H]_0} \quad \text{Eq. 6}$$

To set the equation as a function of the observed chemical shift values that are gathered in the titrations, n_c must be substituted. Since this is a fast exchange system, only a single weighted average peak of complex and free DAC will be observed. This observed chemical shift (δ_o) can be defined by **Equation 7** where n_h and n_c are mol fractions of host and complex, and δ_h and δ_c represent the chemical shift of host and complex, respectively.

$$\delta_o = n_h \delta_h + n_c \delta_c \quad \text{Eq. 7}$$

Equation 7 can be rewritten as a function of n_c by substituting $n_h = 1 - n_c$ to yield **Equation 8**.

$$n_c = \frac{\delta_h - \delta_o}{\delta_h - \delta_c} \quad \text{Eq. 8}$$

Inserting **Equation 8** into **Equation 5** and rearranging to isolate the observed chemical shift will yield our equation for fitting the titration data **Equation 9** where **b** is defined by **Equation 6** ($\Delta\delta = \delta_h - \delta_c$).

$$\delta_o = \delta_h - \left(\frac{\Delta\delta}{2}\right) \left(b - \sqrt{b^2 - 4R}\right) \quad \text{Eq. 9}$$

A titration with a larger data set was then conducted and the newly derived fitting formula was applied. **Figure 2.4a** presents the stacked carbon spectra zoomed in on the C2 peak of the DAC as well as the plot of chemical shift vs. HFIP equivalents with the fitting curve in **Figure 2.4b**.

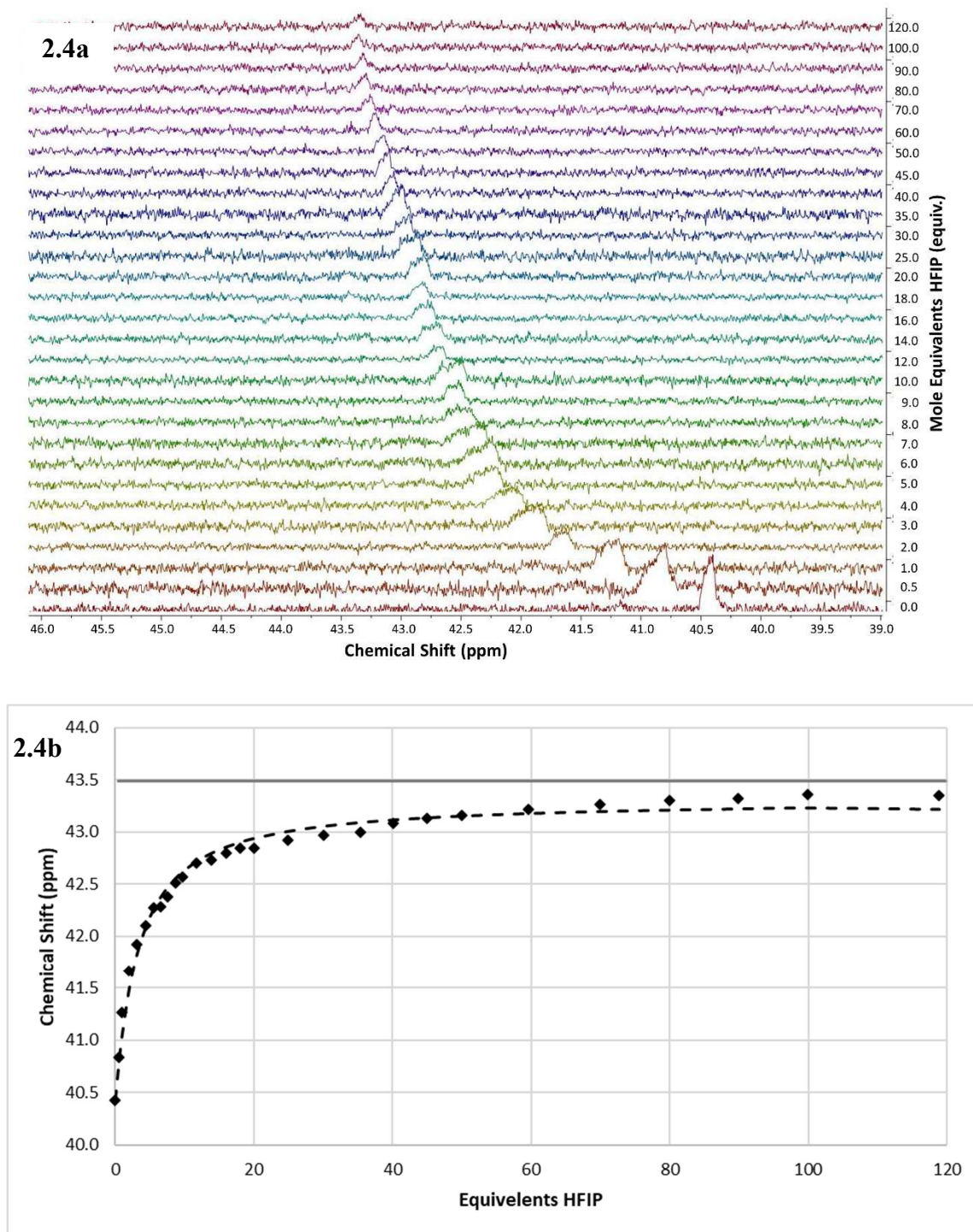


Figure 2.4: Stacked ^{13}C Spectra (2.4a) and initial fitting of expanded data set (2.4b)

It was observed that there was a repeating error pattern between the observed and calculated chemical shifts. The calculated data fit below the experimental data then

above and then below again. The proposed reason for this pattern was that this hemimalonate DAC-HFIP complex was not 1:1 but 2:2 stoichiometry. This is due to the dimerization of the DACs through their carboxylic acid groups (**Figure 2.5**), and therefore more states of the complex are possible such as 2 DAC to 1 HFIP. The solution to this issue was to run a dilution titration to determine what concentration was low enough to limit the interaction between DACs so that the effect on chemical shift was negligible. For this titration, the chemical shift of C^2 was collected at different DAC concentrations from 1 M to 1 mM (**Figure 2.6**). This was performed in the absence of HFIP to isolate the DAC's intermolecular effects. In the plotted data the beginning of a plateau is observed at very low concentrations. This data set would have been expanded to lower concentrations to provide more conclusive results, however, the signal-to-noise ratio became too high to run carbon spectra in a reasonable timeframe. Therefore, this led to the selected concentration for titration experiments being 5 mM DAC.

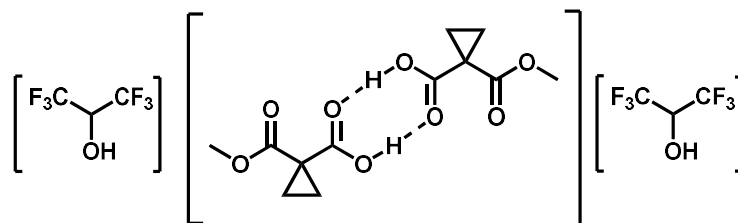


Figure 2.5: Dimerization of hemimalonate 2.1a in 2:2 complex with HFIP

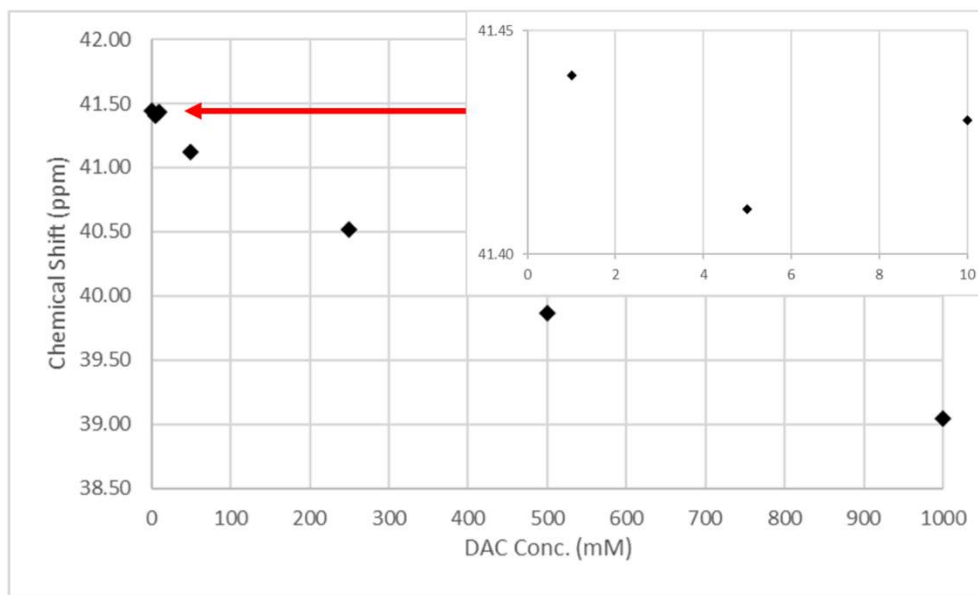


Figure 2.6: Hemimalonate 2.1a dilution experiment

2.1.3. HFIP Titration of Hemimalonate and Diester DAC

The first question to address was how HFIP interacts with the hemimalonate DAC vs the diester DAC. All titrations were run on a 600MHz NMR spectrometer. Titrations of the DACs were run with HFIP mol equivalents ranging from 0-100. Data points were collected in higher density between 0-10 equivalents as this is where the most rapid change occurs, 22 data points were collected in total. These titrations were plotted in **Figure 2.7** and **Figure 2.8** for the hemimalonate and diester DACs, respectively. Applying the fit to these plots reveals that the dilution experiment results proved successful as a significantly tighter fit is now achieved between experimental data and curve.

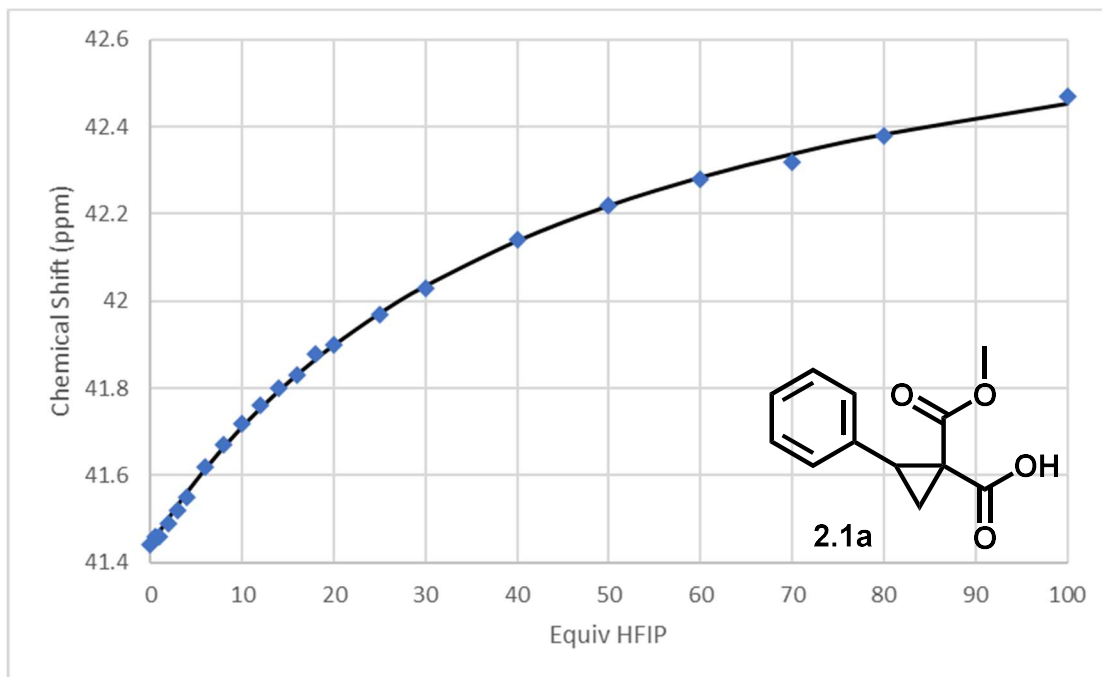


Figure 2.7: Hemimalonate 2.1a and HFIP titration. Blue points represent experimental data, black line represents the calculated fit

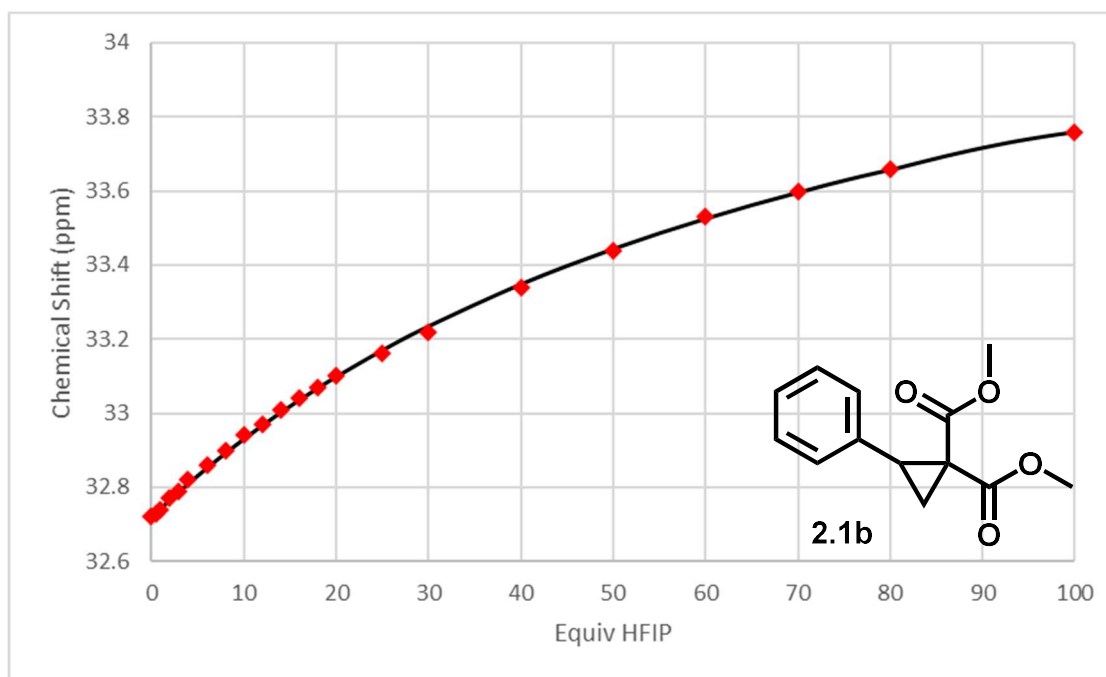


Figure 2.8: Diester 2.1b and HFIP titration. Red points represent experimental data, black line represents the calculated fit

The first observation to note is that the hemimalonate DAC in the absence of HFIP has a C2 position with a chemical shift of 41.44 ppm vs the diester's 32.72 ppm. Similar to the experiment done by Waser, this illustrates how this change to the carboxylic acid substituent increases the electrophilic nature of the C2 position. This observation supports previous observations of the hemimalonate's increased reactivity, such as reacting without a catalyst, unlike the diester. Using equations 9 and 6 an observed chemical shift value was calculated for each R data point (ratio of HFIP to DAC) collected in the titration. A least squares method was used with the Microsoft Excel solver program to best fit the calculated and experimental chemical shifts by manipulating unknowns K and δ_c . For the hemimalonate $K = 4.7 \times 10^{-3} \text{ M}^{-1}$ and $\delta_c = 42.88 \text{ ppm}$ and for the diester $K = 2.6 \times 10^{-3} \text{ M}^{-1}$ and $\delta_c = 34.55 \text{ ppm}$.

2.1.4. Comparison with Metal Catalyst Titration

To compare the effectiveness of HFIP as a method of activation to the more commonly used Lewis acid catalyst methods, similar titration experiments needed to be run using one of these catalysts. There are many examples of Lewis acid catalyst use with DACs, for this experiment the goal was to find a Lewis acid catalyst that was both relatively inexpensive and commonly used in similar reactions so a reasonable mol percent benchmark could be determined. Scandium triflate ($\text{Sc}(\text{OTf})_3$) was selected as a good comparison for both these reasons. A recent example of scandium triflate's use in DAC chemistry is found in a methodology paper by More.³⁶ In this work a diethyl ester DAC **2.2** was used for the ring opening addition with sulfoximine **2.3** nucleophiles (**Scheme 2.1**). Following testing of other Lewis acid catalysts such as bismuth and ytterbium triflate, 10 mol% $\text{Sc}(\text{OTf})_3$ was selected to catalyze this reaction with yields up to 94%. While this is only one example, many other procedures using $\text{Sc}(\text{OTf})_3$ use between 5

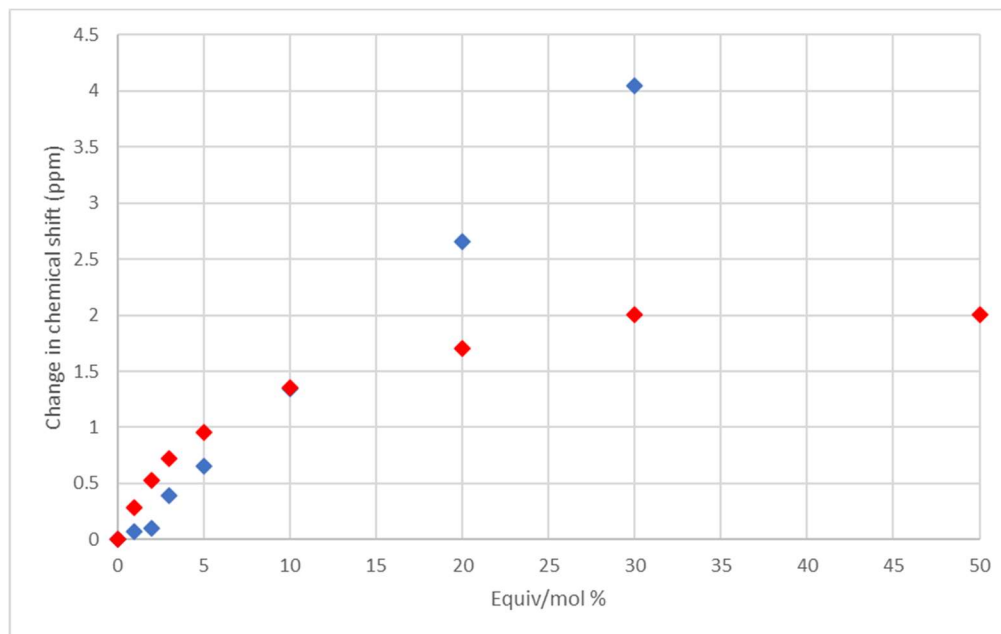


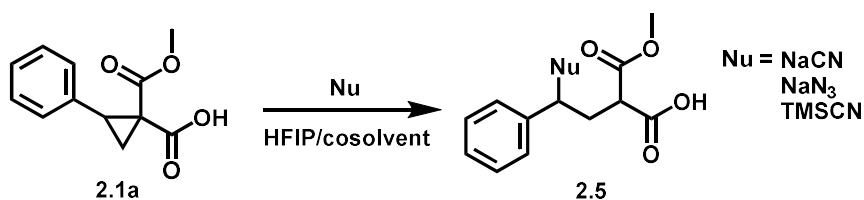
Figure 2.10: ^{13}C NMR titration of diester 2.1b with $\text{Sc}(\text{OTf})_3$. Blue represents Sc titration data, red shows HFIP titration data

Red data points were used for HFIP and are using the x-axis scale in equivalents of HFIP. Blue data points were used for $\text{Sc}(\text{OTf})_3$ and are using the x-axis scale in mol percent $\text{Sc}(\text{OTf})_3$. Since HFIP is a solvent usually used in >20 equivalents and $\text{Sc}(\text{OTf})_3$ catalyst is used in mol percent amount, generally 10%, two different units are used on the x-axis to give a more practical comparison. In both cases, it is observed that $\text{Sc}(\text{OTf})_3$ has a stronger effect on the DACs than HFIP, especially if equal molar amounts of the two are considered. While $\text{Sc}(\text{OTf})_3$ potentially could have a stronger effect, the practical 10 mol% used in DAC ring-opening reactions was shown to cause a change in chemical shift of about 1.1 ppm on the hemimalonate and 1.3 ppm on the diester. In comparison, this change in chemical shift can be achieved with 5 equivalents of HFIP with the hemimalonate or about 10 equivalents with the diester. This is important to note as the method used previously by the Kerr group and in this work around 25 equivalents of HFIP are used. In running these experiments it was observed that the solubility of $\text{Sc}(\text{OTf})_3$ was fairly poor, as reported in similar studies.³⁷ Other solvents were tested to address this solubility problem but the HFIP system did not function properly in those conditions. Additionally, $\text{Sc}(\text{OTf})_3$ caused a lower signal-to-

noise ratio at low concentrations. For this reason, the data gathered in **Figure 2.9** and **Figure 2.10** were run using a DAC concentration of 100 mM. This meant the dimerization effect would be more prominent but I was mainly interested in the direct comparison between HFIP and $\text{Sc}(\text{OTf})_3$ rather than the fit for this study.

2.2. Ring Opening Reactions with Thiol Nucleophiles

Following the previous work done by the Kerr group on the hemimalonate cyclopropane ring opening catalyzed by HFIP and using indole nucleophiles, this work set out to determine what other nucleophiles were compatible with this method. Some earlier work looked at cyanide and azide-based nucleophiles to ring open the hemimalonate DAC. The sodium salts of both were first tested under the indole ring opening conditions which resulted in no indication of the intended product. Trimethylsilyl cyanide was also selected as a potentially better alternative for introducing the cyanide nucleophile into the system which uses organic solvents but again was unsuccessful. In a similar mindset, a phase transfer catalyst tetrabutylammonium iodide was employed in addition to the sodium cyanide and azide salts to make the ions more compatible with the organic system.

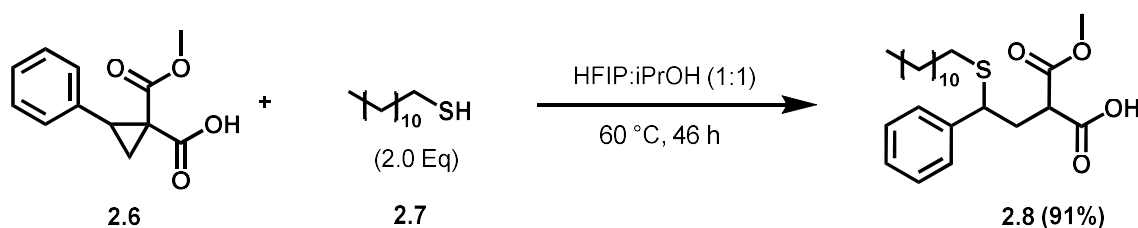


Scheme 2.2: Proposed nucleophiles for hemimalonate DAC ring opening

None of these reagents yielded the intended adduct, as summarized in **Scheme 2.2**, and therefore were set aside as potential nucleophiles. Attention was turned to thiol nucleophiles, as the work by Nolin that was discussed in the introduction showed successful results with these sulfur-based nucleophiles. Dodecane thiol was selected as the model substrate and after running the reaction for about 24 h the intended adduct was isolated, although the reaction was incomplete. Thiol nucleophiles were therefore set as the target for investigation.

2.2.1. Reaction Optimization

Hemimalonate DAC ring opening with dodecane thiol was optimized to the conditions shown in **Scheme 2.3** yielding ring open adduct **2.8** in 91%. These conditions were then applied to benzenethiol to begin the substrate scope of thiophenols.



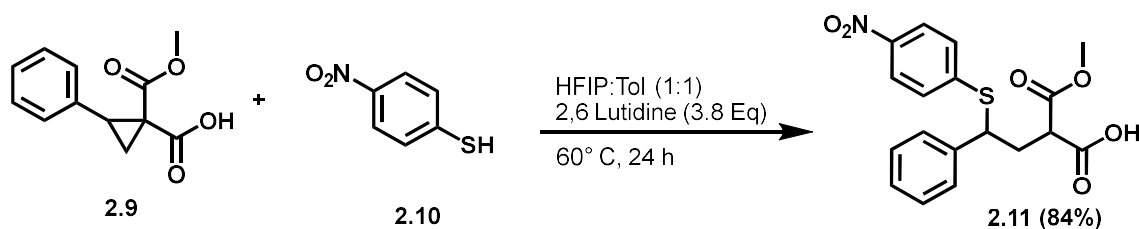
Scheme 2.3: Optimized addition of dodecane thiol to DAC 2.6

It was found under the previously used dodecane thiol conditions that this reaction did not go to completion, so conditions were reoptimized for the thiophenols. Increasing the reaction time to 4 days appeared to push the reaction closer to completion but significant starting material still remained. Increasing the amount of benzenethiol to 5 equivalents drove the reaction to completion with a yield of 80%. Ideally, this would be accomplished with less starting material. Through a brief solvent scope, it was found that switching to toluene as the cosolvent gave comparable results to the dodecanethiol addition. **Table 2.1** summarizes the adjustments made to the reaction conditions for benzenethiol. Cosolvent listed is in a 50:50 ratio with HFIP in all cases, previous work found varying from this ratio did not help.

Entry	Thiophenol Eq.	Cosolvent	Time (h)	Yield (%)
1	2	iPrOH	48	Inc.
2	2	iPrOH	96	Inc.
3	5	iPrOH	48	80
4	5	Toluene	48	88
5	2	Toluene	48	88
6	2	MeCN	48	No rxn

Table 2.1: Optimization of ring opening conditions for thiophenol, temp at 60 °C (Inc. = incomplete, No rxn = no reaction)

Incomplete reactions (Inc.) are listed as such as they showed a large amount of cyclopropane remaining and separating the product from starting cyclopropane proved to be difficult. With optimized conditions for the addition of benzenethiol, the substrate scope was carried out beginning with a variety of para-substituted benzenethiol substrates. Substrates with stronger electron donor groups performed well while electron-withdrawing substituted reagents had significantly lower yields or did not reach completion. Therefore, reaction optimization was revisited to improve the poorly performing reagents. Introducing a base was considered to help by deprotonating the thiol. The bases considered were organic bases that would not be too strong. 2,6-Lutidine was used by the Kerr group previously in cyclopropane chemistry and therefore this seemed like an ideal choice.³⁸ **Scheme 2.4** shows the revised conditions with the addition of 2,6-lutidine, tested with one of the least reactive substrates p-nitro benzenethiol **2.10**.



Scheme 2.4: p-nitro thiophenol substrate with 2,6-lutidine additive

Under the initial conditions used, p-nitrobenzene thiol did not react to completion with the DAC even after 5 days. Following the introduction of 2,6-lutidine, the reaction went to completion in 24 h and the product **2.11** was isolated in 84% yield. This result suggested that the addition of 2,6-lutidine dramatically increased the reaction rate. With this result, the substrate scope was repeated with the new conditions. In the initial substrate scope, p-methoxy benzenethiol **2.13** was found to react the fastest and result in the highest yield, therefore it was the next substrate to be used with the revised 2,6-lutidine conditions (**Scheme 2.5**).

2.2.2. Substrate Scope

The substrate scope of various thiol compounds was carried out using the now optimized set of conditions “A” or “B” and is summarized in **Figure 2.11**.

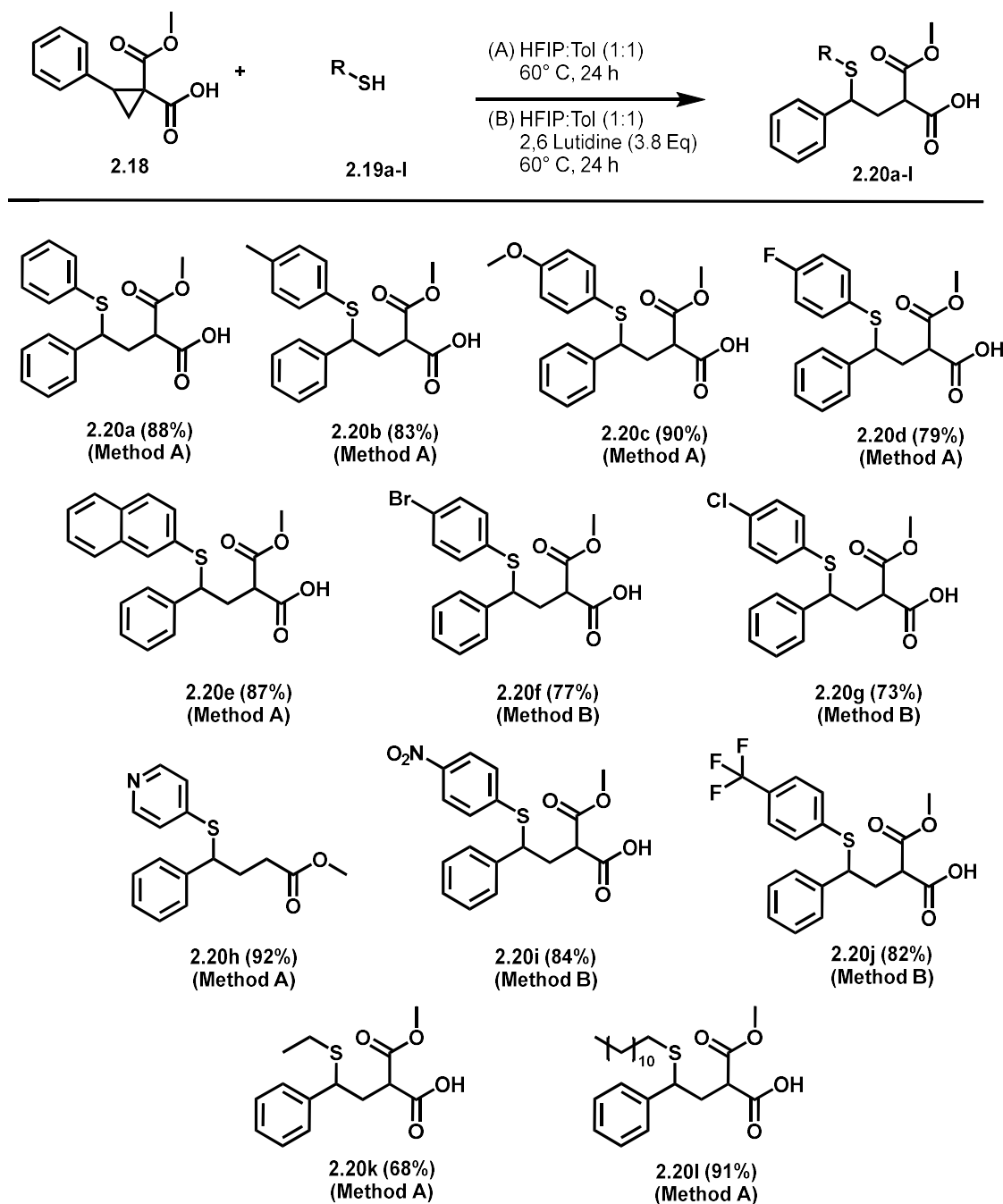


Figure 2.11: Thiol substrate scope

The majority of adducts were successfully synthesized with yields over 80% with some exceptions specifically from the halide-substituted thiophenols. In **Figure 2.12** the ^1H NMR spectra differ from the other adducts by being the only spectrum where additional diastereomeric peaks are not observed. Losing the carboxylic acid group eliminates the second chiral center that would be present, located where the red-colored protons are. Additionally, the doublet of doublets peak around 3.5 ppm is no longer present as seen in the other spectra. This was the signal that correlated to the proton next to the ester and acid group. Instead, now all 4 of the blue and red protons overlap in the 2.3 ppm region.

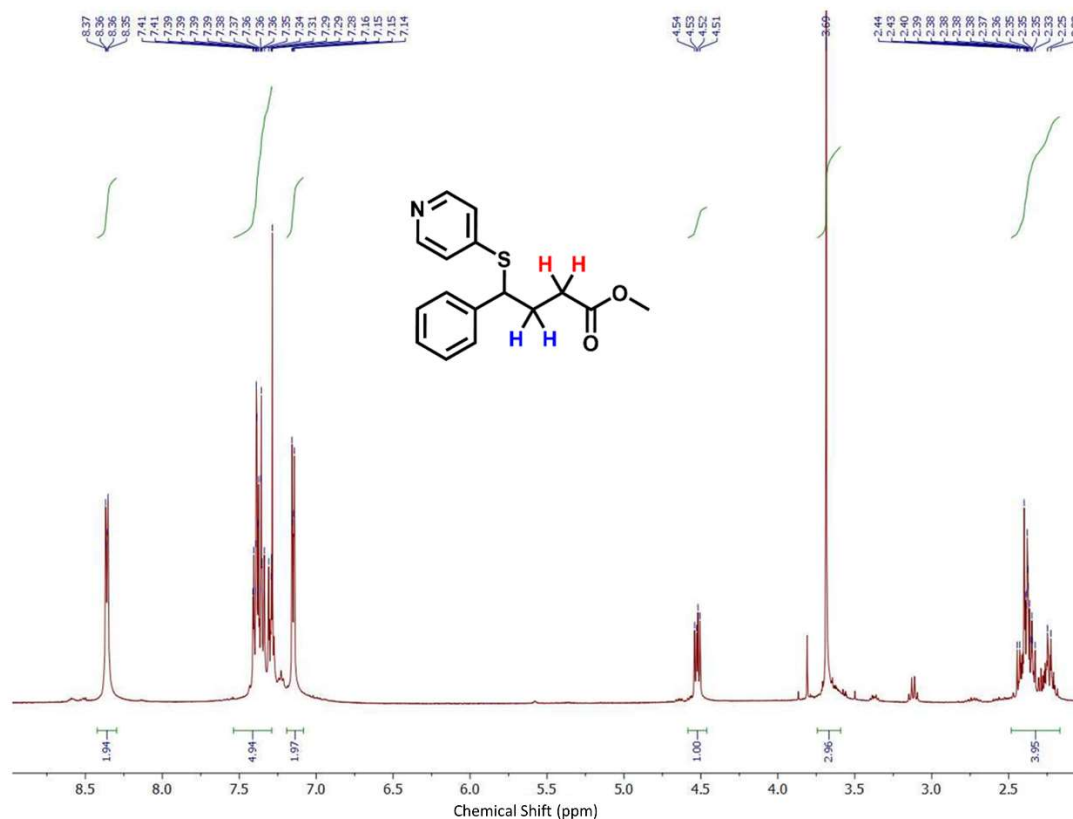


Figure 2.12: Pyridine thiol adduct ^1H spectra

The reason for the decarboxylation, in this case, is likely due to the nitrogen of the pyridine-based reagent deprotonating the carboxylic acid to drive the start of the decarboxylation. It is known from past work with the hemimalonate DAC that decarboxylation will occur during ring opening under certain conditions.³⁹ Besides the

pyridine 4-thiol adduct, the remaining products' NMR spectra show approximately equal ratio diastereomer peaks as a result of the 2 chiral centers.

Several other cyclopropanes were tested to assess donor-group compatibility, as shown in **Figure 2.13**.

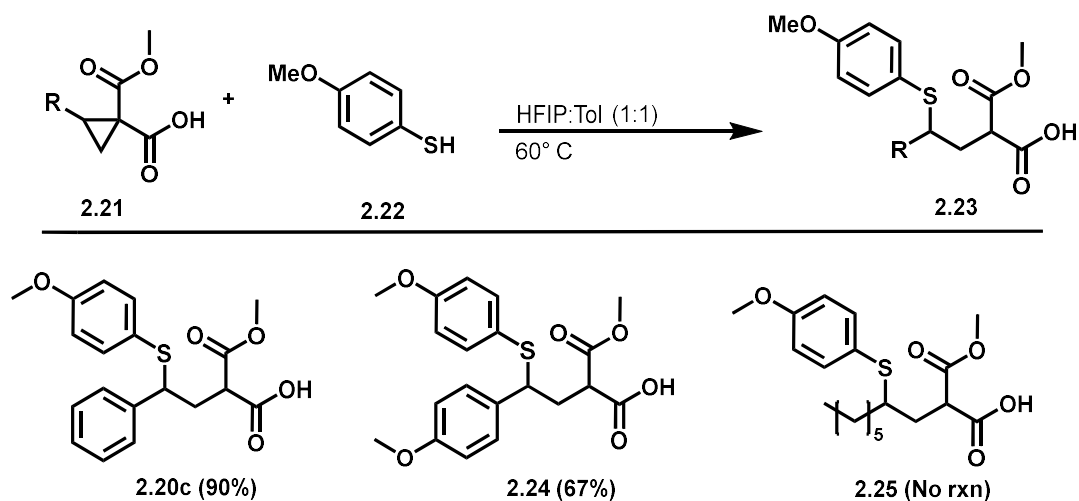


Figure 2.13: DAC donor group substrate scope

p-Methoxy thiophenol was selected for the cyclopropane substrate scope as it performed the best out of the thiophenols. Although limited in examples, these results show that a donor group such as a phenyl group is important for this reaction. The alkyl group introduced in **2.25** is not effective enough at stabilizing the developing partial positive charge and therefore no reaction is observed. The p-methoxyphenyl substituted cyclopropane in **2.24** had a lower yield than expected. This reaction proceeded rapidly compared to others so there was potentially some decomposition occurring with the more reactive reagents.

3. Conclusions and Future Directions

The reactions and synthetic applications possible with donor-acceptor cyclopropanes are of a wide range and continuously expanding. Lewis acid catalysts are an effective means to accomplish these reactions, but developing methods without these compounds allows us to avoid the harmful and expensive downsides of these metals. In places where the products are considered for pharmaceutical development, this becomes even more important. While HFIP used in this research is not an example of a safe alternative, there are other less harmful hydrogen bond donors out there to be studied for this use. Further understanding and improving methods like hydrogen bond donor activation is therefore an important topic in the study of DAC chemistry. NMR spectroscopy titrations have provided the opportunity to visualize and understand the hydrogen bond donor activation method further. These results support the increased reactivity of the hemimalonate DAC previously observed. Significant downfield shift was observed for the donor group carbon in the hemimalonate DAC when compared to the diester (**Figure 3.1**).

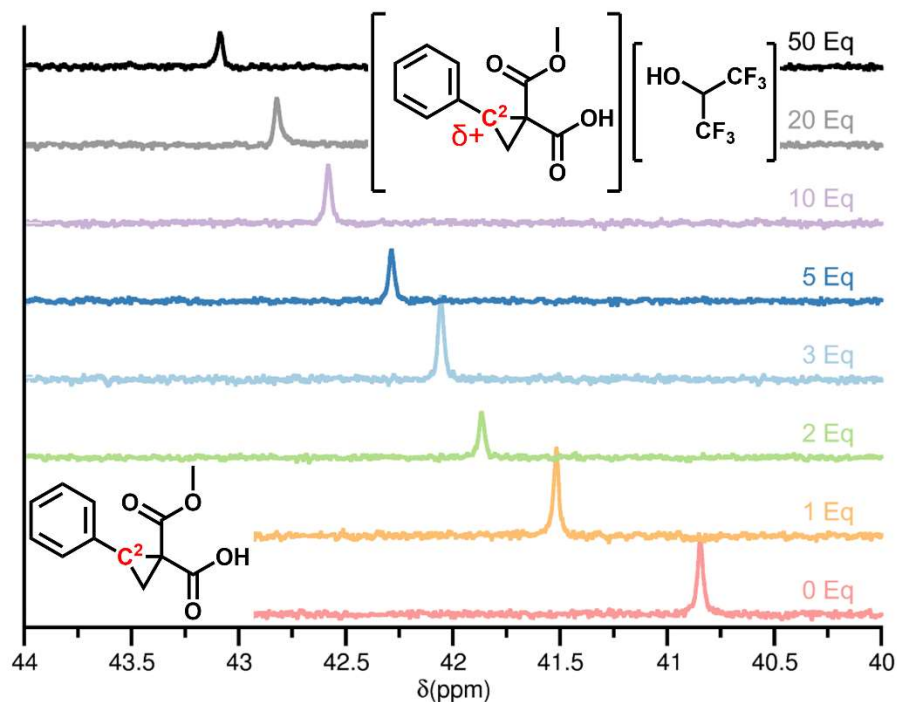
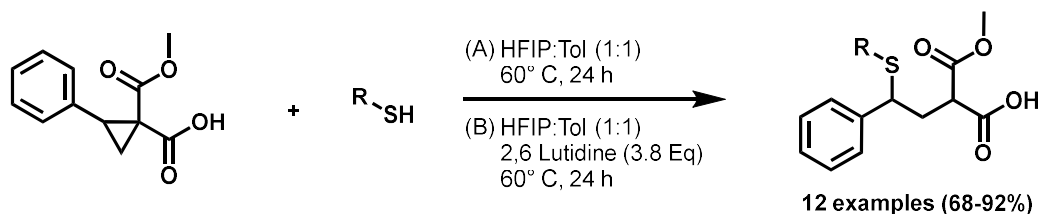


Figure 3.1: Summary of NMR spectroscopy titration method

This reduced electron density indicates a more electrophilic site and therefore a more attractive target for nucleophilic attack. Additionally, a greater understanding of the association structure was gained through the Jobs plot and dilution experiment. These studies led to the proposed 1:1 HFIP binding to DAC or 2:2 in concentrated environments where carboxylic acid dimerization will occur. Using the observed chemical shifts of the titrations and known ratios of HFIP to DAC, a least squares method was used to determine the unknown values K and δ_c . The calculated association constants showed a slightly larger value for the hemimalonate over the diester $K = 4.7 \times 10^{-3} \text{ M}^{-1}$ and $K = 2.6 \times 10^{-3} \text{ M}^{-1}$, respectively.

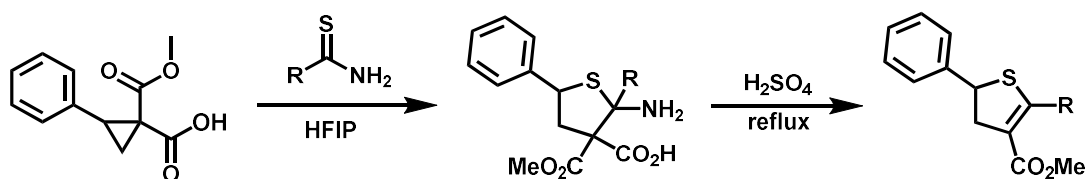
Following the previous work of the Kerr group there was the question of how this mechanism compares against traditional Lewis acid catalyst methods. To answer this, scandium triflate was used as a model catalyst to perform titrations of DACs. While scandium triflate may not have the strongest effect on Lewis acids, it is a commonly used catalyst in DAC reactions and provides a good benchmark for the time being. The results of these titrations showed that 10 equivalents of HFIP can cause an equal or further downfield shift on the target peak than 10 mol% scandium triflate. This was a fascinating observation as the method developed with HFIP uses around 25 equivalents, which based on this data would cause stronger activation than practical amounts of scandium triflate.

For the synthetic portion of the project previous work by the Kerr group on hemimalonate DACs and HFIP was expanded to other nucleophiles. The results of thiol nucleophile ring-opening reactions were reported here (**Scheme 3.1**). A variety of alkyl thiol and thiophenol compounds demonstrated the reaction tolerance for different substituents. It was also found that the additive 2,6-lutidine was able to dramatically increase reaction speed and yield for some of the weaker nucleophiles. Thiols were found to be effective nucleophiles resulting in 12 examples up to 92% yield for pyridine 4-thiol.



Scheme 3.1: Summary of DAC ring opening by thiol nucleophiles

Future work in this area is to expand on the substrate scope of the DACs used with thiols. Further exploration into modifications of the products is also of interest, discovering what can be done with the carboxylic acid group in place of the methyl ester. Additionally, the next steps outside of thiol chemistry would look at expanding the HFIP reaction to include other nucleophiles, such as revisiting azide and cyanide reactions. Future work building off the results reported here is to apply the hemimalonate DAC ring opening by HFIP method to heterocycle targets. There are many examples of DACs used in constructing heterocycle targets and as key pharmaceutical motifs synthesizing them through a route absent of metal-based catalysts is of great interest. Remaining in the field of sulfur-based chemistry, initial work with thioamides has shown promise as a sulfur-based nucleophile for the synthesis of 5-membered sulfur-containing rings. Early work with these compounds and hemimalonate DACs has led to the synthesis of dihydrothiophenes through a one-pot annulation reaction and subsequent decarboxylation and deamination as shown in **Scheme 3.2**.



Scheme 3.2: Initial work on dihydrothiophene synthesis by DAC annulation with thioamides

This reveals a unique pathway towards the synthesis of structures with thiophene cores. This discovery has opened up the consideration of other amide reagents as potential routes to also construct non-sulfur-containing heterocycles.

4. Experimental

4.1. NMR Titrations

The following experiments were all run on a 600 MHz spectrometer in CDCl₃. CDCl₃ used for all titrations was purchased new from Sigma Aldrich, 4Å molecular sieves were added and the bottle was flushed with argon gas before being stored in a desiccator.

Between experiments NMR spectroscopy tubes used were thoroughly cleaned with water and acetone then left in the oven overnight to dry. Before sample preparation, tubes are taken from the oven and a small septum is added before being left to cool in a desiccator until sample preparation.

The peaks of interest for each titration experiment were determined using HSQC NMR spectroscopy.

4.1.1. Sample Preparation: Job's Plot

Jobs plot samples were prepared using 1M stock solutions of hemimalonate DAC and HFIP in CDCl₃. 1 M hemimalonate DAC solution was prepared by dissolving 1.10 g of the DAC in 5 mL CDCl₃. 1 M HFIP solution was prepared with 0.53 mL HFIP and 4.47 mL CDCl₃. 0.5 mL samples were prepared in NMR tubes using the required ratio of stock solutions for cyclopropane mol fractions 0.1, 0.2, 0.3, 0.4, 0.5, 0.6, 0.7, 0.8, 0.9, 1.0.

4.1.2. Sample Preparation: HFIP titrations

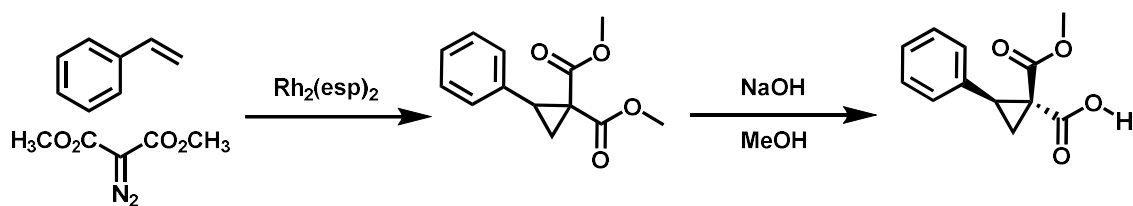
HFIP titrations of hemimalonate and diester cyclopropanes were run at 5 mM cyclopropane with HFIP equivalents ranging from 0-100. Stock solution A (50 mM DAC) was prepared by dissolving 0.25 mmol of the cyclopropane in 5 mL of CDCl₃. Stock solution B (5 mM DAC) was prepared by diluting 1 mL of stock A with 9 mL CDCl₃. Stock solution C (5 mM DAC, 500 mM HFIP) was prepared by diluting 0.5 mL

stock A with 4.236 mL CDCl_3 and 0.264 mL HFIP. Samples for titration were prepared using the required ratios of stock B and C.

4.1.3. Sample Preparation: $\text{Sc}(\text{OTf})_3$ titrations

$\text{Sc}(\text{OTf})_3$ titrations of hemimalonate and diester cyclopropanes were run at 100 mM cyclopropane with $\text{Sc}(\text{OTf})_3$ mol% ranging from 0-100%. Stock solution A (100 mM DAC) was prepared by dissolving 0.001 mol of desired cyclopropane in 10 mL CDCl_3 . Stock solution B (100 mM DAC, 100 mol% $\text{Sc}(\text{OTf})_3$) was prepared by dissolving 0.1477 g $\text{Sc}(\text{OTf})_3$ in 3 mL of stock solution A. Samples for the titration were prepared using the required ratios of stock solutions A and B.

4.2. Synthesis of Cyclopropanes



Synthesis of cyclopropane starting materials as previously reported by the Kerr group²⁷.

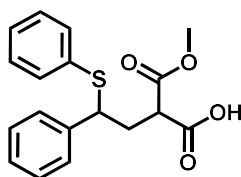
4.3. General Procedures for Ring Opening Additions

General Procedure A: To a reaction flask equipped with a stir bar was added 100 mg (0.45 mmol) of hemimalonate cyclopropane **2.18** followed by 1.2 mL toluene and 1.2 mL HFIP. Once the cyclopropane was completely dissolved thiol **2.19a-2.19e**, **2.19h**, **2.19k**, or **2.19l** (0.91 mmol) was added. The flask was then purged with argon gas, sealed with a rubber septum, and an argon-filled balloon was inserted into the septum. The reaction was left to stir in a 60 °C oil bath for 24-48 h. After confirmation of cyclopropane consumption via TLC the reaction was concentrated in vacuo. The resulting mixture was then purified via flash chromatography (1% MeOH, 1% AcOH v/v in DCM)

General Procedure B: To a reaction flask equipped with a stir bar was added 100 mg (0.45 mmol) of hemimalonate cyclopropane **2.18** followed by 1.2 mL toluene and 1.2 mL HFIP. Once the cyclopropane was completely dissolved thiol **2.19f**, **2.19g**, **2.19i**, **2.19j** (0.91 mmol) was added followed by 0.2 mL 2,6-lutidine (1.7 mmol). The flask was then purged with argon gas, sealed with a rubber septum, and an argon-filled balloon was inserted into the septum. The reaction was left to stir in a 60 °C oil bath for 24-48 h. After confirmation of cyclopropane consumption via TLC the reaction was diluted with 5 mL DCM and transferred to a separatory funnel. The mixture was acidified with 5 mL of 5% H₂SO₄ and then extracted with 3x5 mL DCM. The organic layers were combined, washed with brine, dried on MgSO₄, filtered, and then concentrated in vacuo. The resulting mixture was then purified via flash chromatography (1% MeOH, 1% AcOH v/v in DCM)

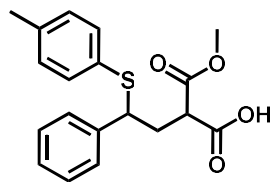
Note: due to the two chiral centers of the products an approximately 1:1 mix of diastereomers is present, this results in twice as many carbon NMR peaks however not all are differentiable due to overlapping.

4.4. Characterization of ring open adducts



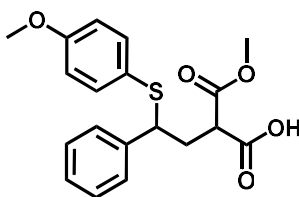
2-Methoxycarbonyl-4-phenyl-4-(phenylthio)butyric acid (2.20a)

2.20a was prepared following general procedure A. Reagents employed: cyclopropane **2.18** (100 mg, 0.45 mmol), thiol **2.19a** (93 μ L, 0.91 mmol), toluene (1.2 mL) and HFIP (1.2 mL). The reaction was stirred on heat for 48 h. **2.20a** (131 mg, 88%) was obtained as a yellow oil: ¹H NMR (400 MHz, CDCl₃) δ 7.28-7.19 (m, 10H), 4.20 (dd, 1H), 3.73 and 3.67 (s, 3H), 3.52 (dd, 1H), 2.65-2.45 (ddd, 2H).; ¹³C NMR (101 MHz, CDCl₃) δ 174.4, 169.2, 140.4, 140.3, 134.0, 132.8, 129.0, 128.8, 128.0, 127.9, 127.8, 127.6, 53.0, 51.2, 51.1, 49.73, 49.67, 34.9.



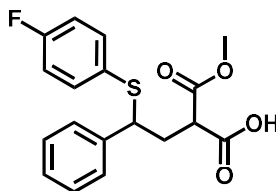
Methoxycarbonyl-4-phenyl-4-(p-tolylthio)butyric acid (**2.20b**)

2.20b was prepared following general procedure A. Reagents employed: cyclopropane **2.18** (100 mg, 0.45 mmol), thiol **2.19b** (113 mg, 0.91 mmol), toluene (1.2 mL) and HFIP (1.2 mL). The reaction was stirred on heat for 24 h. **2.20b** (129 mg, 83%) was obtained as a yellow oil: $^1\text{H NMR}$ (400 MHz, CDCl_3) δ 7.32 (m, 2H), 7.26 (m, 3H), 7.21 (m, 2H), 7.1 (m, 2H), 4.2 (dd, 1H), 3.78 and 3.72 (s, 3H), 3.60 (dd, 1H), 2.62 (ddd, 1H), 2.54 (ddd, 1H), 2.34 (s, 3H).; $^{13}\text{C NMR}$ (101 MHz, CDCl_3) δ 169.5, 140.5, 138.0, 133.5, 130.1, 129.8, 128.7, 128.00, 127.97, 127.80, 127.76, 53.0, 51.5, 51.4, 34.8, 21.3.



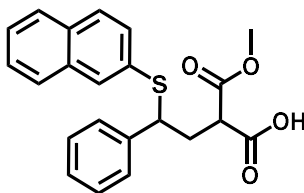
2-Methoxycarbonyl-4-(p-methoxyphenylthio)-4-phenylbutyric acid (**2.20c**)

2.20c was prepared following general procedure A. Reagents employed: cyclopropane **2.18** (100 mg, 0.45 mmol), thiol **2.19c** (112 μL , 0.91 mmol), toluene (1.2 mL) and HFIP (1.2 mL). The reaction was stirred on heat for 24 h. **2.20c** (146 mg, 90%) was obtained as a yellow oil: $^1\text{H NMR}$ (400 MHz, CDCl_3) δ 7.30-7.12 (m, 7H), 6.74 (dd, 2H), 4.02 (dd, 1H), 3.76 and 3.73 (s, 3H), 3.56 (dd, 1H), 2.60-2.43 (m, 2H).; $^{13}\text{C NMR}$ (101 MHz, CDCl_3) δ 174.3, 169.3, 160.0, 140.7, 140.6, 136.28, 136.27, 128.64, 128.62, 128.4, 128.01, 127.97, 127.69, 127.65, 123.83, 123.79, 114.5, 55.4, 52.9, 52.3, 52.2, 49.8, 34.39.



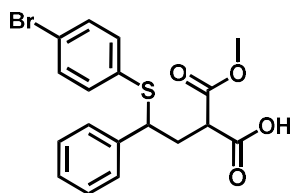
4-(p-fluorophenylthio)-2-methoxycarbonyl-4-phenylbutyric acid (**2.20d**)

2.20d was prepared following general procedure A. Reagents employed: cyclopropane **2.18** (100 mg, 0.45 mmol), thiol **2.19d** (97 μ L, 0.91 mmol), toluene (1.2 mL) and HFIP (1.2 mL). The reaction was stirred for 48 h. **2.20d** (124 mg, 79%) was obtained as a yellow oil: $^1\text{H NMR}$ (400 MHz, CDCl_3) δ 7.26-7.15 (m, 7H), 6.90 (m, 2H), 4.09 (dd, 1H), 3.73 and 3.68 (s, 3H), 3.54 (dd, 1H), 2.61-2.44 (m, 2H).; $^{13}\text{C NMR}$ (101 MHz, CDCl_3) δ 169.5, 140.5, 138.0, 133.5, 130.1, 129.8, 128.7, 128.00, 127.97, 127.80, 127.76, 53.0, 51.5, 51.4, 34.8, 21.3.



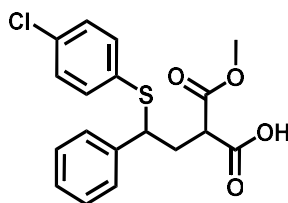
2-methoxycarbonyl-4-(2-naphthylthio)-4-phenylbutyric acid (**2.20e**)

2.20e was prepared following general procedure A. Reagents employed: cyclopropane **2.18** (100 mg, 0.45 mmol), thiol **2.19e** (146, 0.91 mmol), toluene (1.2 mL) and HFIP (1.2 mL). The reaction was stirred on heat for 24 h. **2.20e** (149 mg, 87%) was obtained as a yellow oil: $^1\text{H NMR}$ (400 MHz, CDCl_3) δ 7.80-7.75 (m, 2H), 7.72-7.67 (m, 2H), 7.46-7.43 (m, 2H), 7.34 (t, 1H), 7.30-7.23 (m, 5H), 4.35 (dd, 1H), 3.74 and 3.65 (s, 3H), 3.57 (dd, 1H), 2.67 (ddd, 1H), 2.57 (ddd, 1H).; $^{13}\text{C NMR}$ (101 MHz, CDCl_3) δ 174.3, 169.3, 146.7, 140.3, 140.2, 133.68, 133.66, 132.48, 132.46, 131.6, 131.5, 131.4, 131.3, 129.71, 129.66, 128.84, 128.83, 128.4, 128.00, 127.97, 127.92, 127.88, 127.7, 127.6, 126.5, 126.31, 126.29, 60.66, 52.89, 52.88, 51.0, 50.9, 49.8, 35.0, 34.9, 29.8, 21.2, 14.3.



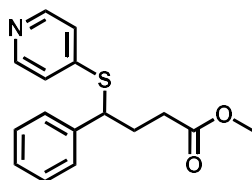
4-(p-bromophenylthio)-2-methoxycarbonyl-4-phenylbutyric acid (2.20f)

2.20f was prepared following general procedure B. Reagents employed: cyclopropane **2.18** (100 mg, 0.45 mmol), thiol **2.19f** (172 mg, 0.91 mmol), toluene (1.2 mL), HFIP (1.2 mL) and 2,6-lutidine (0.2 mL, 1.8 mmol). The reaction was stirred on heat for 24 h. **2.20f** (142 mg, 77%) was obtained as a yellow oil: $^1\text{H NMR}$ (400 MHz, CDCl_3) δ 7.36-7.07 (m, 9H), 4.17 (dd, 1H), 3.73 (s, 3H), 3.50 (dd, 1H), 2.60-2.44 (m, 2H).



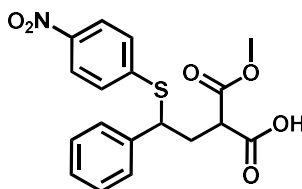
4-(p-chlorophenylthio)-2-methoxycarbonyl-4-phenylbutyric acid (2.20g)

2.20g was prepared following general procedure B. Reagents employed: cyclopropane **2.18** (100 mg, 0.45 mmol), thiol **2.19g** (132 mg, 0.91 mmol), toluene (1.2 mL), HFIP (1.2 mL) and 2,6-lutidine (0.2 mL, 1.8 mmol). The reaction was stirred on heat for 36 h. **2.20g** (120 mg, 73%) was obtained as a yellow oil: $^1\text{H NMR}$ (400 MHz, CDCl_3) δ 7.34-7.15 (m, 9H), 4.16 (dd, 1H), 3.75 and 3.69 (s, 3H), 3.51 (dd, 1H), 2.61-2.45 (m, 2H); $^{13}\text{C NMR}$ (101 MHz, CDCl_3) δ 173.8, 169.1, 169.2, 140.0, 139.9, 134.3, 134.0, 132.3, 129.12, 129.05, 128.9, 128.8, 128.1, 128.03, 127.96, 127.93, 127.89, 53.04, 51.4, 51.3, 49.53, 49.45, 34.74, 34.68.



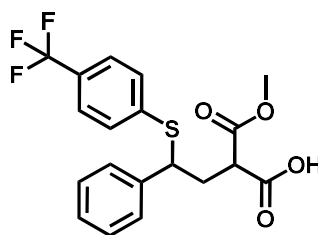
methyl 4-phenyl-4-(4-pyridylthio)butyrate (2.20h)

2.20h was prepared following general procedure A. Reagents employed: cyclopropane **2.18** (100 mg, 0.45 mmol), thiol **2.19h** (101 mg, 0.91 mmol), toluene (1.2 mL) and HFIP (1.2 mL). The reaction was stirred on heat for 24 h. The product was purified via flash chromatography (10% EtOAc v/v in hexanes). **2.20h** (119 mg, 92%) was obtained as a yellow oil: $^1\text{H NMR}$ (400 MHz, CDCl_3) δ 8.3 (d, 2H), 7.39-7.26 (m, 5H), 7.1 (d, 2H), 4.5 (dd, 1H), 3.7 (s, 3H), 2.42-2.20 (m, 4H).; $^{13}\text{C NMR}$ (101 MHz, CDCl_3) δ 173.2, 149.1, 148.4, 129.1, 128.1, 127.8, 122.1, 51.9, 49.2, 31.7, 31.5.



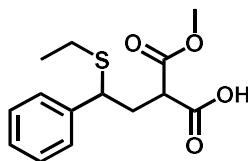
2-methoxycarbonyl-4-(p-nitrophenylthio)-4-phenylbutyric acid (2.20i)

2.20i was prepared following general procedure B. Reagents employed: cyclopropane **2.18** (100 mg, 0.45 mmol), thiol **2.19i** (141 mg, 0.91 mmol), toluene (1.2 mL), HFIP (1.2 mL) and 2,6-lutidine (0.2 mL, 1.8 mmol). The reaction was stirred on heat for 24 h. **2.20i** (141 mg, 84%) was obtained as a yellow oil: $^1\text{H NMR}$ (400 MHz, CDCl_3) δ 8.1 (d, 2H), 7.39-7.26 (m, 7H), 4.5 (dd, 1H), 3.78 and 3.71 (s, 3H), 3.4 (dd, 1H), 2.6 (ddd, 1H), 2.5 (ddd, 1H). $^{13}\text{C NMR}$ (101 MHz, CDCl_3) δ 129.2, 128.8, 128.7, 128.5, 127.8, 127.7, 124.0, 123.9, 53.1, 35.1.



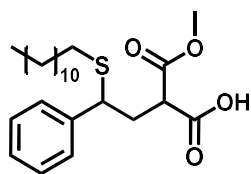
2-methoxycarbonyl-4-phenyl-4-[p-(trifluoromethyl)phenylthio]butyric acid (**2.20j**)

2.20j was prepared following general procedure B. Reagents employed: cyclopropane **2.18** (100 mg, 0.45 mmol), benzene thiol **2.19j** (162 mg, 0.91 mmol), toluene (1.2 mL), HFIP (1.2 mL) and 2,6-lutidine (0.2 mL, 1.8 mmol). The reaction was stirred on heat for 24 h. **2.20j** (146 mg, 82%) was obtained as a yellow oil: $^1\text{H NMR}$ (400 MHz, CDCl_3) δ 7.45-7.17 (m, 9H), 4.3 (dd, 1H), 3.76 and 3.69 (s, 3H), 3.50 (dd, 1H), 2.62-2.49 (m, 2H); $^{13}\text{C NMR}$ (101 MHz, CDCl_3) δ 169.1, 139.5, 135.6, 135.5, 135.4, 135.3, 129.31, 129.29, 129.0, 128.8, 128.7, 128.2, 128.0, 127.9, 124.22, 124.16, 53.1, 50.9, 50.8, 49.5, 34.7, 34.6.



4-(ethylthio)-2-methoxycarbonyl-4-phenylbutyric acid (**2.20k**)

2.20k was prepared following general procedure A with changes of solvent from toluene to isopropanol and thiol equivalents from 2.0 Eq to 10.0 Eq. Reagents employed: cyclopropane **2.18** (100 mg, 0.45 mmol), thiol **2.19k** (328 μL , 4.55 mmol), isopropanol (1.2 mL) and HFIP (1.2 mL). The reaction was stirred on heat for 48 h. **2.20k** (86 mg, 68%) was obtained as a yellow oil: $^1\text{H NMR}$ (400 MHz, CDCl_3) δ 7.30-7.22 (m, 5H), 3.82 (m, 1H), 3.73 (s, 3H), 3.47 (m, 1H), 2.55-2.36 (m, 2H), 2.36-2.27 (m, 2H), 1.12 (t, 3H); $^{13}\text{C NMR}$ (101 MHz, CDCl_3) δ 174.3, 169.4, 169.3, 141.3, 128.8, 128.6, 127.94, 127.89, 127.70, 127.68, 52.93, 52.91, 49.80, 49.76, 47.07, 47.05, 35.21, 35.19, 25.27, 25.23, 14.49.



2-methoxycarbonyl-4-phenyl-4-(dodecylthio)butyric acid (**2.201**)

2.201 was prepared following general procedure A with changes of solvent from toluene to isopropanol. Reagents employed: cyclopropane **2.18** (100 mg, 0.45 mmol), thiol **2.191** (184 mg, 0.91 mmol), isopropanol (1.2 mL), and HFIP (1.2 mL). The reaction was stirred for 48 h. **2.201** (173 mg, 91%) was obtained as a yellow oil: $^1\text{H NMR}$ (400 MHz, CDCl_3) δ 7.34-7.23 (m, 5H), 3.8 (dd, 1H), 3.75 and 3.71 (s, 3H), 3.5 (dd, 1H), 2.53-2.37 (m, 2H), 2.37-2.23 (m, 2H), 1.44 (tt, 2H), 1.31-1.21 (m, 18H), 0.88 (t, 3H).; $^{13}\text{C NMR}$ (101 MHz, CDCl_3) δ 169.3, 141.2, 128.7, 127.83, 127.80, 127.59, 127.56, 52.9, 49.4, 47.29, 47.27, 35.2, 31.9, 31.2, 29.7, 29.6, 29.5, 29.4, 29.22, 29.17, 28.9, 22.7, 14.16.

5. References

Donor acceptor cyclopropane review articles see: ^{40–48}

- (1) Ouellette, R. J.; Rawn, J. D. *Organic Chemistry (Second Edition)*; 2018.
- (2) Good, W. D.; Smith, N. K. Enthalpies of Combustion of Toluene, Benzene, Cyclohexane, Cyclohexene, Methylcyclopentane, 1-Methylcyclopentene, and n-Hexane. *J. Chem. Eng. Data* **1969**, *14* (3), 102–106.
- (3) Ghosh, K.; Das, S. Recent Advances in Ring-Opening of Donor Acceptor Cyclopropanes Using C-Nucleophiles. *Org. Biomol. Chem.* **2021**, *19* (5), 965–982. <https://doi.org/10.1039/d0ob02437f>.
- (4) Al Mamari, H. H. Developments and Uses of Lewis Acids: From Conventional Catalysts to Modern Green Catalysts. In *Electrophile and Lewis Acid*; 2023.
- (5) Corma, A.; García, H. Lewis Acids: From Conventional Homogeneous to Green Homogeneous and Heterogeneous Catalysis. *Chem. Rev.* **2003**, *103* (11), 4307–4365. <https://doi.org/10.1021/cr030680z>.
- (6) Budynina, E. M.; Ivanov, K. L.; Sorokin, I. D.; Melnikov, M. Y. Ring Opening of Donor-Acceptor Cyclopropanes with N-Nucleo-Philes. *Synth.* **2017**, *49* (14), 3035–3068. <https://doi.org/10.1055/s-0036-1589021>.
- (7) Boichenko, M. A.; Andreev, I. A.; Chagarovskiy, A. O.; Levina, I. I.; Zhokhov, S. S.; Trushkov, I. V.; Ivanova, O. A. Ring Opening of Donor-Acceptor Cyclopropanes with Cyanide Ion and Its Surrogates. *J. Org. Chem.* **2020**, *85* (2), 1146–1157. <https://doi.org/10.1021/acs.joc.9b03098>.
- (8) Harrington, P.; Kerr, M. A. The High Pressure Reaction of Cyclopropanes with Indoles Catalyzed by Ytterbium Triflate. *Tetrahedron Lett.* **1997**, *38* (34), 5949–5952. [https://doi.org/10.1016/S0040-4039\(97\)01351-8](https://doi.org/10.1016/S0040-4039(97)01351-8).
- (9) Braun, C. M.; Shema, A. M.; Dulin, C. C.; Nolin, K. A. The Homologous Conjugate Addition of Thiols to Electron-Deficient Cyclopropanes Catalyzed by a Calcium(II) Complex. *Tetrahedron Lett.* **2013**, *54* (44), 5889–5891.

<https://doi.org/10.1016/j.tetlet.2013.08.102>.

- (10) Kerr, M. A.; Carson, C. A. Heterocycles from Cyclopropanes: Applications in Natural Product Synthesis. *Chem. Soc. Rev.* **2009**, *38* (11), 3051–3060.
- (11) Young, I. S.; Kerr, M. A. A Homo [3 + 2] Dipolar Cycloaddition: The Reaction of Nitrones with Cyclopropanes. *Angew. Chemie - Int. Ed.* **2003**, *42* (26), 3023–3026. <https://doi.org/10.1002/anie.200351573>.
- (12) Young, I. S.; Williams, J. L.; Kerr, M. A. Diastereoselective Synthesis of Pyrrolidines Using a Nitronone/Cyclopropane Cycloaddition: Synthesis of the Tetracyclic Core of Nakadomarin A. *Org. Lett.* **2005**, *7* (5), 953–955. <https://doi.org/10.1021/ol0501018>.
- (13) Carson, C. A.; Kerr, M. A. Diastereoselective Synthesis of Pyrrolidines via the Yb(OTf)₃ Catalyzed Three-Component Reaction of Aldehydes, Amines, and 1,1-Cyclopropanediester. *J. Org. Chem.* **2005**, *70* (20), 8242–8244. <https://doi.org/10.1021/jo0512251>.
- (14) Jackson, S. K.; Karadeolian, A.; Driega, A. B.; Kerr, M. A. Stereodivergent Methodology for the Synthesis of Complex Pyrrolidines. *J. Am. Chem. Soc.* **2008**, *130* (12), 4196–4201. <https://doi.org/10.1021/ja710289k>.
- (15) Lebold, T. P.; Kerr, M. A. Stereodivergent Synthesis of Fused Bicyclopiprazolidines: Access to Piprazolines and Pyrrolidines. *Org. Lett.* **2009**, *11* (19), 4354–4357. <https://doi.org/10.1021/ol901744e>.
- (16) Lebold, T. P.; Leduc, A. B.; Kerr, M. A. Zn(II)-Catalyzed Synthesis of Piperidines from Propargyl Amines and Cyclopropanes. *Org. Lett.* **2009**, *11* (16), 3770–3772. <https://doi.org/10.1021/ol901435k>.
- (17) Leduc, A. B.; Lebold, T. P.; Kerr, M. A. Synthesis of Tetrahydropyrans from Propargyl Alcohols and 1,1-Cyclopropanediester: A One-Pot Ring-Opening/Conia-Ene Protocol. *J. Org. Chem.* **2009**, *74* (21), 8414–8416. <https://doi.org/10.1021/jo9019122>.

- (18) Grover, H. K.; Lebold, T. P.; Kerr, M. A. Tandem Cyclopropane Ring-Opening/Conia-Ene Reactions of 2-Alkynyl Indoles: A [3 + 3] Annulative Route to Tetrahydrocarbazoles. *Org. Lett.* **2011**, *13* (2), 220–223. <https://doi.org/10.1021/ol102627e>.
- (19) Pohlhaus, P. D.; Sanders, S. D.; Parsons, A. T.; Li, W.; Johnson, J. S. Scope and Mechanism for Lewis Acid-Catalyzed Cycloadditions of Aldehydes and Donor-Acceptor Cyclopropanes: Evidence for a Stereospecific Intimate Ion Pair Pathway. *J. Am. Chem. Soc.* **2008**, *130* (27), 8642–8650. <https://doi.org/10.1021/ja8015928>.
- (20) Vitaku, E.; Smith, D. T.; Njardarson, J. T. Analysis of the Structural Diversity, Substitution Patterns, and Frequency of Nitrogen Heterocycles among U.S. FDA Approved Pharmaceuticals. *J. Med. Chem.* **2014**, *57* (24), 10257–10274. <https://doi.org/10.1021/jm501100b>.
- (21) Carson, C. A.; Kerr, M. A. Total Synthesis of FR901483. *Org. Lett.* **2009**, *11* (3), 777–779. <https://doi.org/10.1021/ol802870c>.
- (22) Carson, C. A.; Kerr, M. A. Total Synthesis of (+)-Phyllantidine. *Angew. Chemie - Int. Ed.* **2006**, *45* (39), 6560–6563. <https://doi.org/10.1002/anie.200602569>.
- (23) Boeckman, R. K.; Wang, H.; Rugg, K. W.; Genung, N. E.; Chen, K.; Ryder, T. R. A Scalable Total Synthesis of (-)-Nakadomarin A. *Org. Lett.* **2016**, *18* (23), 6136–6139. <https://doi.org/10.1021/acs.orglett.6b03137>.
- (24) Leduc, A. B.; Kerr, M. A. Total Synthesis of (-)-Allosecurinine. *Angew. Chemie - Int. Ed.* **2008**, *47* (41), 7945–7948. <https://doi.org/10.1002/anie.200803257>.
- (25) Karadeolian, A.; Kerr, M. A. Total Synthesis of (+)-Isatisine A. *J. Org. Chem.* **2010**, *75* (20), 6830–6841. <https://doi.org/10.1021/jo101209y>.
- (26) Emmett, M. R.; Kerr, M. A. Nucleophilic Ring Opening of Cyclopropane Hemimalonates Using Internal Brønsted Acid Activation. *Org. Lett.* **2011**, *13* (16), 4180–4183. <https://doi.org/10.1021/ol201486x>.

- (27) Irwin, L. C.; Renwick, C. R.; Kerr, M. A. Nucleophilic Opening of Donor-Acceptor Cyclopropanes with Indoles via Hydrogen Bond Activation with 1,1,1,3,3,3-Hexafluoroisopropanol. *J. Org. Chem.* **2018**, *83* (11), 6235–6242. <https://doi.org/10.1021/acs.joc.8b00894>.
- (28) Richmond, E.; Vuković, V. D.; Moran, J. Nucleophilic Ring Opening of Donor-Acceptor Cyclopropanes Catalyzed by a Brønsted Acid in Hexafluoroisopropanol. *Org. Lett.* **2018**, *20* (3), 574–577. <https://doi.org/10.1021/acs.orglett.7b03688>.
- (29) Bonato, M.; Corrà, F.; Bellio, M.; Guidolin, L.; Tallandini, L.; Irato, P.; Santovito, G. Pfas Environmental Pollution and Antioxidant Responses: An Overview of the Impact on Human Field. *Int. J. Environ. Res. Public Health* **2020**, *17* (21), 1–45. <https://doi.org/10.3390/ijerph17218020>.
- (30) Feng, Y.; Chen, X. B.; Yuan, W. G.; Huang, S.; Li, M.; Yang, X. L. Comparison of the Level of Free Hexafluoro-Isopropanol in Adults' Blood and the Incidence of Emergence Agitation After Anesthesia With Different Concentrations of Sevoflurane in Laparoscopic Gastrointestinal Surgery: A Randomized Controlled Clinical Trial. *Clin. Ther.* **2019**, *41* (11), 2263–2272. <https://doi.org/10.1016/j.clinthera.2019.08.022>.
- (31) Sheff, J. T.; Lucius, A. L.; Owens, S. B.; Gray, G. M. Generally Applicable NMR Titration Methods for the Determination of Equilibrium Constants for Coordination Complexes: Syntheses and Characterizations of Metallacrown Ethers with α,ω -Bis(Phosphite)- Polyether Ligands and Determination of Equilibrium Bindin. *Organometallics* **2011**, *30* (21), 5695–5709. <https://doi.org/10.1021/om200580t>.
- (32) Macomber, R. S. An Introduction to NMR Titration for Studying Rapid Reversible Complexation. *J. Chem. Educ.* **1992**, *69* (5), 375–378. <https://doi.org/10.1021/ed069p375>.
- (33) Suleymanov, A.; Du, E. Le; Dong, Z.; Muriel, B.; Scopelliti, R.; Farzaneh, F.-T.;

- Waser, J.; Severin, K. Triazene-Activated Donor – Acceptor Cyclopropanes: Ring-Opening and (3 + 2) Annulation Reactions. *Org. Lett.* **2020**, *22* (11), 4517–4522. <https://doi.org/https://dx.doi.org/10.1021/acs.orglett.0c01527>.
- (34) Renny, J. S.; Tomasevich, L. L.; Tallmadge, E. H.; Collum, D. B. Method of Continuous Variations: Applications of Job Plots to the Study of Molecular Associations in Organometallic Chemistry. *Angew. Chemie - Int. Ed.* **2013**, *52* (46), 11998–12013. <https://doi.org/10.1002/anie.201304157>.
- (35) Thordarson, P. Determining Association Constants from Titration Experiments in Supramolecular Chemistry. *Chem. Soc. Rev.* **2011**, *40* (3), 1305–1323. <https://doi.org/10.1039/c0cs00062k>.
- (36) More, S. G.; Suryavanshi, G. Lewis Acid Triggered N-Alkylation of Sulfoximines through Nucleophilic Ring-Opening of Donor-Acceptor Cyclopropanes: Synthesis of γ -Sulfoximino Malonic Diesters. *Org. Biomol. Chem.* **2022**, *20* (12), 2518–2529. <https://doi.org/10.1039/d2ob00213b>.
- (37) Jennings, J. J.; Wigman, B. W.; Armstrong, B. M.; Franz, A. K. NMR Quantification of the Effects of Ligands and Counterions on Lewis Acid Catalysis. *J. Org. Chem.* **2019**, *84* (24), 15845–15853. <https://doi.org/10.1021/acs.joc.9b02107>.
- (38) Cochrane, S.; Kerr, M. A. 3,4-Annulated Indoles via Tandem Cyclopropane Ring-Opening/Conia-Ene and Michael Addition/Conia-Ene Reactions. *Org. Lett.* **2022**, *24* (30), 5509–5512.
- (39) Emmett, M. R. The Synthesis and Reactivity of Novel Donor-Acceptor Cyclopropanes and Progress Towards Pyrrolidine Alkaloids. *Electronic Thesis and Dissertation Repository.* **2014**, 2267.
- (40) Reissig, H. U.; Zimmer, R. Donor - Acceptor-Substituted Cyclopropane Derivatives and Their Application in Organic Synthesis. *Chem. Rev.* **2003**, *103* (4), 1151–1196. <https://doi.org/10.1021/cr010016n>.

- (41) Schneider, T. F.; Kaschel, J.; Werz, D. B. A New Golden Age for Donor-Acceptor Cyclopropanes. *Angew. Chemie - Int. Ed.* **2014**, *53* (22), 5504–5523. <https://doi.org/10.1002/anie.201309886>.
- (42) Nicolaou, K. C.; Chen, J. S. Rapid Formation of Molecular Complexity in Organic Synthesis Issue Reviewing the Latest Advances in Reaction Development And. *Chem. Soc. Rev.* **2009**, *38* (11), 2993–3009.
- (43) Werz, D. B.; Biju, A. T. Uncovering the Neglected Similarities of Arynes and Donor-Acceptor Cyclopropanes. *Angew. Chemie - Int. Ed.* **2019**.
- (44) Lebold, T. P.; Kerr, M. A. Intramolecular Annulations of Donor-Acceptor Cyclopropanes. *Pure Appl. Chem.* **2010**, *82* (9), 1797–1812. <https://doi.org/10.1351/PAC-CON-09-09-28>.
- (45) Grover, H. K.; Emmett, M. R.; Kerr, M. A. Carbocycles from Donor-Acceptor Cyclopropanes. *Org. Biomol. Chem.* **2015**, *13* (3), 655–671. <https://doi.org/10.1039/c4ob02117g>.
- (46) Pagenkopf, B. L.; Vemula, N. Cycloadditions of Donor–Acceptor Cyclopropanes and Nitriles. *European J. Org. Chem.* **2017**, *2017* (18), 2561–2567. <https://doi.org/10.1002/ejoc.201700201>.
- (47) Kerr, M. A. The Annulation of Nitrones and Donor-Acceptor Cyclopropanes: A Personal Account of Our Adventures to Date. *Isr. J. Chem.* **2016**, *56* (6–7), 476–487. <https://doi.org/10.1002/ijch.201500095>.
- (48) Ivanova, O. A.; Trushkov, I. V. Donor-Acceptor Cyclopropanes in the Synthesis of Carbocycles. *Chem. Rec.* **2019**, *19* (11), 2189–2208. <https://doi.org/10.1002/tcr.201800166>.

Appendix

Table A.1: HFIP titration of hemimalonate 200 mM

Hemimalonate DAC (200mM) - HFIP						
Run	HFIP Eq	obs shift (ppm)	calc shift (ppm)	diff	diff^2	
1	0	40.43	40.43	0.0000	0.0000	
2	0.5	40.84	40.76	-0.0776	0.0060	
3	1	41.26	41.04	-0.2229	0.0497	
4	2	41.66	41.49	-0.1682	0.0283	
5	3	41.92	41.81	-0.1133	0.0128	
6	4	42.10	42.10	0.0014	0.0000	
7	5	42.27	42.26	-0.0141	0.0002	
8	7	42.28	42.38	0.0965	0.0093	
9	8	42.38	42.47	0.0930	0.0086	
10	9	42.51	42.55	0.0418	0.0017	
11	10	42.57	42.62	0.0473	0.0022	
12	12	42.70	42.72	0.0197	0.0004	
12	14	42.73	42.80	0.0660	0.0044	
13	16	42.80	42.85	0.0550	0.0030	
14	18	42.84	42.90	0.0619	0.0038	
15	20	42.84	42.94	0.0985	0.0097	
16	25	42.92	43.01	0.0862	0.0074	
17	30	42.97	43.05	0.0838	0.0070	
18	35	43.00	43.09	0.0903	0.0081	
19	40	43.08	43.12	0.0351	0.0012	
20	45	43.13	43.14	0.0056	0.0000	
21	50	43.16	43.15	-0.0076	0.0001	
22	60	43.22	43.18	-0.0432	0.0019	
23	70	43.26	43.20	-0.0638	0.0041	
24	80	43.30	43.21	-0.0899	0.0081	
25	90	43.32	43.22	-0.0990	0.0098	
26	100	43.36	43.23	-0.1303	0.0170	
27	120	43.35	43.22	-0.1334	0.0178	
k	0.0017	δc	43.49	Sum:	0.2228	

Table A.2: Jobs plot HFIP titration of hemimalonate, total concentration 1 M

Jobs Plot							
DAC conc (mM)	DAC mole fraction	HFIP mole fraction	Shift (ppm)	Shift - DAC shift (ppm)	calc [H]	calc [G]	calc [HmGn]
100	0.1	0.9	41.77	2.82	40.88	840.88	59.12
200	0.2	0.8	41.53	2.58	91.82	691.82	108.18
300	0.3	0.7	41.23	2.28	156.60	556.60	143.40
400	0.4	0.6	41.00	2.05	228.09	428.09	171.91
500	0.5	0.5	40.67	1.72	319.71	319.71	180.29
600	0.6	0.4	40.34	1.39	425.16	225.16	174.84
700	0.7	0.3	40.01	1.06	544.44	144.44	155.56
800	0.8	0.2	39.66	0.71	680.92	80.92	119.08
900	0.9	0.1	39.31	0.36	832.08	32.08	67.92
1000	1	0	38.95	0.00	1000	0	0
Complex shift estimate:		43.72					
Complex shift - host shift:		4.77					
Fit formula:	=(-741.85*(B17^2))+ (727.66*B17)+2.0088						
Fit x value:	0.4904	(excel solver for highest y value)					
Fit y value (mM):	180.44						

Table A.3: HFIP titration of hemimalonate 5 mM

Hemimalonate DAC (5mM) - HFIP						
Run	HFIP Eq	obs shift (ppm)	calc shift (ppm)	diff	diff^2	
1	0	41.44	41.44	0.0000	0.0000	
2	0.5	41.46	41.46	-0.0035	0.0000	
3	1	41.46	41.47	0.0127	0.0002	
4	2	41.49	41.50	0.0140	0.0002	
5	3	41.52	41.53	0.0139	0.0002	
6	4	41.55	41.56	0.0126	0.0002	
7	6	41.62	41.62	-0.0034	0.0000	
8	8	41.67	41.67	-0.0036	0.0000	
9	10	41.72	41.71	-0.0075	0.0001	
10	12	41.76	41.76	-0.0048	0.0000	
11	14	41.80	41.80	-0.0050	0.0000	
12	16	41.83	41.83	0.0021	0.0000	
13	18	41.88	41.87	-0.0132	0.0002	
14	20	41.90	41.90	-0.0006	0.0000	
15	25	41.97	41.97	0.0023	0.0000	
16	30	42.03	42.04	0.0052	0.0000	
17	40	42.14	42.14	-0.0017	0.0000	
18	50	42.22	42.22	-0.0008	0.0000	
19	60	42.28	42.28	0.0043	0.0000	
20	70	42.32	42.34	0.0178	0.0003	
21	80	42.38	42.38	0.0026	0.0000	
22	100	42.47	42.45	-0.0168	0.0003	
k	0.0047	δc	42.88	Sum:	0.0017	

Table A.4: HFIP titration of diester 5 mM

Diester DAC (5mM) - HFIP					
Run	HFIP Eq	obs shift (ppm)	calc shift (ppm)	diff	diff^2
1	0	32.72	32.72	0.0000	0.0000
2	0.5	32.73	32.73	0.0018	0.0000
3	1	32.74	32.74	0.0035	0.0000
4	2	32.77	32.77	-0.0036	0.0000
5	3	32.79	32.79	-0.0012	0.0000
6	4	32.82	32.81	-0.0094	0.0001
7	6	32.86	32.85	-0.0074	0.0001
8	8	32.90	32.89	-0.0073	0.0001
9	10	32.94	32.93	-0.0091	0.0001
10	12	32.97	32.97	-0.0025	0.0000
11	14	33.01	33.00	-0.0075	0.0001
12	16	33.04	33.04	-0.0041	0.0000
12	18	33.07	33.07	-0.0020	0.0000
13	20	33.10	33.10	-0.0013	0.0000
14	25	33.16	33.17	0.0104	0.0001
15	30	33.22	33.24	0.0153	0.0002
16	40	33.34	33.35	0.0086	0.0001
17	50	33.44	33.44	0.0040	0.0000
18	60	33.53	33.53	-0.0045	0.0000
19	70	33.60	33.60	-0.0041	0.0000
20	80	33.66	33.66	-0.0027	0.0000
21	100	33.76	33.76	-0.0007	0.0000
k	0.0026	δc	34.55	Sum:	0.0009

Table A.5: HFIP and Sc(OTf)₃ titration of hemimalonate 100 mM

Hemimalonate (100mM) DAC - Sc			Hemimalonate (100mM) DAC - HFIP		
Run	Sc mol %	obs shift (ppm)	Run	HFIP Eq	obs shift (ppm)
1	0	40.88	1	0	40.88
2	1	40.9	2	1	41.36
3	2	40.93	3	2	41.68
4	3	40.98	4	3	41.91
5	5	41.18	5	5	42.23
6	10	41.99	6	10	42.52
7	20	N/A	7	20	42.9
8	30	44.07	8	30	43.25
9	50	45.33	9	50	43.26

Table A.6: HFIP and Sc(OTf)₃ titration of diester 100 mM

Diester DAC (100mM) - SC			Diester DAC (100mM) - HFIP		
Run	Sc mol %	obs shift (ppm)	Run	HFIP Eq	obs shift (ppm)
1	0	32.58	1	0	32.70
2	1	32.65	2	1	32.99
3	2	32.68	3	2	33.23
4	3	32.97	4	3	33.42
5	5	33.23	5	5	33.66
6	10	33.92	6	10	34.05
7	20	35.24	7	20	34.40
8	30	36.63	8	30	34.71
9	50	40.15	9	50	34.71

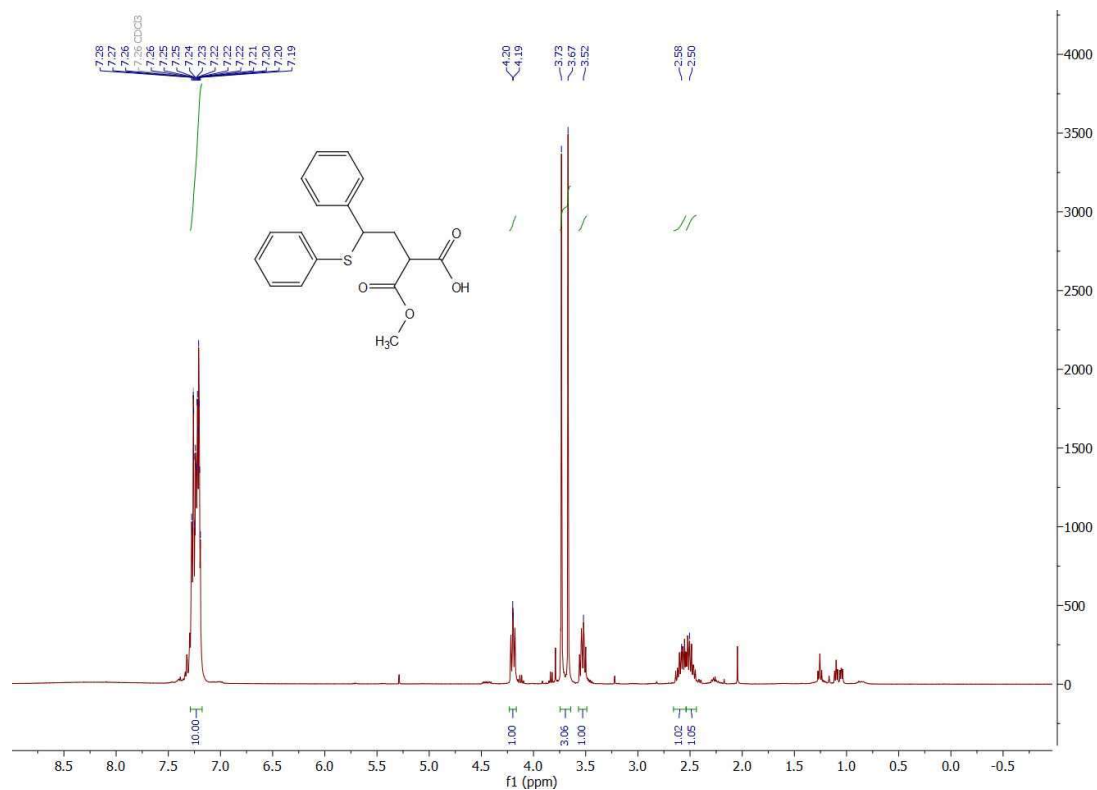
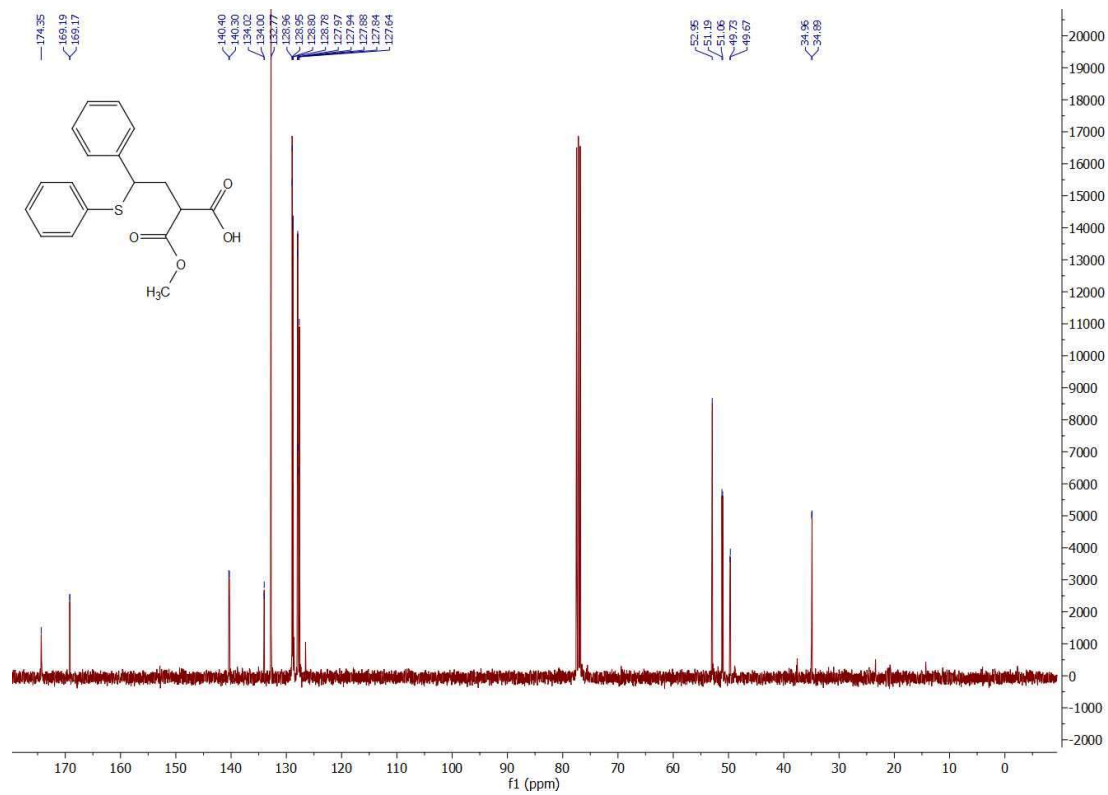
Figure A.1: ^1H NMR Spectra for 2.20aFigure A.2: ^{13}C NMR Spectra for 2.20a

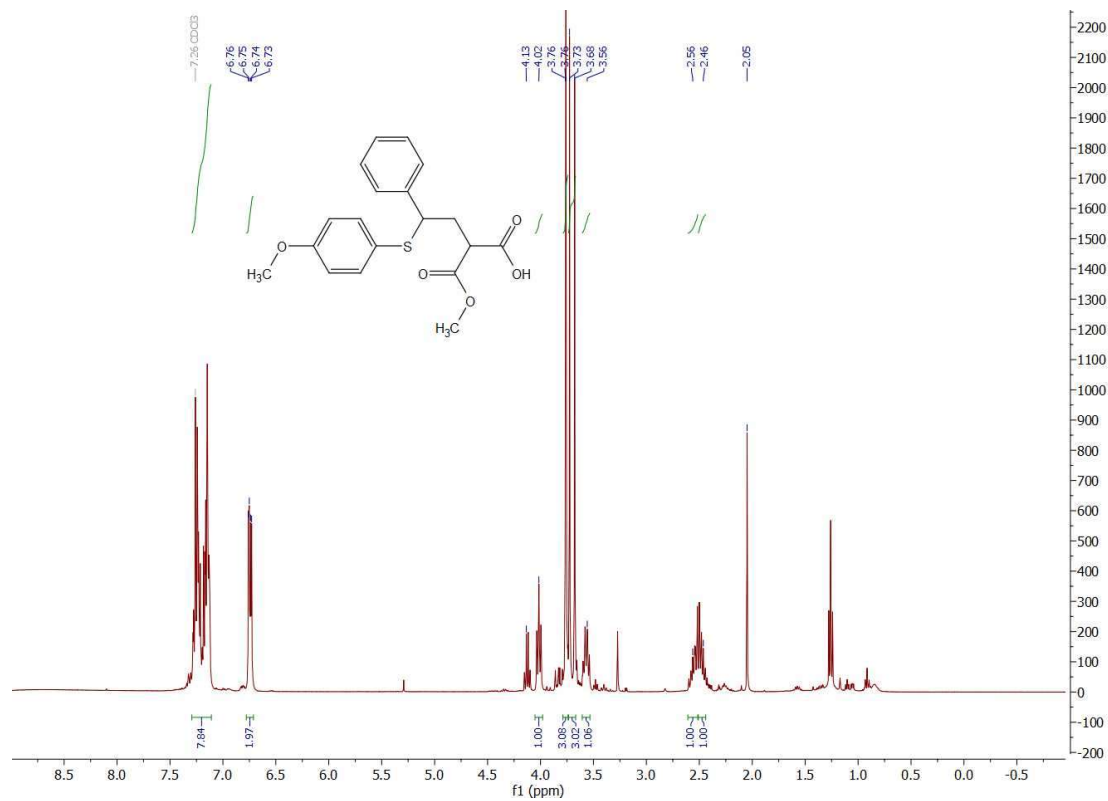
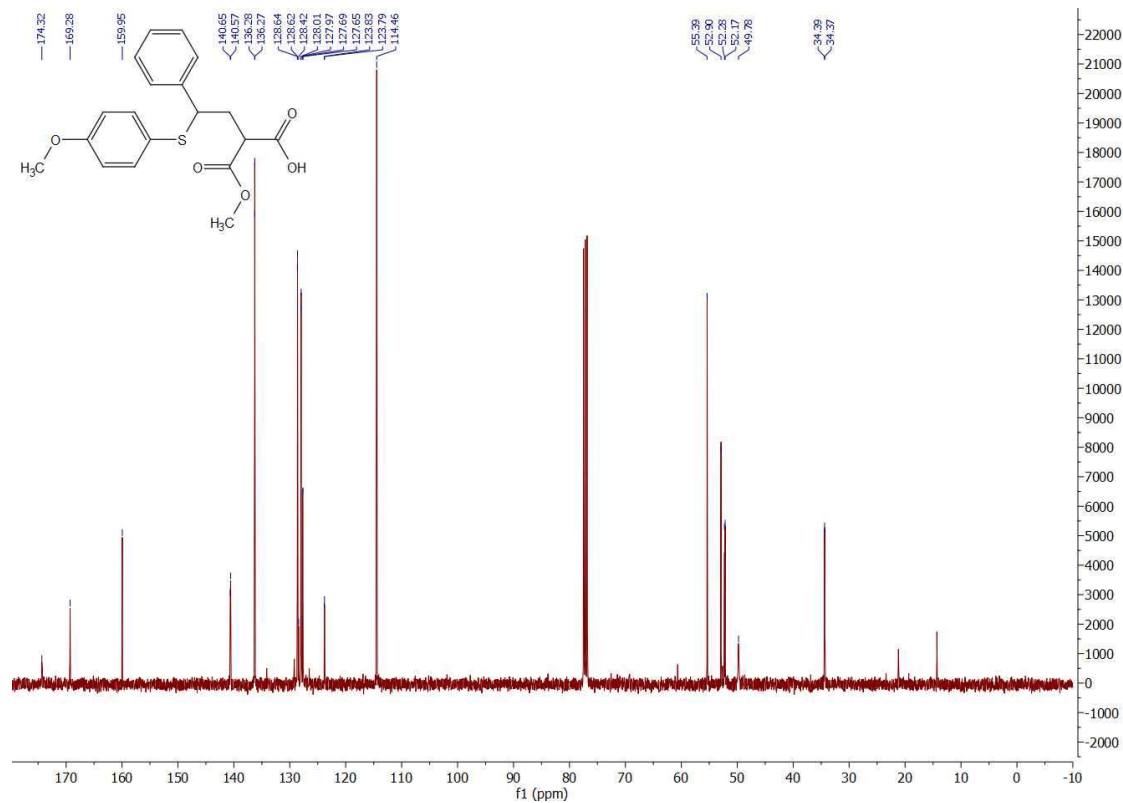
Figure A.5: ^1H NMR Spectra for 2.20cFigure A.6: ^{13}C NMR Spectra for 2.20c

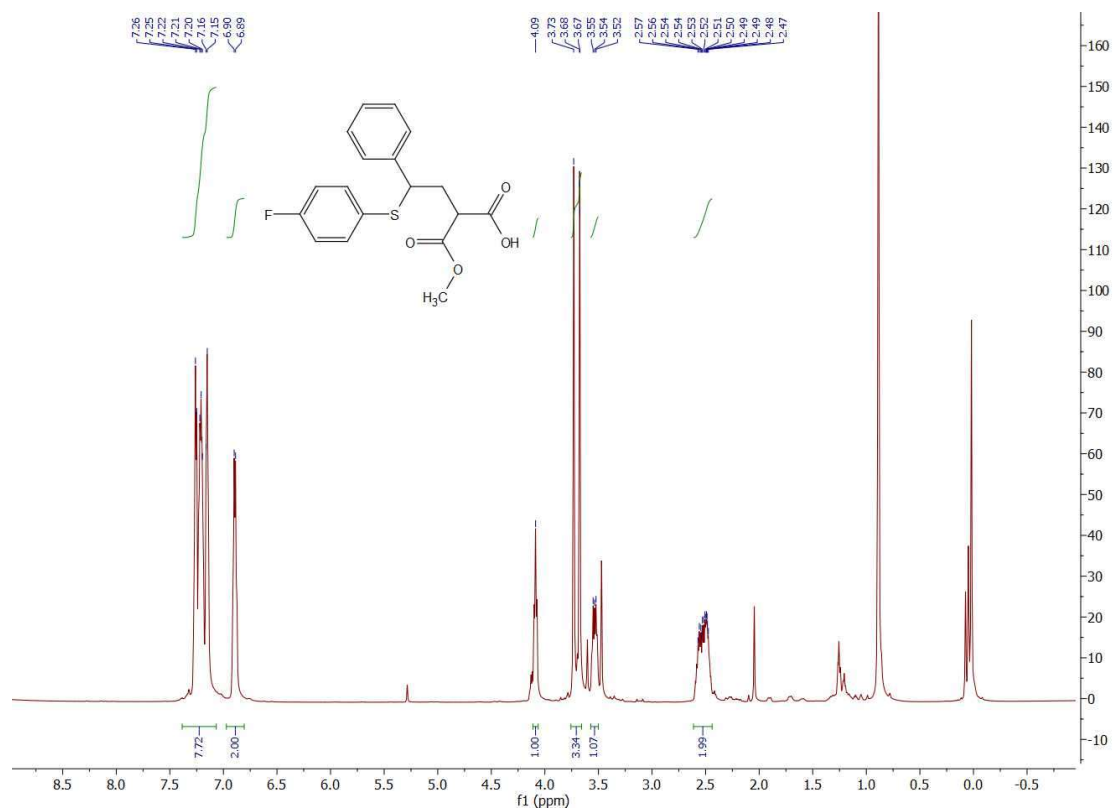
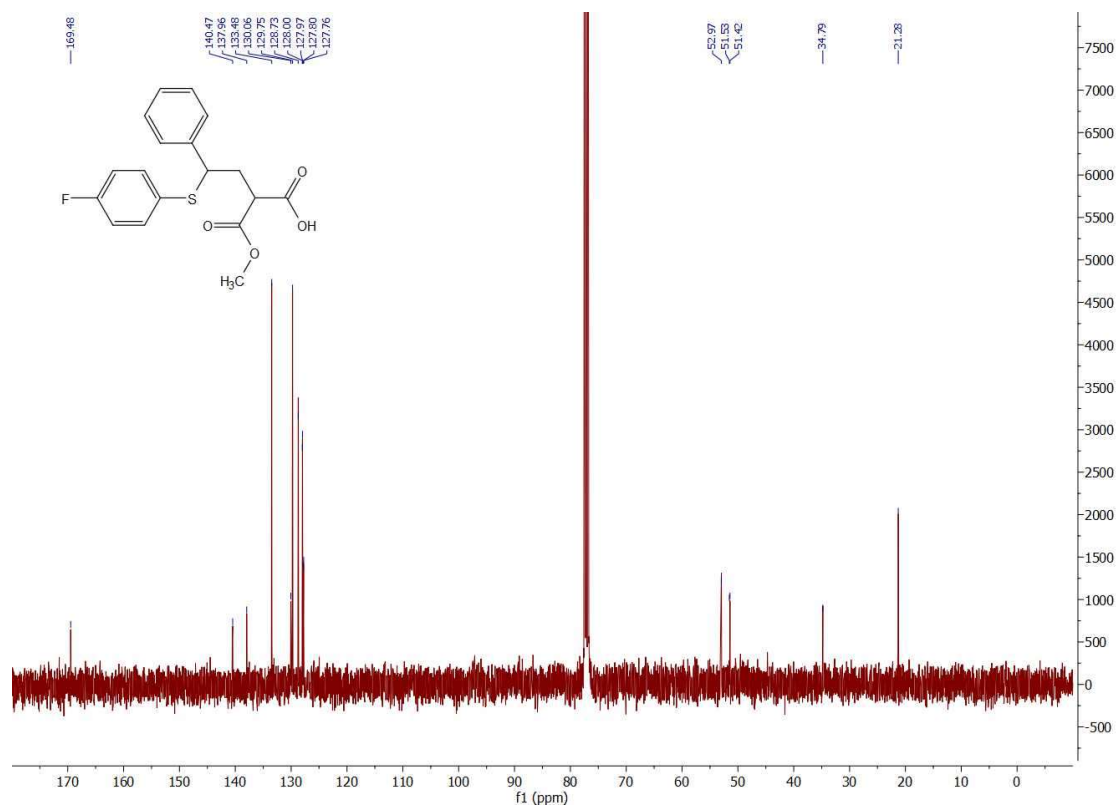
Figure A.7: ^1H NMR Spectra for 2.20dFigure A.8: ^{13}C NMR Spectra for 2.20d

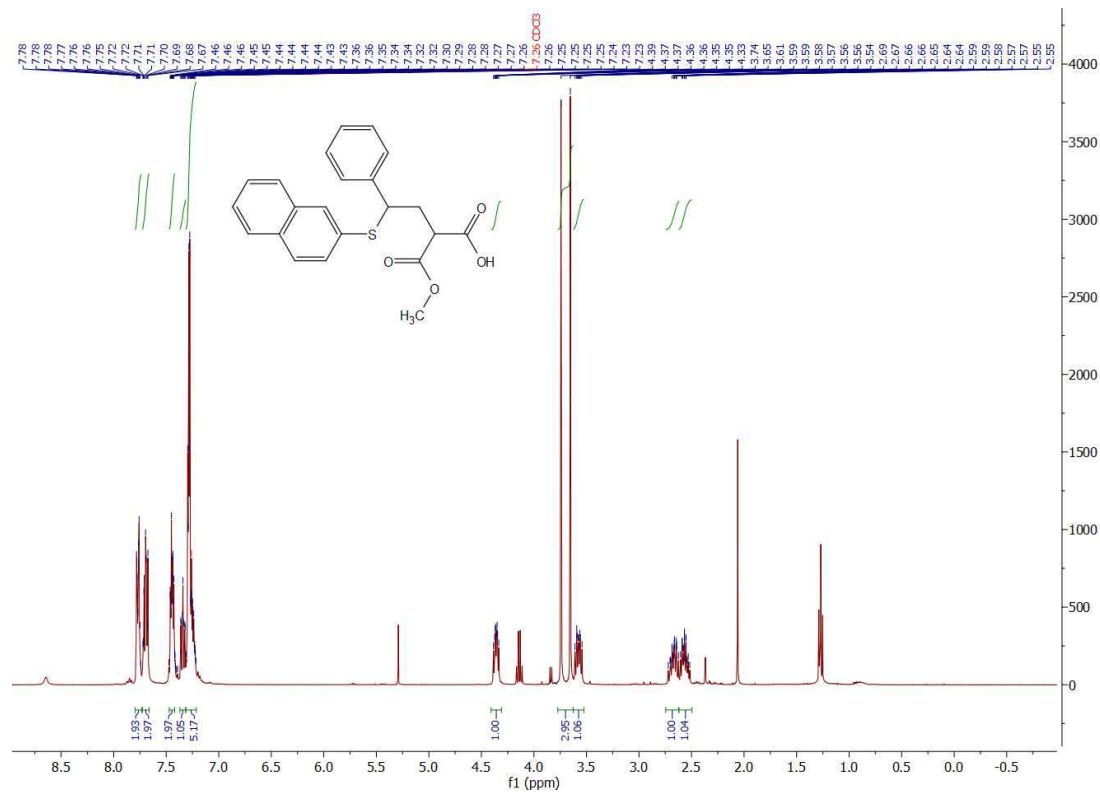
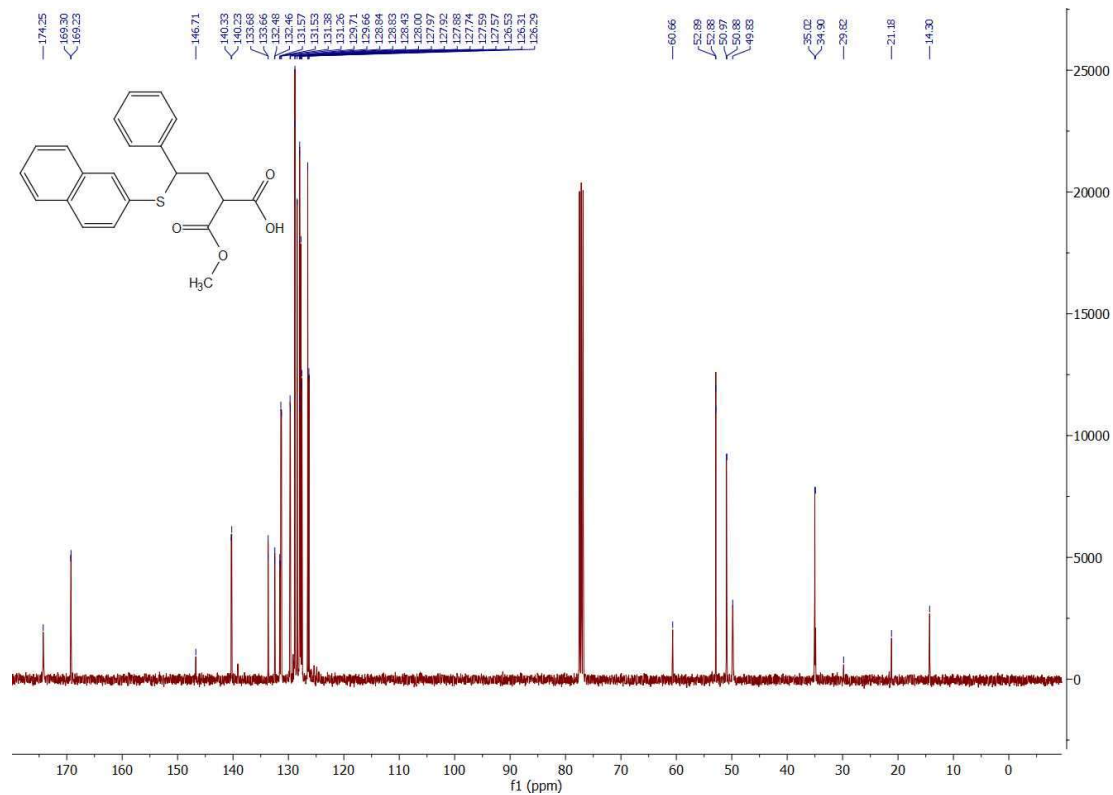
Figure A.9: ^1H NMR Spectra for 2.20eFigure A.10: ^{13}C NMR Spectra for 2.20e

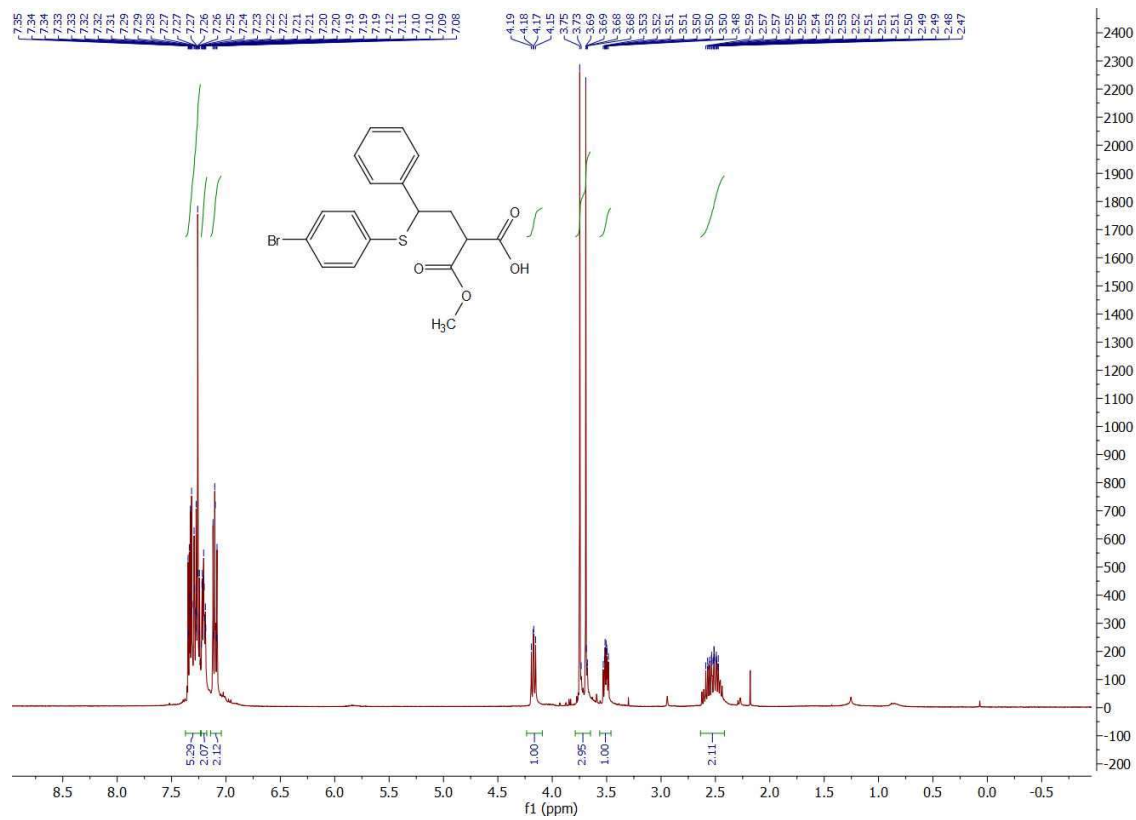
Figure A.11: ^1H NMR Spectra for 2.20f

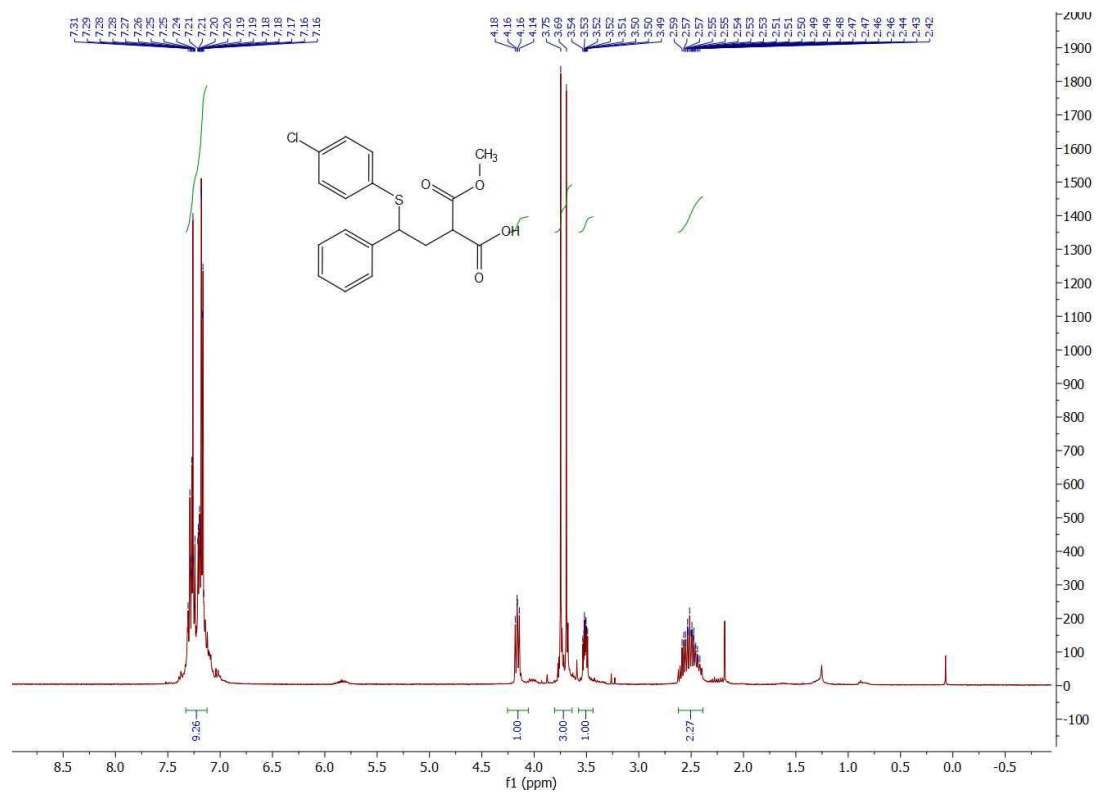
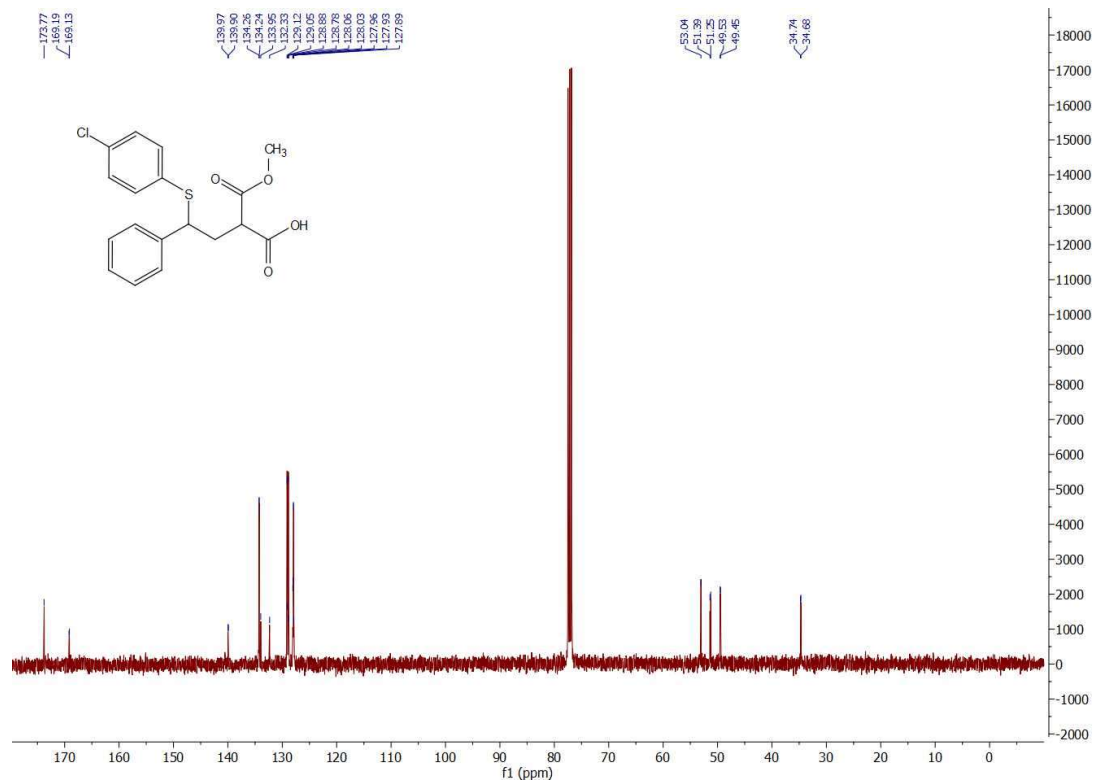
Figure A.12: ^1H NMR Spectra for 2.20gFigure A.13: ^{13}C NMR Spectra for 2.20g

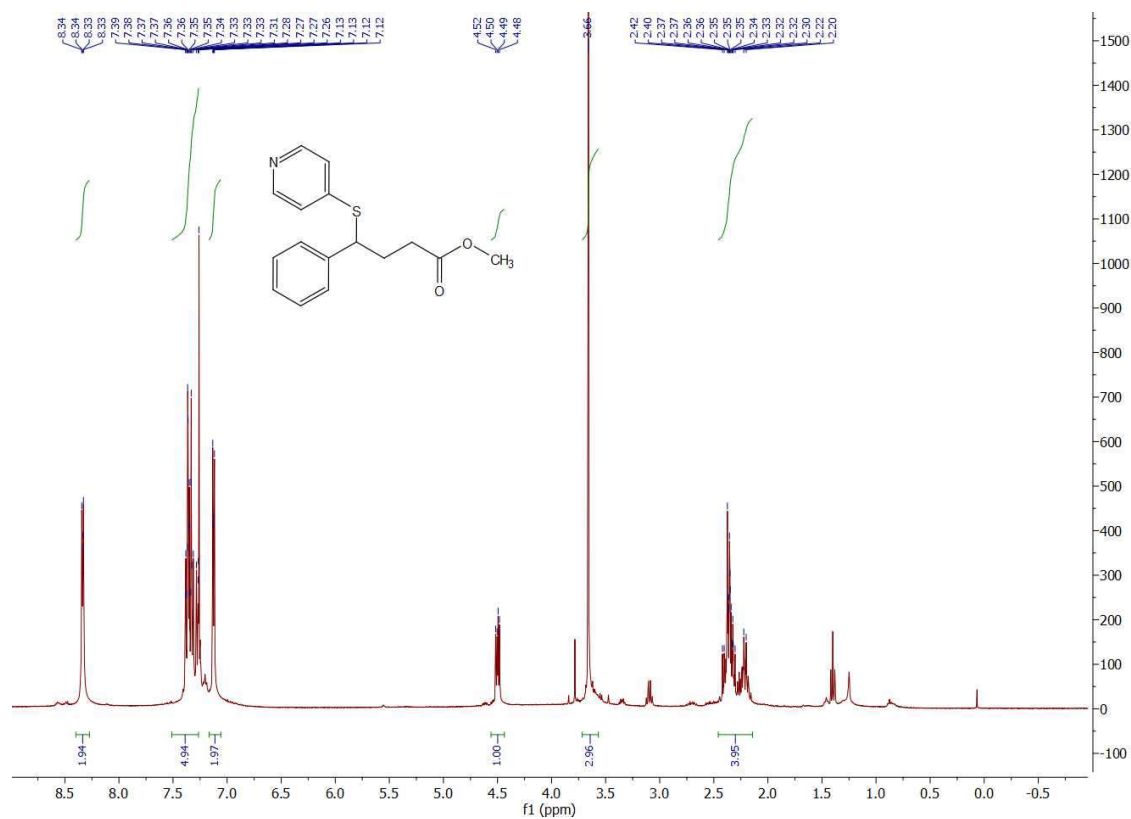
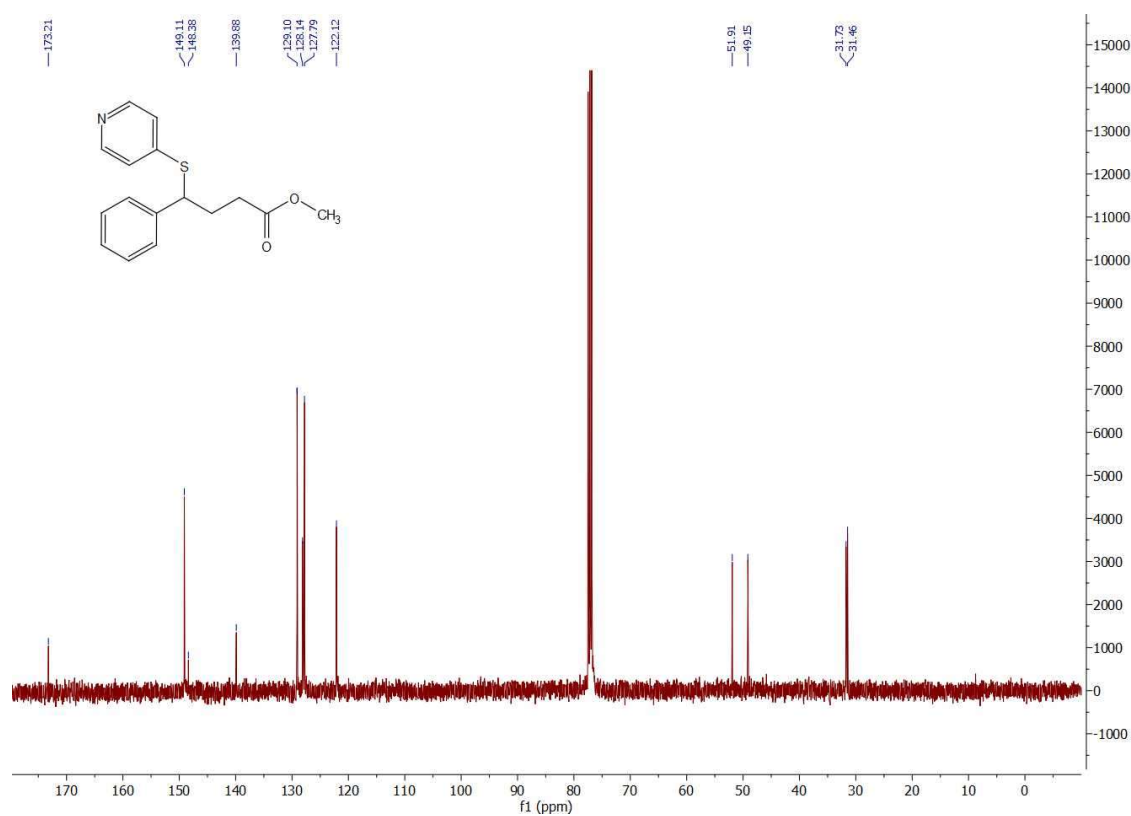
Figure A.14: ^1H NMR Spectra for 2.20hFigure A.15: ^{13}C NMR Spectra for 2.20h

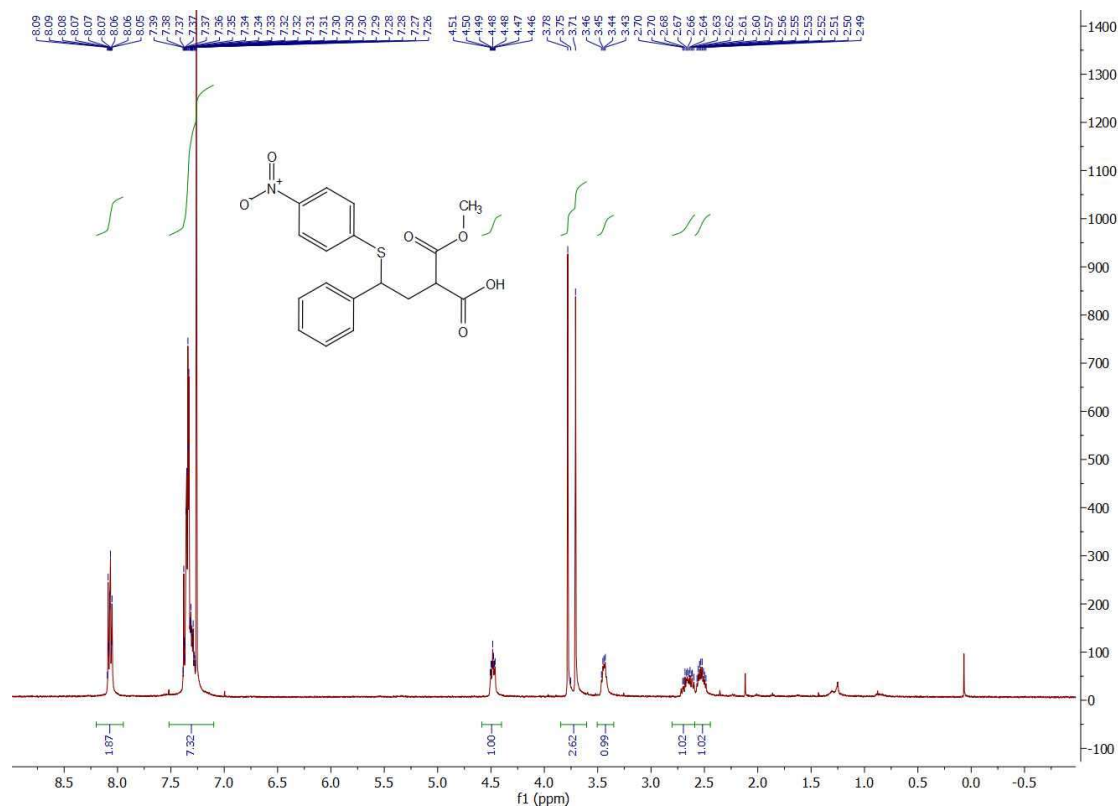
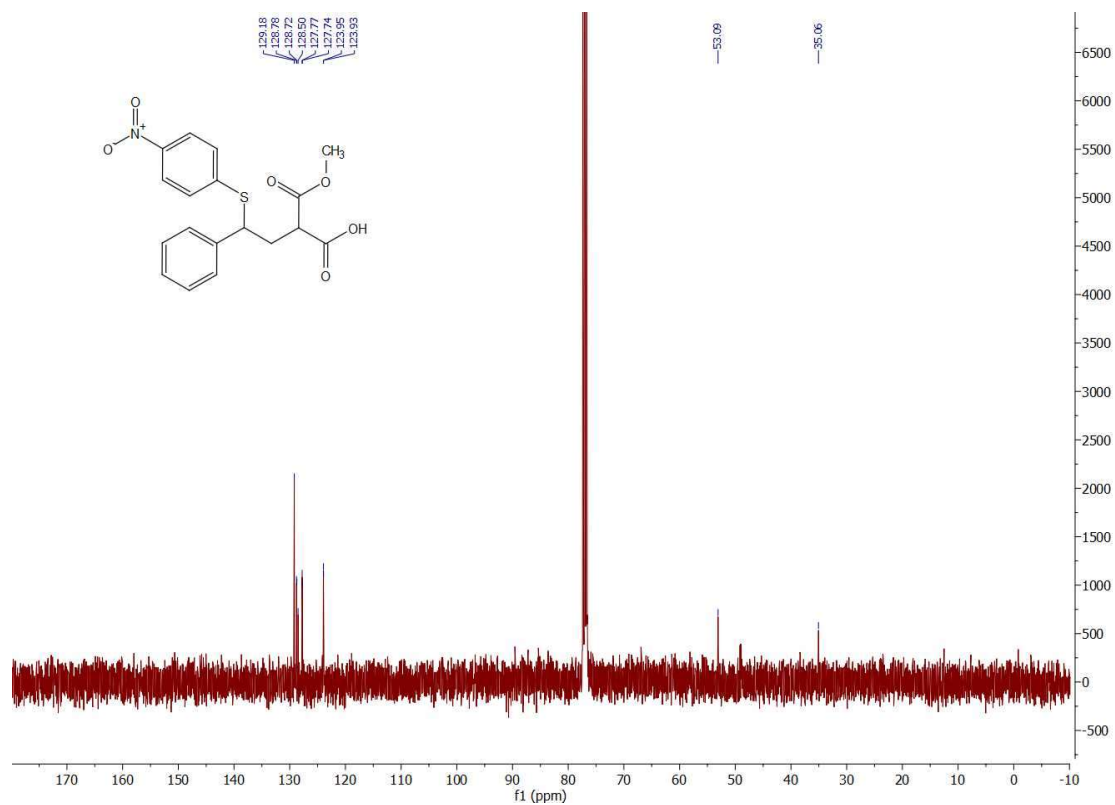
Figure A.16: ^1H NMR Spectra for 2.20iFigure A.17: ^{13}C NMR Spectra for 2.20i

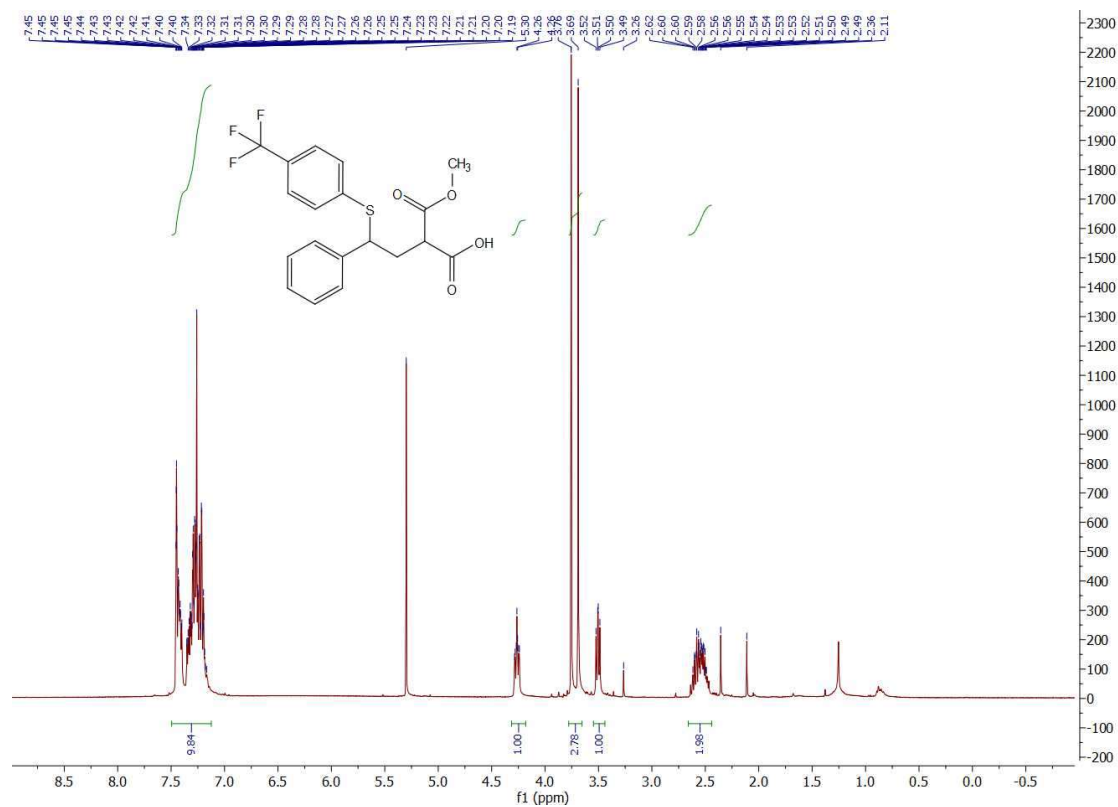
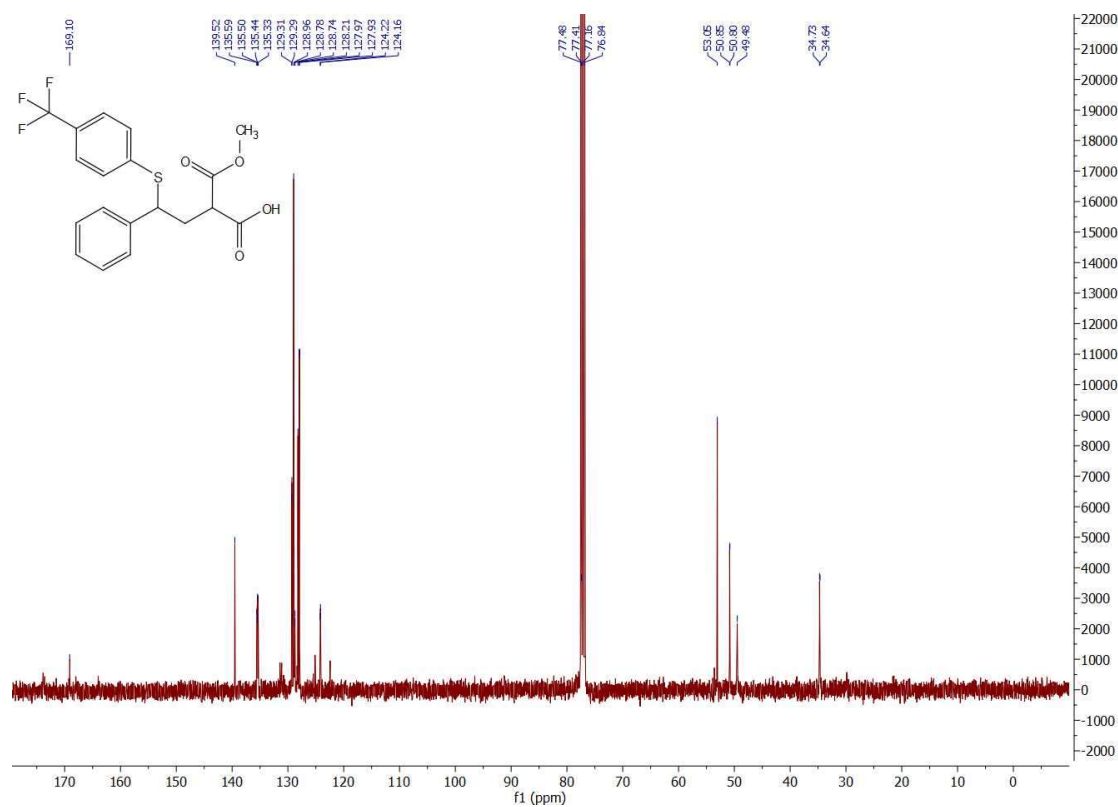
Figure A.18: ^1H NMR Spectra for 2.20jFigure A.19: ^{13}C NMR Spectra for 2.20j

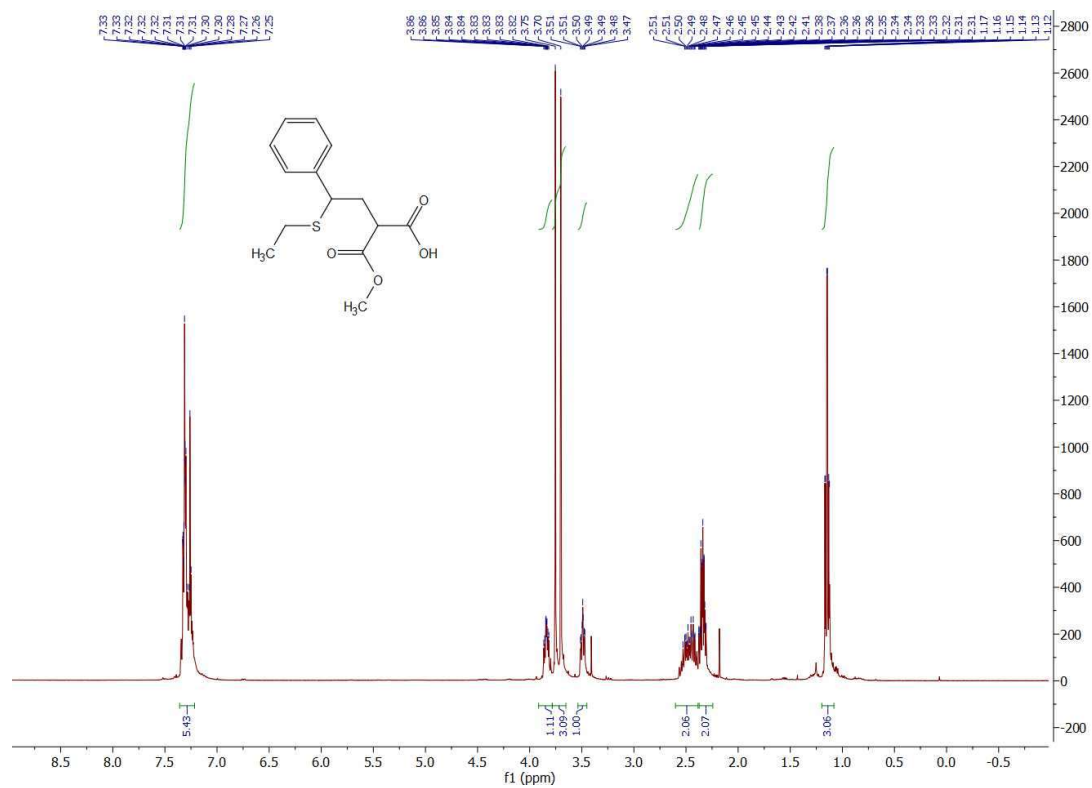
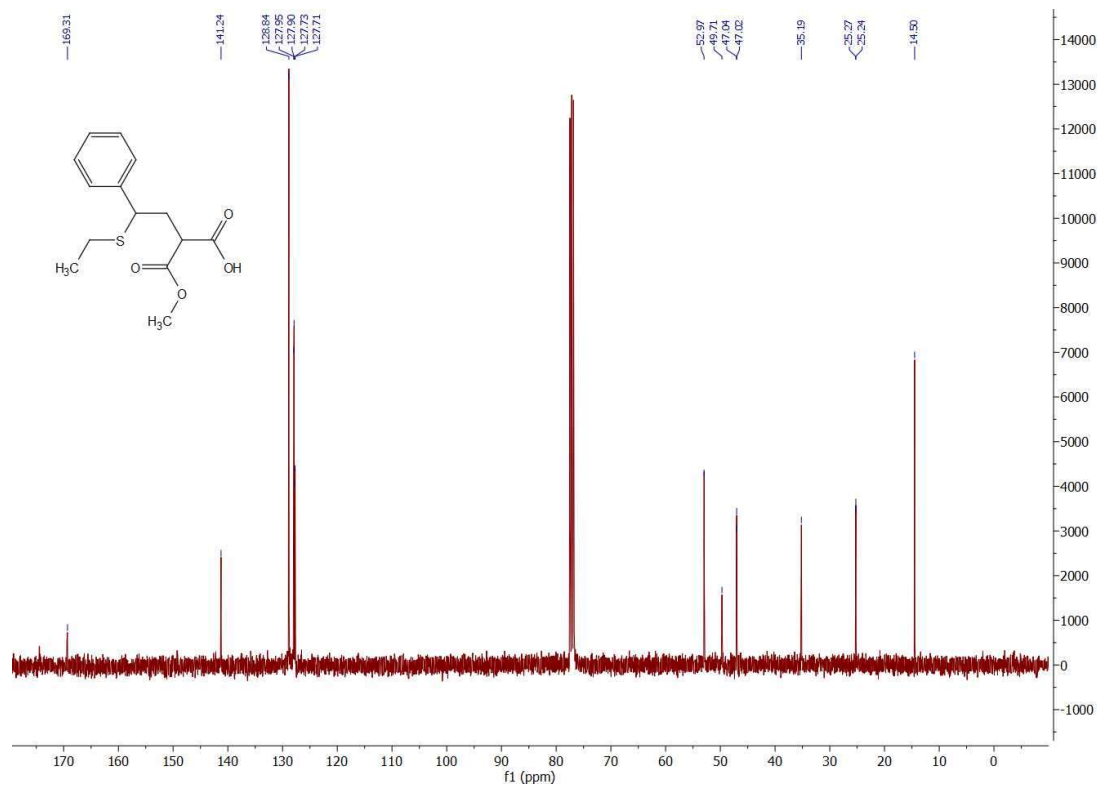
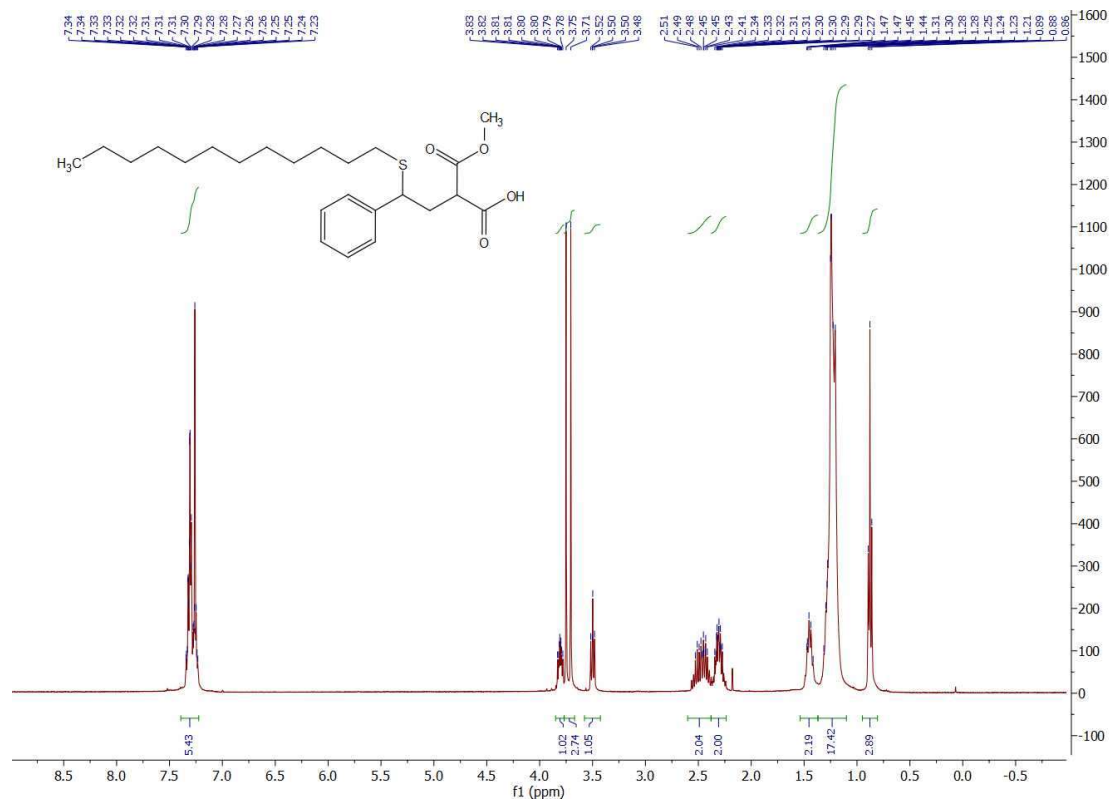
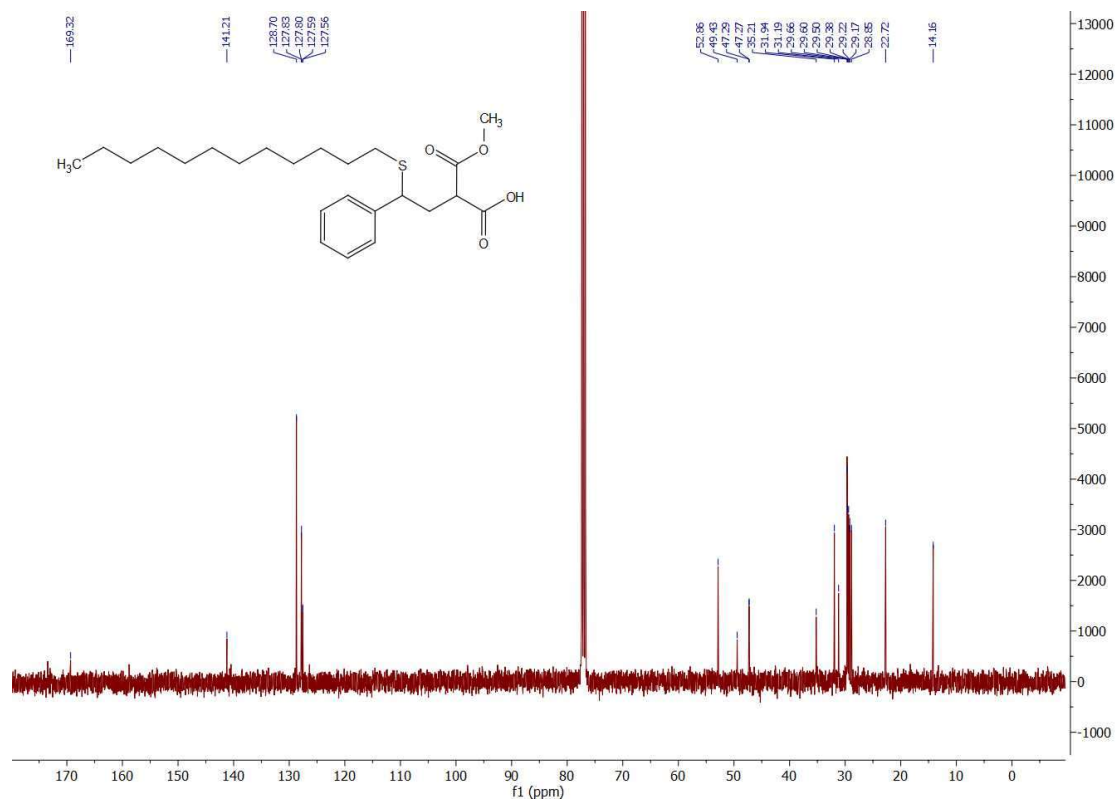
Figure A.20: ^1H NMR Spectra for 2.20kFigure A.21: ^{13}C NMR Spectra for 2.20k

Figure A.22: ^1H NMR Spectra for 2.201Figure A.23: ^{13}C NMR Spectra for 2.201

Curriculum Vitae

Name: Matthew Pamenter

Post-secondary Education and Degrees: **Bachelor of Science, Honors Specialization in Chemistry**
University of Western Ontario
London, Ontario, Canada
2016-2021

Master of Science, Organic Chemistry
The University of Western Ontario
London, Ontario, Canada
2021-present

Research Experience **Masters Student**
The University of Western Ontario
Supervisor: M. A. Kerr
2021-present

- Developed method for ring opening reaction of cyclopropanes with thiol-based reagents
- Used NMR spectroscopy titrations to study the host-guest interaction between cyclopropanes and a hydrogen bond donor or catalyst

Undergraduate Research Project
The University of Western Ontario
Supervisor: M. A. Kerr
2020-2021

- Attempted to expand previous group work ring opening hemimalonate cyclopropanes to new classes of nucleophiles
- Looked at how the ^{13}C NMR spectra of cyclopropanes were affected by the addition of a hydrogen bond donor

Honors and Awards: **Deans Honor List**
The University of Western Ontario
2018, 2019, 2020

Work Experience **Teaching Assistant**
The University of Western Ontario
2021-2023

- Chem 2283 and Chem 3373:
 - As head TA maintained communication between course supervisor and TAs regarding student problems and grading.
 - Assisted students through experiments in the laboratory, ran NMR spectra for samples made by students, and graded lab reports.
 - Held office-hour help sessions regarding lab material.